WIND ANALYSIS IN RELATION TO THE DEVELOPMENT

OF WIND POWER

By

LE ROY ANDREW GIBSON

Bachelor of Science
University of Utah
Salt Lake City, Utah
1958

Master of Science
Oklahoma State University
Stillwater, Oklahoma
1962

Submitted to the Faculty of the Graduate College
of the Oklahoma State University
in partial fulfillment of the requirements
for the Degree of
DOCTOR OF PHILOSOPHY
May, 1969

WIND ANALYSIS IN RELATION TO THE DEVELOPMENT

OF WIND POWER

Thesis Approved:

Kenneth A. McCollom
Thesis Adviser

Arthur M. Breipohl

Paul A. McCollum

James E. Shamblin

N. N. Durham
Dean of the Graduate College

ii

iii

TABLE OF CONTENTS

LIST OF TABLES

LIST OF FIGURES

CHAPTER I

INTRODUCTION

Electric power consumption in the United States has almost doubled
every ten years since 1900. This means that in every successive ten year
period we consume more energy resources than we consumed in all past
history (1). This also means that our vast reserves of natural energy
resources stored in the form of fossil fuels of oil, coals, gas, etc.,
are being depleted. No one knows how much energy remains in the earth
but with the ever increasing consumption of this stored energy research-
ers have begun investigating methods for obtaining and storing other
forms of energy.

Investigations for utilization of other sources of energy have been
taking place all over the world (2). The investigations have occured in
both technologically developed countries and in the developing countries.
Developing countries are considered to be those backward countries who
are striving to enter the mainstream of economic progress enjoyed by the
West. The developing countries also have the most to gain from the de-
velopment of new sources of energy. Some of the sources of energy that
are now being considered are wind energy, solar energy directly from the
sun, and tidal energy. These energy sources are categorized as unconven-
tional energy sources and are being developed not as a replacement for
but as a supplement to the more conventional sources of energy. For
example, the unconventional energy systems can provide for electrification

1

of remote farms, stations, and other areas where power transmission lines
to available power stations are not economically feasible. In some areas
such as in developing countries, these unconventional sources may provide
the energy necessary for essential life sustaining requirements and may
be the only energy source available. Here, the unconventional energy
can be used to increase agricultural productivity by providing power for
irrigation and for drying grain crops.

Applications of unconventional energy sources to small energy sys-
tems may provide power for modern communication systems. For example,
the power requirements of solid state microwave radio links are very low
(200 to 300 watts) and could be adequately met by a storage system
charged by a small wind electric generator or solar energy converter.

The School of Electrical Engineering at Oklahoma State University
has been and is presently engaged in research programs to develop and
provide an economic energy conversion and storage system for these uncon-
ventional energy sources for possible use in developing countries (3,4).
The heart of this conversion system is an energy storage subsystem using
electrolysis cells to produce hydrogen and oxygen gases and a direct con-
version fuel cell to recombine the gases when needed as electricity.
Figure 1 depicts the basic building blocks of a typical system. This
system takes the energy developed by the wind generator or solar gener-
ator and converts this energy to hydrogen and oxygen. The hydrogen and
oxygen are then stored under pressure until the demand occurs. When the
demand occurs, the fuel cell recombines the two gases to obtain a direct
current electrical voltage. This voltage output can then be used either
in the direct current form, be inverted to provide alternating current
power, or perhaps be converted in an internal combustion engine to
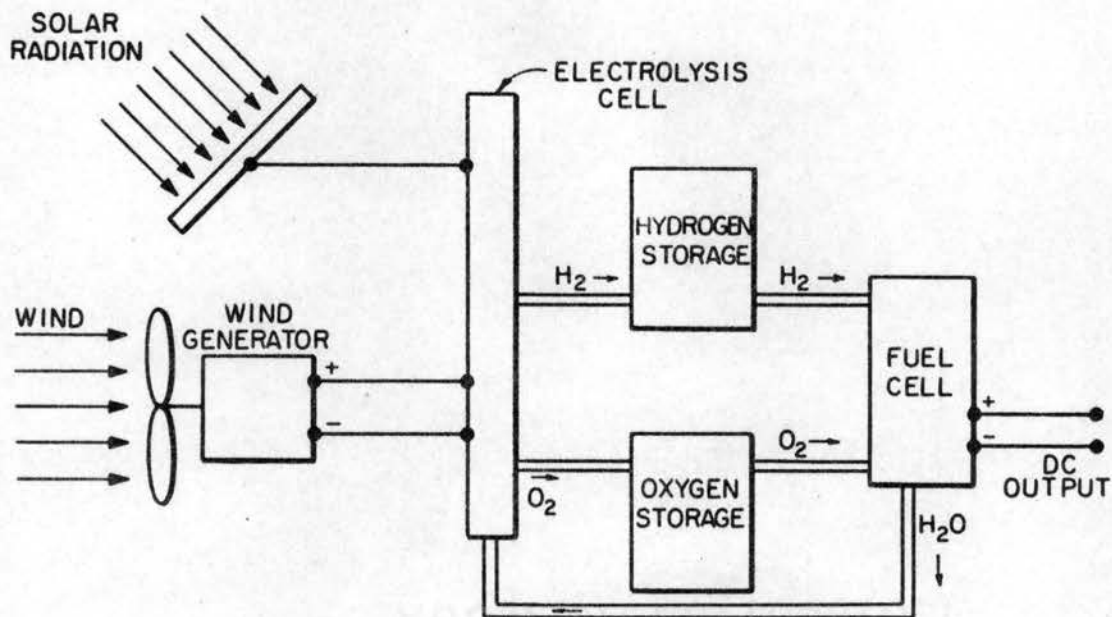
Figure 1. A Solar or Wind Electrical Energy System With
Intermediate Energy Storage

mechanical energy for pumping water.

Research has progressed satisfactorily on the storage part of the
system but little has been done about studying the characteristics of
the input from the unconventional energy sources. A designer of such an
energy system must have considerable information about the input. For
example, the design of wind energy conversion equipment requires the
knowledge of the energy available in the wind. A good correlation must
be made between wind data that are presently available from standard
meteorological stations and the energy that can be extracted for use.

The unconventional energy sources have a great advantage of being
free inexhaustible supplies of energy. However, because the wind velocity
is quite high in Oklahoma and because it can be measured quite easily,
it was selected as the first input to investigate for the energy

conversion and storage system. Man has always used the energy from the wind. Through the years, the wind has been used to pump water, to power ships, to recharge batteries, to winnow grain, and to generate electrical power. However, the use of the wind as an electrical energy source has not been attractive because of excessive expenses involved in storing the energy to be available during times of little or no wind. The electrolysis and fuel cell storage system may be able to reduce the cost of the storage to such a degree that wind energy systems, at least on a small scale, may be practical and economical.

The purpose of this dissertation is to make a detailed analysis of the wind to provide a designer of an energy conversion system with necessary information about its characteristics. The research was divided into three major areas. The first was to obtain a model of the wind which could be used to simulate the wind input for the energy conversion system, the second was to determine the predictability of the wind, and the third was to provide a method to obtain velocity duration curves without manual analysis of excessively long wind records as well as to verify through its use the dependability of energy estimates using only one-minute hourly averages available at many meteorological stations.

Chapter II presents a review of wind energy developments and previous methods used for modeling the wind. Chapter III develops the model of the wind which is an extension of previous work on models of the wind derived for wind loading of structures. Chapter IV presents the analysis of the frequency content of the wind. Chapter V discusses the design and operation of a velocity distribution analyzer, methods for obtaining velocity duration curves and comparisons of velocity duration curves obtained from the different methods. Chapter VI describes the research

conclusions and limitations; this chapter also outlines some direction

for future research.

REVIEW OF LITERATURE

Conversion of wind energy to rotating shaft movement is an age old technology. However, little has been done in optimizing the equipment required to convert wind energy to electrical energy. Most of the technology previously has been directed toward converting wind energy to mechanical energy, e.g. windmills for direct pumping of water. The newest impetus for again concentrating on an electrical energy conversion system is that variations of electrical output with varying wind is not a problem when good energy storage is available. An energy storage system of the form described in Chapter I is superior to the previous practical alternative, that of storage batteries.

Wind Power

Although the wind has been used to do work for many centuries, wind power generation has only been investigated seriously since the original work done by A. Betz (5) in 1927. Since that time, many individuals in many countries have investigated wind power utilization. The results of these investigations in general have led to conclusions that wind energy is not economical and not easy to use because of the variations of electrical output with varying wind velocities. The use of wind power generation plants in the United States was quite common in the thirties in the rural areas of the plain states before conventional forms of electrical power were extended through transmission lines from the larger cities. Putnam (6) in the early forties attempted to connect a large wind

generator to the Vermont power system but he met with failure due to the lack of funds, mechanical failures and the inability of the wind generated electricity to be as economical as other forms; Golding (7) in England in the early fifties did extensive research in attempting to use the wind on a large scale in the United Kingdom. His work also declined because of the inability at that time of the wind generated electricity to compete with other forms of energy. Others in many countries have done extensive research in an attempt to use the wind. Much of the work prior to 1961 was reported in a United Nations' publication of the Proceedings of the Conference on New Sources of Energy which was held in Rome in August of 1961 (2). The most recent wind research has been done in India (8,9,10,11).

The Necessity for Additional Wind Analysis

Since so many have attempted to harness the wind and use the wind energy with little success, why is it important to again investigate it as an energy source? Many answers to this question could be given but those of primary importance are:

(1) There is the prospect of developing an economical and efficient method for storing the energy. This storage method has come about as a result of recent research in electrolysis processes and fuel cell technology.

(2) There are increasing demands on our natural resources that are required to generate electrical power so all possible sources of energy should be investigated before it is too late.

(3) Developing countries may be able to use these energy sources much more rapidly than waiting for the ultimate development of

large central power plants.

The analysis of the wind has been a vital part of the research of each attempt to use the wind. Putnam (6) conducted a wind survey to determine the best location for his wind generator that operated for a number of years in Vermont. Golding (7) also performed an extensive wind analysis in England. Others since Golding have also done detailed analysis of the wind. These wind studies were in most cases limited to the use of hourly measurements to obtain the wind velocity information. These hourly measurements are almost standard throughout the world and are obtained by taking the average each hour for one minute, i.e. the wind speed in averaged for one minute every hour to obtain the hourly wind measurements. This one-minute hourly average is recorded in the meteorological records as the wind velocity for the entire hour. This procedure for obtaining one-minute hourly averages is outlined in the U. S. Weather Bureau Manual of Surface Observations (12).

Some of the researchers did consider effects of the wind between the hourly measurements; however, the hourly measurements were used in most studies because these measurements were the only available wind data. Thus the effects of variations over shorter time periods essentially were ignored. The variations over shorter time periods are referred to as wind gusts. The gustiness of the wind is a measure of the deviations of the wind velocity from the mean wind velocity. The variations over short time periods can have a significant effect on the estimated power for a specific location. As an example of how the variations within an hour might effect the estimated power, assume that the hourly speed was 10 miles per hour and was constant for a one hour period; then using a six foot diameter propeller results in an energy generated of

approximately 100 watts. If however, during this one-hour period gusts of wind of 20 miles per hour had an accumulated time of eight minutes while the average remained at 10, the total energy would be approximately doubled or 200 watts.

In attempt to adequately consider the effects of the short term variations, Golding (7) defined an Energy Pattern Factor. This factor is defined as the total energy in the wind divided by the energy calculated by cubing the mean wind velocity. A large pattern factor for a given location normally indicates that the short term variations have either a few large long duration gusts or a number of shorter duration gusts that causes the actual power to be much larger than the power estimated by cubing the mean velocity. He stated that the Energy Pattern Factor was usually close to unity unless the fluctuation pattern (gust durations) was wide therefore he considered the factor as not too important in energy estimates. He also concluded that the factor was not important because a wind driven machine may not be able to take advantage of the fast fluctuations because of the large inertia of the system.

Recent studies in India have resulted in conclusions that the Energy Pattern Factor should not be ignored in selecting potential wind power sites. Ramakrishman and Venkiteshwaran (13) found that the Energy Pattern Factor was much larger than unity at many sites. This would indicate that Golding's first reason for ignoring the Energy Pattern Factor might not hold true for all potential sites.

Since there is an apparent contradiction as to whether or not the Energy Pattern Factor should be ignored, further analysis of the short duration variations is indicated.

The Energy Pattern Factor requires the true mean velocity and not

the mean velocity of the one-minute hourly averages. Therefore, in addition to further analysis of the short duration variations, a comparison between the actual and the estimated power using one-minute hourly measurements should be made.

Formulas for Energy Extraction

The wind is air in motion and since air has mass, the wind has kinetic energy when the mass has velocity. The kinetic energy is $\frac{1}{2}$ the product of mass and velocity squared. The mass of air passing in unit time is the product of air density, wind velocity and cross sectional area. The kinetic energy passing through the area per unit time then is:

$$\frac{\text{Kinetic Energy}}{\text{Hour}} = \frac{1}{2}(\rho AV)V^2 = \frac{1}{2}(\rho AV^3) \qquad (2\text{-}1)$$

where

ρ = air density, mass per unit volume, pounds/ft^3;

V = wind velocity, in miles per hour;

A = area through which the wind passes, in square feet.

The kinetic energy in Equation 2-1 above represents the total available energy in the wind. This energy can be converted to power in kilowatts by introducing a non-dimensional constant k, where $k = 2.14 \times 10^{-3}$. Therefore, the expression for the maximum theoretical power in the wind is:

$$P \text{ (in kilowatts)} = 2.14 \, \rho AV^3 \times 10^{-3} \qquad . \qquad (2\text{-}2)$$

Golding (7) expressed this equation in a more general form by combining the constants k and ρ into a general constant K. He expressed K for

various units used for P, A and V. Table I is a reproduction from Golding, page 22, showing the various value for K. The units used throughout this paper require a value of K = 0.0000053 for all power calculations. Therefore power in kilowatts is:

$$P = 0.0000053 \, AV^3 \qquad . \qquad (2.3)$$

TABLE I

VALUES FOR CONSTANT K AS PRESENTED BY GOLDING

Unit of Power P	Unit of Area A	Unit of Velocity V	Value of K
Kilowatts	Square Feet	Miles Per Hour	0.0000053
Kilowatts	Square Feet	Knots	0.0000081
Horse-Power	Square Feet	Miles Per Hour	0.0000071
Watts	Square Feet	Feet Per Second	0.00168
Kilowatts	Square Metres	Metres Per Second	0.00064
Kilowatts	Square Metres	Kilometres Per Hour	0.0000137

The theoretical maximum power extractable from the wind is not that described in Equation 2.3. The fraction available was determined by Betz (5) in 1927. He showed that the theoretical maximum fraction of the power in the wind which could be extracted by an ideal rotor was 0.593 or 16/27 of the kinetic energy passing through the area per unit of time or 16/27 of power. In addition, the theoretical maximum power

is further reduced by the efficiency of the mechanical and electrical
equipment. The maximum efficiency of a typical propeller wind energy
system is about 60 per cent; therefore, the extractable power is about
36 per cent of the theoretical total power available in the wind.

Energy Estimates for Specific Locations

Energy estimates are made for a potential site by first obtaining
the velocity duration curves, then calculating the power duration curve,
and finally determining the total power from the power duration curve.

The velocity duration curve is a cumulative frequency curve which
shows the duration in hours that the magnitude of the wind velocity
exceeds each unit velocity of hourly mean wind velocity. It is obtained
by examining the wind records for the potential site and recording the
number of times that the velocity magnitude was above each unit velocity
of the wind. The power duration curve then is obtained by cubing the
ordinates of the velocity duration curve and replotting them to any con-
venient scale. The area under the power duration curve represents the
maximum extractable power.

Figures 2a and 2b show the velocity duration and power duration
curves respectively for a two month period for Stillwater, Oklahoma.
There are two methods for obtaining the velocity duration curve shown in
Figure 2a. It can be obtained by rather tedious analysis of wind
recordings, or it can be obtained by using a frequency distribution
analyzer which automatically records the number of hours that the wind
blows in the predetermined velocity level. Most velocity duration curves
are obtained by the manual reduction of existing records. Figure 2b, in
addition to representing the power duration curve, represents an area
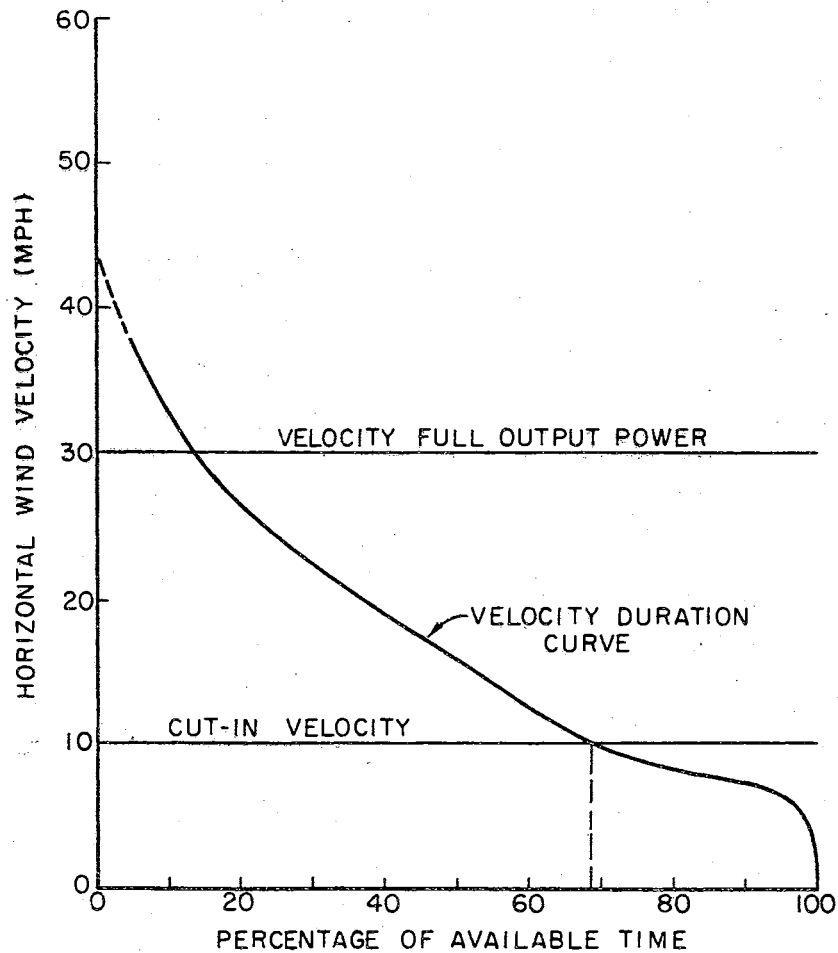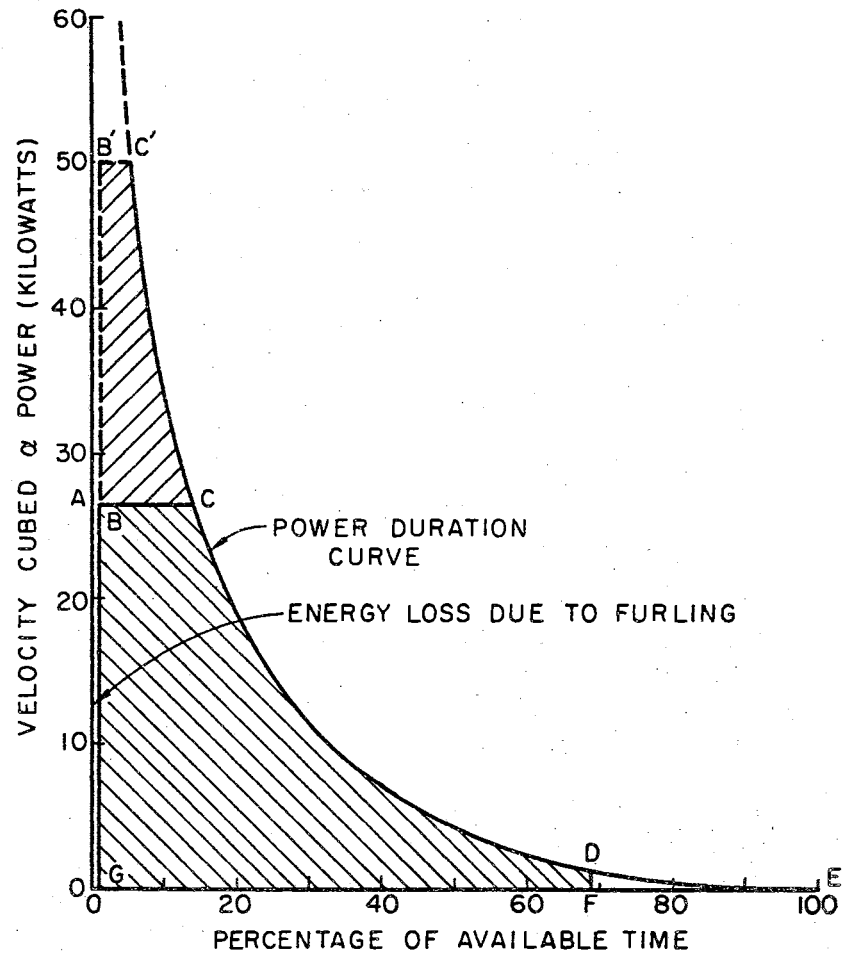
Figure 2. Velocity and Power Duration Curves for Stillwater, Oklahoma (9 March to 9 May, 1968)

that is proportional to the extractable power, shaded areas GBCDF and GB'C'DF. [The areas must be multiplied by the swept area and by the appropriate constant 16/27 K to obtain the maximum extractable power.]

The shaded areas do not include the total area under the power duration curve because a wind generator [can not generate an output for velocities below designed cut-in or turn-on velocities], because most machines are designed to operate at a constant rated output for velocities above some set velocity, and because all machines have some type of safety device to "furl" or stop the machine in excessively high winds.

Furling is accomplished either by changing the pitch of the propellers or by turning the propeller out of the main air stream of the wind. If a constant output voltage were not normally required, the extractable energy would approach the area GB'C'DF. Early wind generators were designed to have a constant output voltage to meet load requirements but wind generators coupled into an electrolysis energy storage system may not need this constant output requirement.

[The cut-in speed is that speed required to overcome the inertia of the system and begin generating an output]. The rated wind speed for most machines is between 25 and 35 miles per hour. In addition to providing a constant output voltage to meet load requirements, machines are designed for [optimum operation when the rated wind speed is between 25 and 35 miles per hour because of economics]. It would be uneconomic to attempt to build a machine which could extract full power for very high winds because high winds do not occur often enough to warrent expense of design.

Effects of Height and Terrain on Wind Profile

Terrain greatly effects the wind profile and therefore effects the output of a wind generator. Studies have been made to determine how the roughness of the terrain alters the wind velocity at various heights (14,15). Results of these studies show that the velocity at any height Y1 is related to some known velocity at height Y2 by the expression:

$$V_{Y1} = V_{Y2} \left[\frac{Y1}{Y2} \right]^{\alpha} \tag{2.4}$$

where α is the power law exponent which varies with surface roughness. Table II was suggested by A. G. Davenport (16) in 1961 to show the effects of terrain on the velocity at different heights. Column 1 indicates the value of α for the various types of terrain. [Results shown in the table can be used to determine the wind velocity at a proposed height for a wind generator when the velocity at some other height were known]

The roughness of the terrain also effects the short term variations of the wind. Scrase (17) and others around 1930 noted two important physical observations about the wind. [They noted that the gustiness of the wind is directly proportional to the average wind velocity and to the surface roughness] The variation of the roughness or drag coefficient is shown in Column 2 of Table II. These important physical observations proved to be useful in the development of the wind model in the next chapter.

The shape of the hill in addition to the type of surface must be considered in selections of potential wind power sites. Frenkiel (18) established criteria for selecting the best type of site for wind power systems.

TABLE II

INFLUENCE OF SURFACE ROUGHNESS ON PARAMETERS RELATING TO WIND
STRUCTURE NEAR THE GROUND

Type of Surface	Power Law Exponent α	Roughness Coefficient K'
(a) Open terrain with very few obstacles: e.g. open grass or farmland with few trees, hedgerows, and other barriers, etc.; prarie; tundra; shores, and low islands of inland lakes; desert	0.16	0.005
(b) Terrain uniformly covered with obstacles 30-50 ft in height: e.g. residential suburbs; small towns; woodland, and scrub. Small fields with bushes, trees, and hedges	0.28	0.015
(c) Terrain with large and irregular objects: e.g. centres of large cities; very broken country with many windbreaks of tall trees, etc.	0.40	0.050

He stated that the topographical features in the near approaches to the hilltop determine the structure of flow over it. He further concluded that a single criterion is sufficient, namely, [the mean wind vertical gradient for the height interval from 10 to 40 meters above the ground] For optimal conditions, the gradient must vanish within 5 per cent. Such flow conditions exist and are a result of regular slopes of about 1 in 3½ (inclination 16°) in the nearest few hundred meters from the hill top. [Very good wind power sites would be those located on hills that exhibit a rise of wind speed of between 5 and 10 per cent in the 10 to 40 meter interval]. Such conditions are a result of smooth

regular slopes of about 1 in 6 (inclination 10°).

Good sites would be those located on hills with a rise in the mean wind velocity in the 10 to 40 meter interval of between 10 to 15 per cent. These would be hills of smooth regular shallow slopes (about 1 in 10) or fairly rough but regular slopes of about 1 in 6. Fair wind power sites would comprise the sites for which the ratio of velocity at 40 meters to the velocity at 10 meters in within the interval (1.15, 1.21). That is, $1.15 < V_{40}/V_{10} < 1.21$. These conditions occur for smooth shallow slopes (1 to 20) and for very rough but regional slopes of 1 in 6 or very steep slopes.

Existing Models for Horizontal Winds

Models for the time variation of the horizontal wind have been developed by Davenport [19] in 1961 and by Merchant [20] in 1965. These models create a representation of the horizontal wind which includes gustiness in high winds and are primarily used by designers of structures to simulate the wind loading on these structures. Both authors assumed that the basic characteristics of the wind were essentially constant (stationary) for the period of time under study and assumed that the wind velocity could be separated into a constant part and a fluctuating (gusting) part. They expressed the horizontal wind speed mathematically as the sum of two functions:

$$V(t) = V_0 + X(t) \tag{2.5}$$

where

V_0 = constant mean wind speed;

$X(t)$ = variations about the mean.

The horizontal wind speed was the only component of the wind considered because the vertical and the lateral components of the wind are normally much smaller than the horizontal component. [The horizontal component is the component parallel to the ground and blowing in the direction of the mean wind speed.] The vertical component results from the wind being deflected up or down by obstructions and the lateral component is small wind variations from side to side resulting from the wind being deflected by the obstructions.

The constant part of Equation 2.5, V_0, is the mean wind speed of the horizontal wind for the period of time being considered. Davenport assumed a [random variable model by letting the gusts or the fluctuating part to be normally distributed with a zero mean and with a variance of σ^2] He defined his variance as:

$$\sigma^2 = 6.0K'V_0^2 \quad \text{why} \quad ? \tag{2.6}$$

where

σ^2 = variance of the fluctuating speeds about the mean,

K' = roughness coefficient determined by the roughness of the terrain as shown in Table II,

V_0 = mean wind speed, miles per hour.

Davenport considered only modeling for the magnitudes of the gusts and did not take into account the fact that [some gusts last longer than others] His model appears to be satisfactory in fitting the magnitudes of the experimental data, as verified by comparing the variance of the experimental data with the variance of his model. His model however is not useful in simulating a realistic model of the wind for wind power applications. That is, if one calculated the extractable power from a

simulated wind record and calculated the extractable power from an actual wind record with the same average wind speed, there would be large deviations between the two calculated powers. This is due to the fact that the actual wind velocity may remain at a relatively constant value for durations up to two and three minutes while the simulated model fluctuates from one extreme to the other much faster. [Also this is due to the fact that independence was assumed in his random variable model]. See Figures 3 and 4 respectively.

Figures 3 and 4 represent an actual and simulated wind velocity respectively using Davenport's model for the latter. The maximum extractable power calculated from the actual curve is P_a = 565 watts and the maximum extractable power calculated from the simulated model is P_s = 508 watts, resulting in an error of approximately 10 per cent. Since Davenport's model is a random variable model this error exists. To reduce the error, a random process model should be used.

In addition, Davenport's model does not simulate the wind for short time periods. This can be seen by comparing a simulated wind record, Figure 5a and 5b with an actual wind record, Figure 6, for a period of only one minute. [The actual wind record does not deviate from a one minute mean nearly as much as the simulated model. This is due to the fact that the model assumes independence]

Merchant's model is a random process model which is more suitable in wind modeling. Merchant assumed that the gusts are normally distributed about the mean to generate his model. However, he defined his variance in a different manner than did Davenport. [Merchant defined the variance of a number of impulses which when added together for a specific time, t, would give the total variance of $X(t)$] The variance of $X(t)$ as
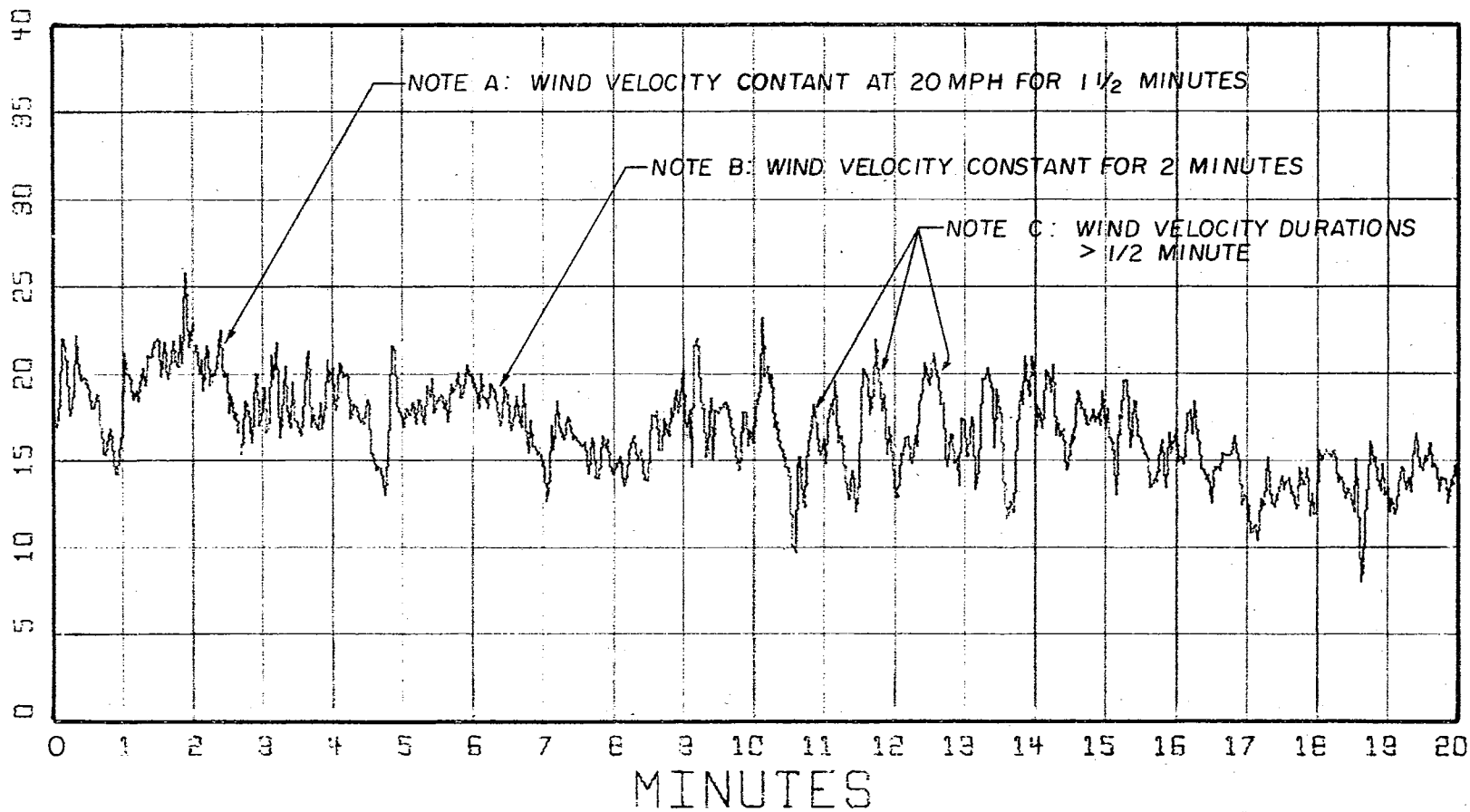
Figure 3. Twenty Minute Actual Wind Record, One Sample Every Two Seconds, Velocity Average = 16.54 MPH
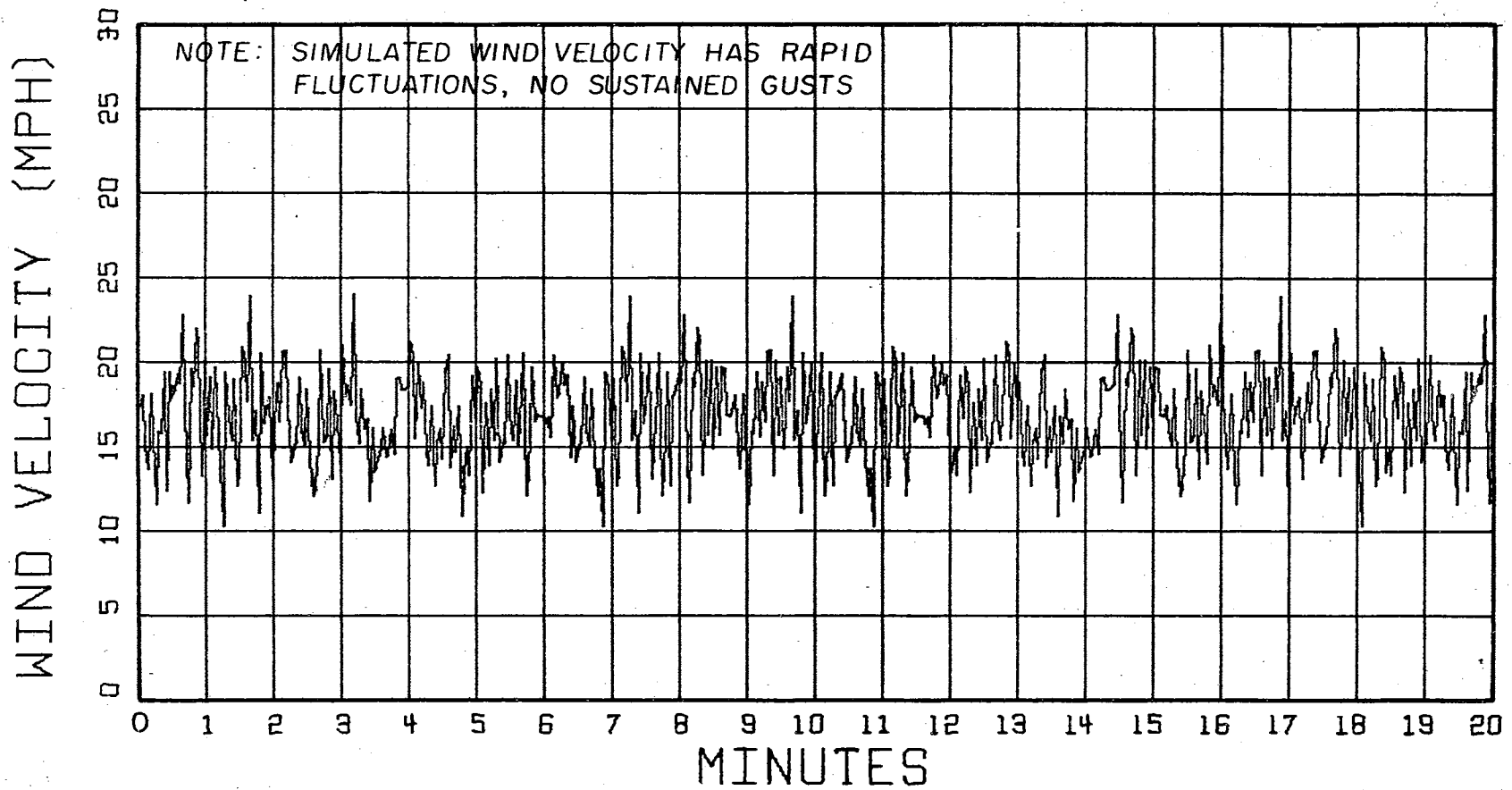
Figure 4. Twenty Minute Simulated Wind Record Using Davenport's Model, 200 Samples, Velocity
Average = 16.50 MPH
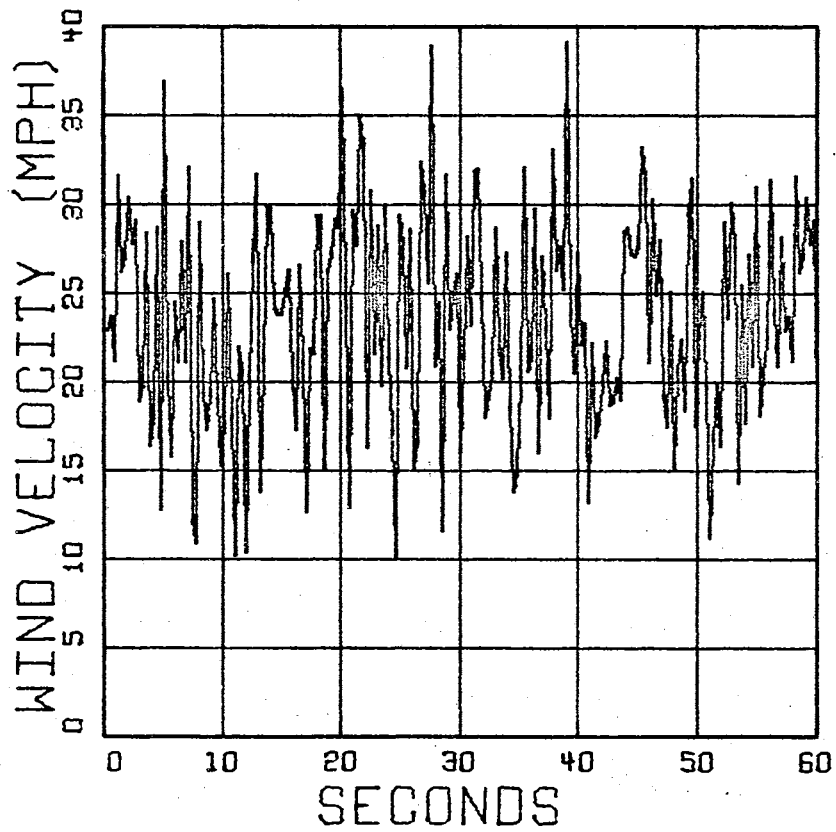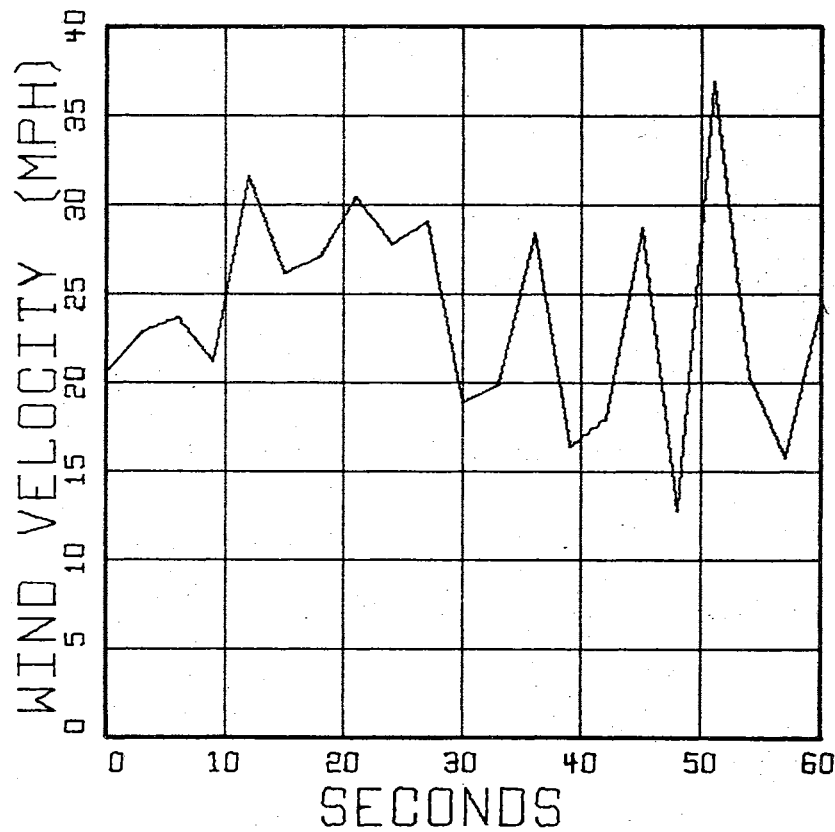
(a) 200 SAMPLES   (b) 20 SAMPLES

Figure 5.   One Minute Simulation of Horizontal Wind Using Davenport's Model, Velocity
Average = 27.2 MPH
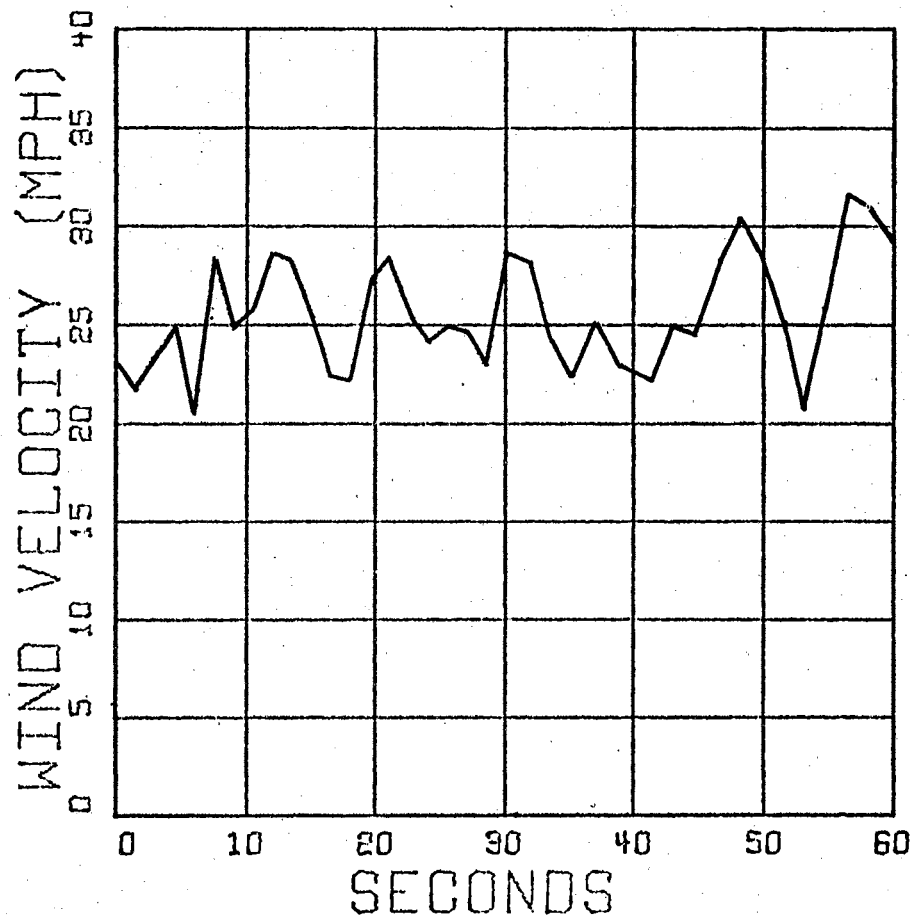
Figure 6. One Minute Actual Wind Record, Two Second
         Samples of Horizontal Wind, Velocity
         Average = 28.0 MPH

determined by Merchant [describes the variance of the gusts as did σ^2

defined by Davenport]

In addition to assuming the magnitudes of the impulses to be

normally distributed, Merchant considered the varying durations of the

gusts. He described his model in such a way that the impulses occurred

randomly according to an [exponential distribution and each impulse had a

width defined by a second exponential distribution]. For a given time t,

there are many impulses that sum together to yield X(t). The impulses

occur at different times T_i and last for different durations D_i. The
impulse function was given analytically as follows:

$$w(t,T,y,D) = \begin{cases} 0 & \text{for } t \leq T \\ y & \text{for } T < t < T + D \\ 0 & \text{for } t \geq T + D \end{cases} \qquad (2.7)$$

where

  y = the magnitude of the impulse.

He expressed his model for the gusts mathematically as a filtered
Poisson process in which occurrences of impulses were Poisson events.
The value of the gust at time t is:

$$X(t) = \sum_{m=1}^{N(t)} w(t,T_m,y_m,D_m) \qquad (2.8)$$

where

  X(t) = the gust velocity at time t;

  N(t) = the Poisson counting process which counts gusts occurring at
    some mean rate;

  w(t) = a function of three real variables known as the impulse
    function;

  T_m = the time of occurrence of the impulses (exponentially distrib-
    uted);

  y_m = the velocity magnitude of the impulse; and

  D_m = the time duration of the impulse (exponentially distributed).

Figure 7 is a reproduction from Merchant's work which shows the
results of his simulation for one anemometer trace. Part (a) is an
actual high speed trace, Part (b) is the square wave approximation to
Part (a), and Part (c) is a simulated sample function of the stochastic
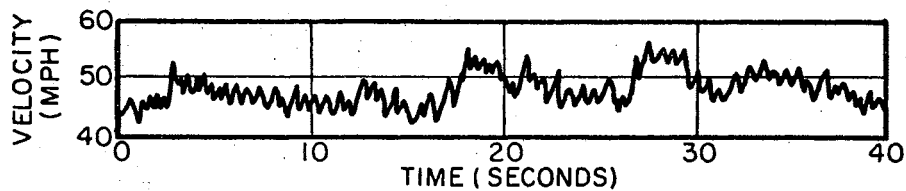
(a) ACTUAL HIGH-SPEED ANEMOMETER TRACE
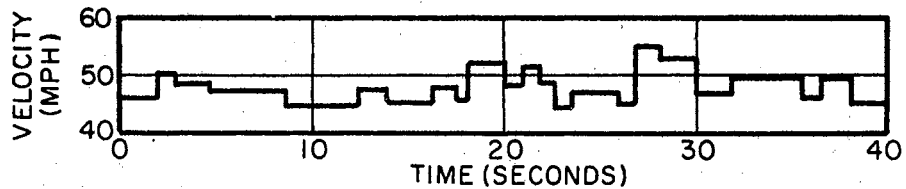
(b) SQUARE-WAVE APPROXIMATION OF ANEMO-
METER TRACE
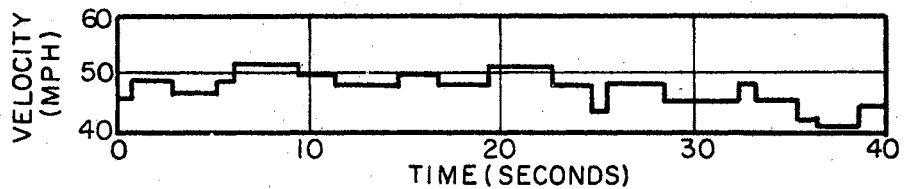
(c) SIMULATED SAMPLE FUNCTION OF THE
STOCHASTIC MODEL

Figure 7. Wind Velocity Recordings Reproduced From
Merchant's Study

model. He manually summed the impulses to obtain trace (c).

The variance associated with this model is obtained from the

following equation:

$$\text{Var}\left[X(t)\right] = \frac{\gamma \sigma_i^2}{\lambda} \qquad (2.9)$$

where

$\lambda = 0.000536 V_0,$

$\gamma = 0.012V_0$, and

$\sigma_i = 0.49K'V_0^2$,

are all parameters of the impulse $w(t,T,y,D)$. Using these parameters to derive an expression for the variance as a function of only K' and V_0, yields

$$\text{Var}\left[X(t)\right] = 10.92K'V_0^2 \qquad\qquad (2.10)$$

which is about 1.8 times larger than the variance obtained by using Davenport's model. The variances calculated from the two models are not the same because one model is a [random variable model while the other is a random process model].

Although Merchant's model considers the characteristics of the wind in a more detailed manner than Davenport, his model is much more complicated and more difficult to generate and to use. Either model can be used to simulate the wind for specific applications to wind loading on structures. However, a more suitable model for applications to wind energy conversion is desirable. A model which simulates the wind better than Davenport's model and which can be obtained in an easier manner should be sought.

CHAPTER III

SIMULATION MODEL OF THE WIND

A suitable computer simulation model of the horizontal wind velocity within a one-hour period would be useful to a designer of the mechanical to electrical energy conversion equipment, i.e. the propeller and generator subsystem. The designer could use the computer simulation of the magnitudes of the velocity to simulate the effects of the input wind variations on the mechanical system while varying such parameters as: the size of the generator; the size, pitch, number, and dimensions of the blades; the total inertia of the system; the load; etc. Since the computer simulation would be useful in the design and since Davenport's and Merchant's models both have shortcomings for this application, a new computer simulation model was generated.

The model developed in this chapter takes into account the variable durations of the gusts while keeping the mechanics of simulation relatively simple. The developed model incorporates ideas from both Merchant and Davenport. That is, [the durations of the gusts were assumed to be exponentially distributed] and the [magnitudes of the gusts were assumed to be normally distributed with a zero mean and a variance defined by Equation 2.6] This model has an advantage over Davenport's model because it considers the varying durations and it has an advantage over Merchant's model because it simulates the experimental data satisfactorily while using a less complicated simulation technique.

This simulation model generates the magnitude of the wind velocity values with magnitudes as defined by Davenport. [The velocity values are then delayed for 1, 2, 3, 4, and 5 time periods in a random manner. Then, by linear extrapolation, velocity magnitudes in between the delayed velocity magnitudes are determined] That is, the simulated wind record is made up of equal spaced discrete velocity magnitudes some of which are determined from the generated normally distributed numbers and some of which are the velocity magnitudes within the delay interval. By delaying the velocity values and by including additional velocity values, the resulting discrete values tend to give the effect of sustaining the wind speed for one, two, or three minutes.

Verification of the quality of the model, i.e. how well the model simulates the actual wind, was accomplished by calculating the actual power from wind velocity records and by calculating the estimated power from the simulated record then comparing the results of the two.

Development of Model

The simulation of the discrete wind velocities was accomplished in the following manner:

1. Normally distributed random variables, $Y(I)$, with a zero mean and a variance of one were generated using a standard library program for the IBM 7040 computer. Reference: Random Normal Number Generator, OSU-0170.

2. Exponentially distributed random variables were generated by a method based on the probability integral transformation as presented by Parzen (21). See Appendix B of this dissertation for details of this procedure.

3. The variance of the fluctuations was calculated using Equation
    2.6 with $K' = 0.005$ and V_0 = average wind velocity of actual
    wind traces over a period of one hour. K' was selected as
    0.005 because the terrain where data were taken was open
    terrain, see Table II.

4. The magnitudes of the gusts were calculated using the equation

    $$X(t) = \sqrt{\sigma^2} \; Y(t) \tag{3.1}$$

    where

    $X(t)$ = magnitude of the gusts, normal random variables with
    mean 0 and variance σ^2;

    σ^2 = variance as defined in step 3;

    $Y(t)$ = the standard normally distributed random variables;

    t = an integer.

    This resulted in the gusts being normally distributed with a
    zero mean and with a variance of σ^2.

5. The magnitudes of the simulated discrete wind speeds at each
    time, t, were then found using Equation 3.2.

    $$V(t) = V_0 + X(t) \tag{3.2}$$

6. A typical wind record has gusts that vary about the average
    velocity and these gusts [last for different intervals of time]
    [The length of the random durations can be simulated by the
    exponential distribution] Therefore the varying durations for
    the gusts were simulated by letting the exponentially distriub-
    uted random number determine the time (Δt) between successive
    occurrences of the discrete magnitudes obtained in step 5. That

is, if a generated exponential number z was such that:

$$0 < z \le 0.5 \qquad \text{then} \qquad \Delta t = 1$$

$$0.5 < z \le 1.5 \qquad \qquad \Delta t = 2$$

$$1.5 < z \le 2.5 \qquad \qquad \Delta t = 3$$

$$2.5 < z \le 3.5 \qquad \qquad \Delta t = 4$$

$$3.5 < z \qquad \qquad \Delta t = 5 \quad .$$

Figure 8 is presented to further describe the procedure. The figure depicts a partial simulation using eight discrete generated velocity magnitudes; $V(t)$, $V(t + 1)$, ..., $V(t + 7)$. These magnitudes are delayed for four, two, one, one, five, and two time periods respectively. By connecting these discrete generated magnitudes with straight lines, a good simulation of the horizontal wind speed at least by visual comparison with actual wind records is obtained.

The values in between the generated magnitudes are next obtained by linear extrapolation thus yielding equally spaced velocity samples to simulate the horizontal wind. The curve in Figure 8 therefore is made up of seventeen equally spaced samples and it was generated by using only eight normally distributed random numbers.

Results of Simulation

Figure 9a was generated by the above simulation for a one hour interval. Comparison of this simulation with an actual trace of the horizontal wind reveals that the simulation does not simulate the high frequency components of the wind. However, if one neglects the high frequency variations in the actual trace, the two curves compare quite well. The simulated curve has peaks and dips that have durations lasting
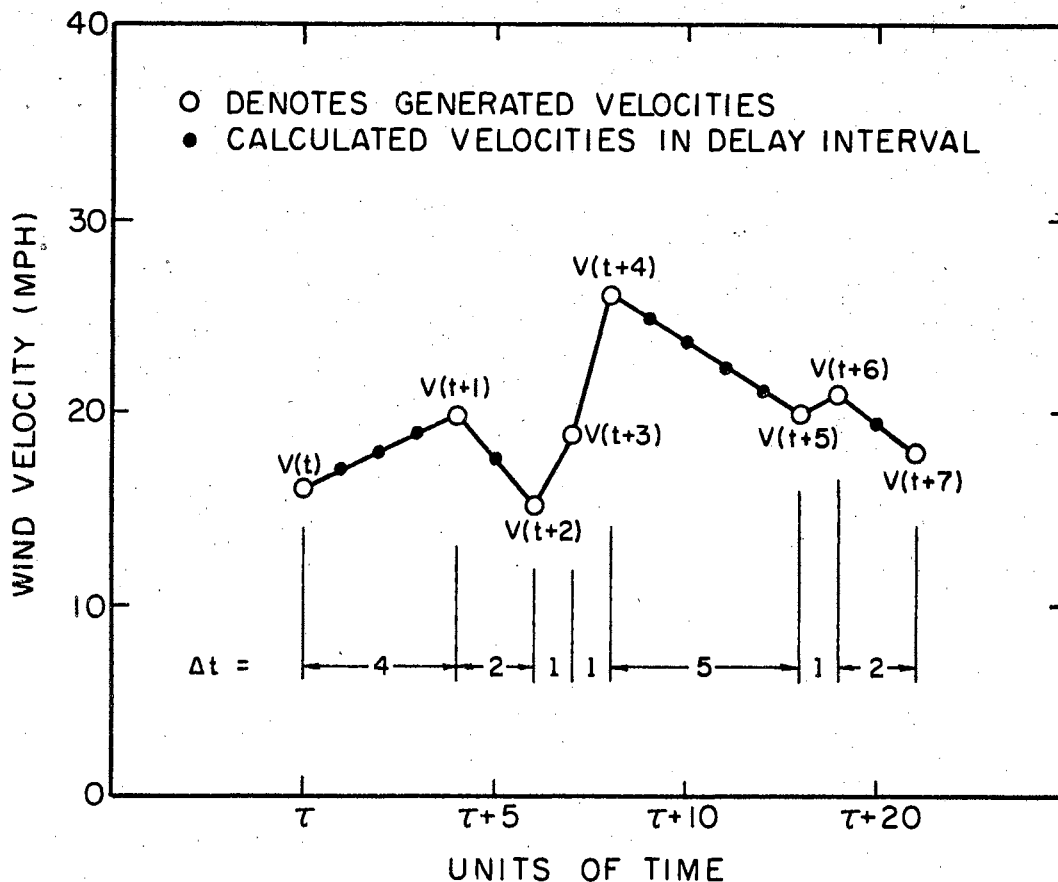
Figure 8. Partial Simulation of Wind Velocity Showing Delays
Between Generated Velocity Values

for periods of one, two and three minutes as does the actual trace. Also

there appears to be one minute peaks which compare with the one minute

peaks of the actual anemometer trace shown in Figure 9b. The high fre-

quency components can be ignored in the simulation of the horizontal wind

for wind power applications because of the size of the wind power system.

The wind power systems are too large to allow the system to follow the

high frequency variations. A good visual comparison between the actual

and simulated traces exists if the high frequency variations are ignored

in the actual trace.
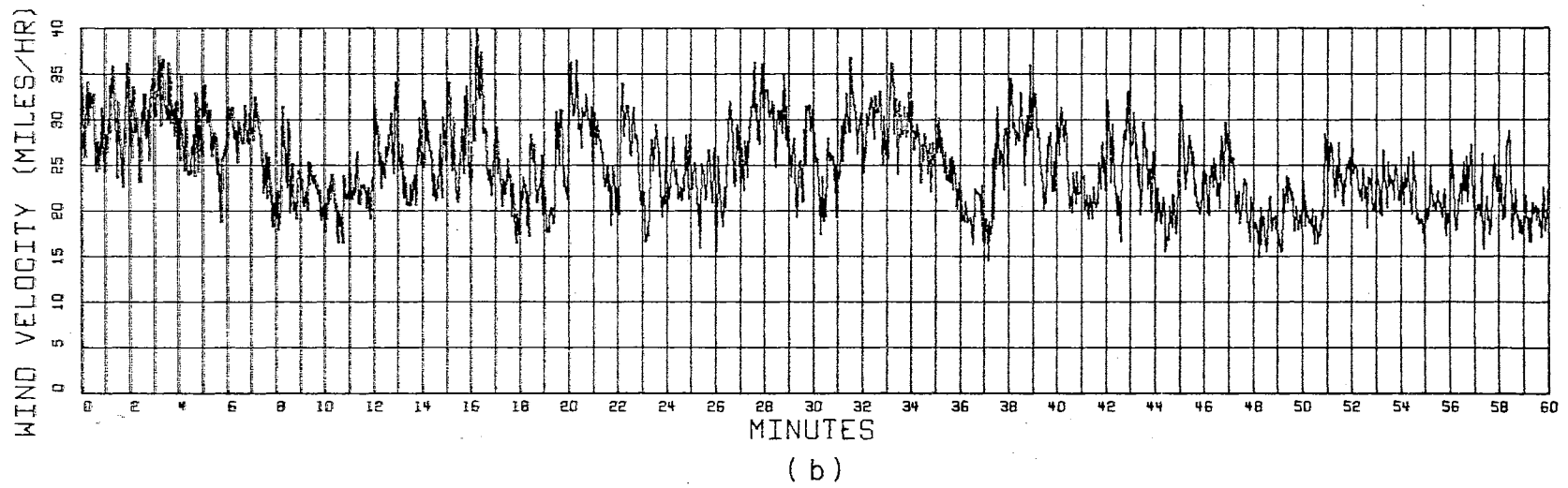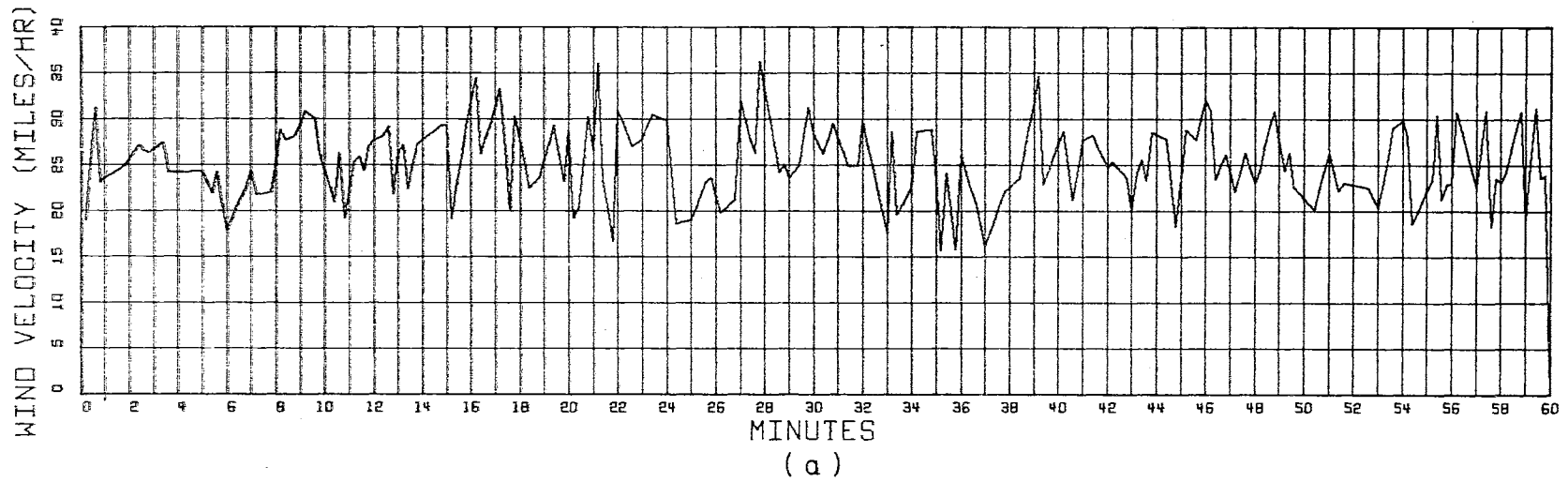
Figure 9. Horizontal Wind Velocity (a) Simulated Wind Velocity, Average Velocity Equal to 25.0 MPH
(b) Actual Anemometer Trace, Average Velocity Equal to 24.94 MPH

A visual comparison with actual data is not sufficient, therefore a comparison of extractable power was made. That is, in an attempt to determine if the model could be used to adequately simulate the wind a number of actual wind velocity records were obtained by sampling at a rate of one sample every two seconds. The theoretical extractable power was then calculated and the results of the calculations were compared to similar calculations using the simulated wind velocity. Comparison of the results revealed that the extractable power can be estimated quite well if one uses 120 or more sample velocities during the hour and if the spacings between the generated samples are exponentially distributed. Table III summarizes the results obtained for these comparisons. For each known average velocity in column two, discrete velocity samples were generated. The number of samples was varied in each comparison in an attempt to determine how many samples would be required for the simulation. Once the discrete samples were obtained, the estimated power for each sample was calculated using Equation 2.3 with the area calculated for a six foot diameter propeller. This estimated power was then compared with the actual power calculated using the actual two second samples of the wind velocity over the hour.

As can be seen from the table, if 25 or 50 samples are used, the estimated power and actual power vary widely. However, if 200 or 250 samples are used, the estimated power is quite close to the actual power.

Sufficient simulations were obtained in order to determine the maximum percentage errors using various numbers of samples. The maximum percentage error between the estimated power and the actual power was essentially unchanged when using five or more simulations. Table IV is a summary of the maximum percentage error between the estimated power

TABLE III

SUMMARY OF HORIZONTAL WIND SIMULATIONS

Date	Average Velocity of Data	Variance of Data	Variance of Model	Number of Samples	Actual Power Watts	#1 Est. Power Watts	#2 Est. Power Watts	#3 Est. Power Watts	#4 Est. Power Watts	#5 Est. Power Watts	#6 Est. Power Watts	#7 Est. Power Watts	#8 Est. Power Watts	#9 Est. Power Watts
30 Apr.	16.53	9.2	8.21	25	498	486	509	495	488	481	504	480	475	473
				50		479	519	495	503	503	495	501	494	519
				100		481	505	501	498	491	496	511	499	498
				120		---	---	---	498	493	501	519	498	502
				150		487	508	506	501	504	499	513	503	498
				200		480	502	501	504	504	497	506	501	496
				250		479	501	501	502	502	498	505	501	499
				300		478	497	500	---	---	---	---	---	---
2 May	13.95	6.1	5.84	25	307	293	306	297	293	289	303	289	285	284
				50		287	312	298	302	302	298	301	297	312
				100		289	304	301	299	295	298	307	300	299
				120		---	---	---	299	296	301	312	299	302
				150		293	306	304	301	303	300	308	303	299
				200		288	302	301	303	303	299	304	301	297
				250		288	301	301	302	301	300	304	301	300
				300		287	309	301	---	---	---	---	---	---
14 May	13.02	7.00	5.09	25	250	237	249	242	239	235	246	235	232	231
				50		234	253	242	245	245	241	245	242	254
				100		235	247	245	243	240	243	250	244	244
				120		---	---	---	243	241	245	254	243	246
				150		238	248	247	245	246	244	251	246	243
				200		235	245	248	246	246	243	247	245	242
				250		234	245	245	245	245	244	247	245	244
				300		234	245	245	---	---	---	---	---	---
24 May	24.94	20.49	18.66	25	1705	1672	1751	1700	1678	1652	1733	1652	1632	1625
				50		1644	1783	1701	1726	1726	1700	1719	1698	1783
				100		1652	1735	1721	1710	1688	1705	1756	1715	1711
				120		----	----	----	1711	1692	1719	1784	1710	1727
				150		1674	1746	1736	1721	1731	1715	1762	1729	1711
				200		1650	1725	1720	1732	1732	1708	1737	1722	1702
				250		1647	1721	1720	1725	1723	1712	1736	1720	1716
				300		1643	1708	1719	----	----	----	----	----	----
28 May	14.94	8.80	6.69	25	370	359	376	365	361	355	372	355	351	349
				50		353	383	366	371	371	365	370	365	383
				100		355	373	370	368	363	366	378	369	368
				120		---	---	---	368	364	370	383	368	371
				150		359	375	373	370	372	369	378	372	368
				200		354	371	370	372	372	367	373	370	366
				250		354	370	370	371	370	368	373	370	369
				300		353	367	369	---	---	---	---	---	---
30 May	15.77	9.70	7.46	25	439	422	442	430	424	417	438	418	413	411
				50		416	450	430	436	437	430	435	429	451
				100		418	439	435	432	427	431	444	433	432
				120		---	---	---	432	428	435	451	432	437
				150		423	441	439	435	438	434	445	437	433
				200		417	436	435	438	438	432	439	435	430
				250		416	435	434	436	436	433	439	435	434
				300		415	432	435	---	---	---	---	---	---
2 June	19.07	10.01	10.90	25	750	---	---	---	751	739	775	738	730	726
				50		---	---	---	772	772	760	769	759	797
				100		---	---	---	765	754	762	785	767	765
				120		---	---	---	765	756	769	770	764	772
				150		---	---	---	774	773	767	788	772	765
				200		---	---	---	771	774	764	777	770	760
				250		---	---	---	771	770	766	776	769	767

and the actual power for various numbers of samples. As the number of samples increases to 300, the actual power is estimated more accurately. The average maximum percentage error varies from 5.81 per cent error for 25 samples to 1.33 per cent error for 300 samples. The selection of the number of samples would probably be best somewhere above 100 samples.

TABLE IV

MAXIMUM PERCENTAGE ERROR OF ESTIMATED POWER VS. ACTUAL POWER

Velocity	Samples							
	25	50	100	120	150	200	250	300
16.53	3.41	4.20	1.17	1.00	1.20	1.20	0.81	0.41
13.95	5.86	6.50	2.93	3.58	1.96	1.96	1.96	2.60
13.02	6.00	6.40	2.80	3.60	2.00	2.00	2.00	2.00
29.94	5.98	4.57	1.76	0.76	2.40	1.17	1.17	0.82
14.94	8.60	4.60	1.89	1.08	1.35	0.54	0.27	0.81
15.77	9.40	5.25	2.74	2.50	0.81	2.50	1.11	1.34
19.07	1.47	2.93	2.00	2.00	3.20	3.20	2.80	----
Totals	40.72	34.45	15.29	14.52	12.92	12.57	10.12	7.98
Av. % Error	5.81	4.92	2.18	2.08	1.85	1.80	1.45	1.33

Since the actual extractable power and the estimated extractable power are sufficiently close, the model appears to be suitable for simulating the horizontal wind. Therefore the designer of the energy conversion equipment can use the model to simulate the effects of the input

wind variation on the mechanical system while varying the system param-

eters.

The input velocity for the model can be varied to allow simulation

of horizontal wind velocities for any desired wind velocity. Also, one-

minute hourly averages can be used as an input for the model to obtain

simulations for more than one hour. Figure 10 is a 24 hour simulation

using one-minute averages as an input to the model. From the figure,

one can see that as the input velocity increases the deviations about

the input become larger. This is also true in actual wind traces.
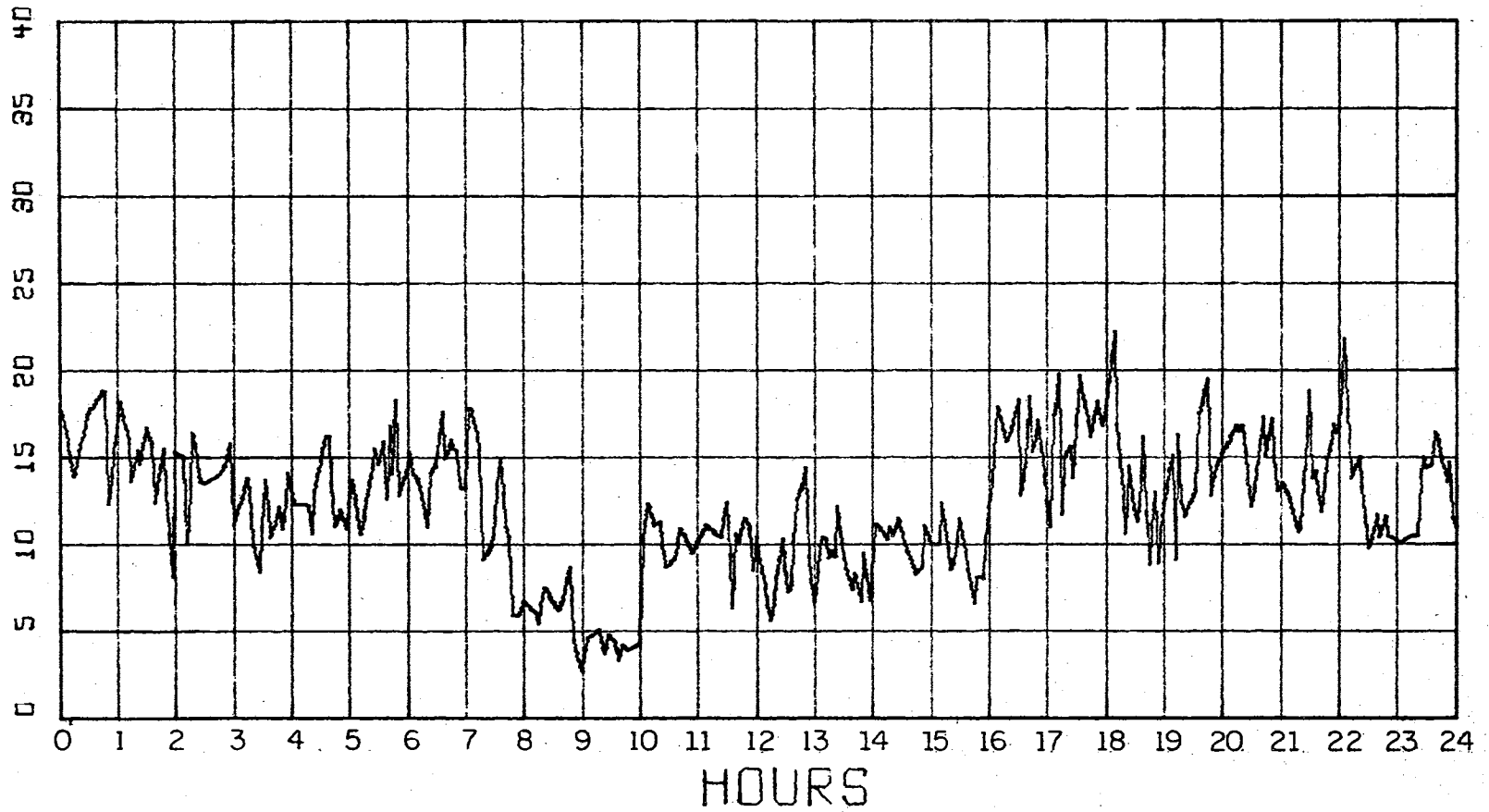
Figure 10. 24-Hour Simulation of Horizontal Wind Velocity Using One-Minute Hourly Averages as Input for the Model

CHAPTER IV

SPECTRUM ANALYSIS OF THE HORIZONTAL WIND

The conventional forms of energy have either been stored for many

years in natural storage deposits such as coal and oil deposits or they

have been stored for only a few years in man-made storage facilities

such as water reservoirs. In either case, the energy is available when

needed because of the storage. The size of the man-made storage facility

is determined by many factors. The size of water reservoirs for example

is related to the supply of rainfall, to the demand for energy, to the

cost per unit of energy, etc. Some of these factors require the reser-

voir to be built as large as possible while others require the size to

be limited. The designer of the reservoirs had to have a knowledge of

the cyclical nature, the maximum yields, and the minimum yields of the

supply in order to optimize their designs.

As in the storage of conventional forms of energy, the size of the

storage for unconventional energy sources is related to the variable

nature of the input. Information about the cyclical nature of the wind,

the maximum winds, the minimum winds, and etc. should be known. Past

research in wind energy systems has not included detailed analysis of

the cyclical nature of the input wind velocity. Researchers used the

seasonal variations of the wind to provide only a gross indication of

the extractable energy for a given location. This gross indication of

seasonal variations was probably sufficient because suitable storage was

not available. However, if a more suitable storage device such as a rechargeable fuel cell is available, it is profitable to provide design information through the analysis of the frequency content of the energy in wind. This would be desirable to optimize the size of the energy storage system and the size of the energy conversion system. This can be accomplished by estimating the spectrum of the wind.

The spectrum determines the density of the square of a variable over different frequency ranges or periods. In this case, the horizontal wind velocity is the variable. Where the wind velocity is the variable, the variance is proportional to the kinetic energy of the fluctuations (30). The spectrum can be estimated by either of two methods. The first uses a lagged products procedure recommended by Tukey (22) to obtain a weighted spectrum and the second uses a Fast Fourier Transform algorithm. Either method yeilds a suitable estimate of the spectrum. Both methods require the basic characteristics of the times series of the horizontal wind velocity to remain essentially constant, i.e. the continuous time series of the horizontal wind velocity should be stationary.

The wind velocity does not meet this requirement entirely but it does meet it if the time series representing the horizontal wind velocity is subdivided into shorter time series that can be considered as stationary. One can analyze the time series of the wind velocity by finding the spectrum of sub-time series with characteristics which are considered essentially constant. That is, the horizontal wind is considered to be made up of a number of shorter duration series which are stationary. R. H. Jones (23) showed that the meteorological time series consisting of periodic components such as annual variations and random components that are deviations from the annual can be analyzed by piecing together

various portions of the spectrum. Snyder (24) also verified that spectrum analysis techniques could be used on time series that are not entirely stationary. He generalized the notion of a stationary random function to include random functions whose statistical properties vary slowly with time, i.e. Quasi-Stationary time series. His paper provides a justification and clarification of the procedure for dividing Quasi-Stationary time series into many sub-series to obtain the spectrum.

Since the wind velocity fits into the above category, a number of partial spectra will be calculated by one of the two methods stated earlier and then will be combined to obtain the complete spectrum of the horizontal wind.

Errors in Spectrum Estimates

Before estimating the complete spectrum, sources of errors in the spectrum analysis techniques must be considered. There are two major sources of error. The first source of error is due to the data being averaged and the second source of error is related to problems caused by aliasing. The averaging process reduces the spectral intensity at a given frequency and aliasing removes energy from high frequencies and makes it appear at lower frequencies.

The piecing together of the various parts of the spectrum necessarily dictates that some sort of averaging is performed. For example, the 24 hour averages, $Y_{24}(t)$, used to obtain one part of the spectrum are obtained by averaging the one-minute hourly measurements. When these measurements are averaged, the resultant time series is devoid of high frequencies. Therefore, averaging acts like a filter which eliminates the high frequencies from the record. The errors in the spectral estimate

can be eliminated by multiplying the spectral estimate by a factor of the form $(Sin\pi\omega\frac{T}{2}/\pi\omega\frac{T}{2})^2$. For example if

$$Y_{24}(t) = \frac{X(t) + X(t + 1) + \cdots + X(t + 24)}{24} \qquad (4.1)$$

where

$Y_{24}(t)$ = arithmetic mean averaged over period T = 24 hours, and

X(t) = measurement at time t, t measured in hours,

then the spectrum estimate as a function of frequency (ω) will be:

$$S_{Y_{24}}(\omega) = S_X(\omega) \cdot \left[\frac{Sin\pi\omega\frac{T}{2}}{\pi\omega\frac{T}{2}}\right]^2 \qquad (4.2)$$

where

$S_X(\omega)$ = spectrum of X(t);

$S_{Y_{24}}(\omega)$ = spectrum of $Y_{24}(t)$; and

T = period used to obtain the average.

It is clear that $S_X(\omega)$ the spectrum of X can be derived from the estimated spectrum of $Y_{24}(t)$ with the aid of Equation 4.2.

Aliasing is a source of error which occurs as a result of digitizing or converting continuous data into discrete numbers. If the sampled values are separated too far apart, the sampled values could represent either low or high frequencies in the original data. Figure 11 presented by Griffith, et al. (25) indicates how the sampling introduces fictitious frequencies. The solid curve with a period of two days represents the time series to be sampled and analyzed. With the readings taken every three days, e.g. at points A, B, C, and D, a fictitious oscillation occurs. The dotted line connecting the points results in a curve with a period of six days. The original record contained no cycle of this
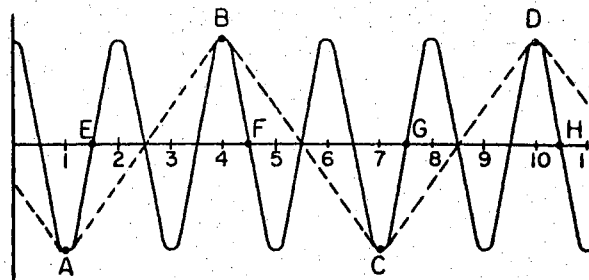
Figure 11. Production of
"Aliasing"

period. If sampling had occurred at points E, F, G, and H, no fictitious

oscillation would appear. Therefore aliasing is greatly influenced by

the sampling. To show how the spectrum is altered by the effects of

aliasing Figures 12 and 13 were reproduced from Bendat and Piersol (26)

and Lumly and Panofsky (27) respectively. The axes were relabeled for

consistency in this report. The cutoff frequency, ω_c, known as the

Nyquist or folding frequency, is the frequency above which frequencies

will be folded back.
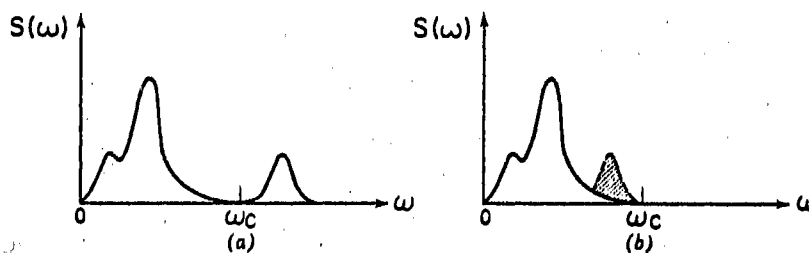
Figure 12. Aliased Power Spectra Due to Folding
(a) True Spectra (b) Aliased Spectra
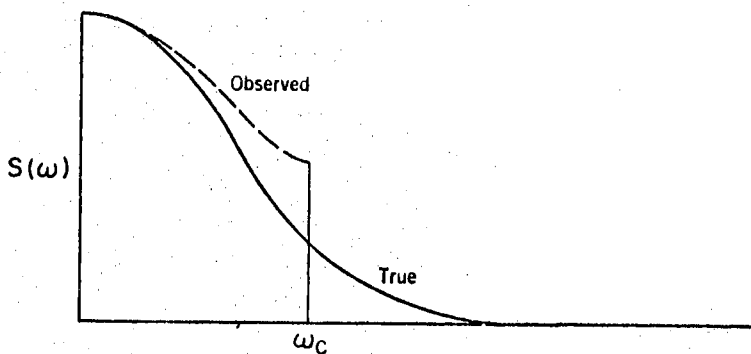
Figure 13. A Spectral Estimate Showing the
Characteristic Effect of
Aliasing, ω_c is the Nyquist
Frequency

Once the major sources of error are known, the estimated spectrum

for the various parts of the spectrum can be obtained and modified to

eliminate the effects of averaging and aliasing to obtain the true

spectrum.

Procedure for Obtaining the Spectrum

The horizontal wind velocity spectrum was estimated by obtaining

spectral estimates for seven different frequency ranges. This resulted

in a total spectrum estimate in a frequency range from 0.0007 to 900

cycles/hour. The estimates were obtained by using Tukey's (22) lagged

products method. This method was chosen over the Fast Fourier Transform

algorithm because it was more suitable for the number of sample observa-

tions and the number of lag products used. Gentleman and Sande (28)

indicated that for lags less than 75 and for samples up to 8000 that the

lagged products method was more practical. Tukey's procedure uses N

observations to calculate autocorrelation coefficients with lags of 0 to

m. Next the m + 1 coefficients are subjected to a cosine transform. The transformed values are then smoothed using a three-term moving average. The smoothed m + 1 terms form estimates of the spectrum.

No one set of computing formulas is prescribed for calculating the spectrum. Tukey (22) presented one set in his paper and he along with Blackman (29) presented another set. Other sets of computing formulas have also been presented; however, those originally given by Tukey were arbitrarily chosen to obtain the various parts of the spectrum in this study. N observations were used to calculate autocorrelation coefficients with lags of 0 to m. The coefficients were then transformed to obtain the apparent power at the m + 1 frequencies. The transformations were then smoothed by a three-term moving average with weights of 0.23, 0.54, and 0.23, to obtain the estimate of the power spectrum at the m + 1 frequencies. This three-term moving average is called Hamming (after R. W. Hamming). The m + 1 spectral estimates occur at frequencies determined by:

$$f_r = \frac{r}{2m\Delta t} \qquad (4.3)$$

where

  $r = 0, 1, 2, \ldots, m$ is the lag number;

  m = number of lags; and

  Δt = sampling interval.

The choice of m determines the frequency resolution of the spectrum. For good frequency resolution, m should be selected as large as possible. However, for economic reasons, to keep the number of calculations to a reasonable minimum, the size of m should be chosen as small as possible. A scheme was devised by Griffith et al. (25) to obtain good resolution

but still keep m small. The scheme used was to estimate different parts of the spectrum separately then piece them together later.

To understand better the choice of m, the following example is presented from Griffith's paper. Let N = 1000 be the number of observations, let m = 6, and let the time between equally spaced data be one day, then the spectrum estimates occur at frequencies: zero cycles/day, 1/12 cycles/day, 2/12 cycles/day, ..., 6/12 cycles as found by using Equation 4.3. The first spectrum estimate at frequency, f_0, applies to a frequency of zero cycles/day, the second spectrum estimate plotted at 1/12 cycles/day measures the average estimate of the spectrum from 0 to 1/6 cycles/day even though the entire spectral estimate is plotted at 1/12 cycles/day. The third spectral estimate will appear at a frequency of 2/12 cycles/day and so forth up to 6/12 cycles/day. Since the second estimate measures the average estimate from 0 to 1/6 cycles/day, all the variations of velocities with periods larger than six days have been lumped into a single estimate at 1/12 cycles/day. If estimates are desired with periods greater than six days, say two months or 50 days, m would have to be increased to about 60 or larger. With m = 60 the amount of computation becomes excessive and the high frequency resolution is greater than is actually needed. To avoid choosing m so large, different samples are used to obtain the spectrum. Good resolution for periods between two and 10 days is obtained by choosing the number of lags to be 10 and choosing the sample period Δt of five days. That is, Δt is five day non-overlapping averages.

The number of lags selected to estimate the various parts of the spectrum in this study ranged from m = 6 to m = 30. The lower number being used when the number of observations were limited. In all cases

however, the number of lags were less than one-tenth of the sample size. Bendat and Piersol (26) recommend that m be less than one-tenth of the sample size to avoid instabilities in the estimates. Choosing m equal to one-tenth of the number of observations can result in the spectral estimate differing from the actual spectrum by an amount of 0.316 as determined by the normalized standard error in Equation 4.4.

The normalized standard error equation is

$$\varepsilon = \sqrt{\frac{m}{n}} \qquad (4.4)$$

where

ε = normalized standard error defined by Bendat and Piersol;

m = number of lags; and

N = number of observations.

Normally ε would be kept at about 0.10, however, errors up to 0.30 would not be extreme in many applications of the power spectrum. Many applications of the power spectrum are for gross indications of frequency content.

The equations used to obtain the spectrum are:

$$R_p = \frac{X_1 X_{p+1} + X_2 X_{p+2} + \cdots + X_{N-p} X_N}{N - p} \qquad (4.5)$$

where

R_p = autocorrelation coefficient;

p = the lag number which varies from 0 to m;

N = the number of observations; and

X = the sample value of the variable (wind velocity) minus the mean wind velocity for the time $N\Delta t$.

$$L_h = \frac{1}{2m} R_0 + R_m + \frac{1}{m} \sum_{p=1}^{m-1} R_p, \quad h = 0$$

$$L_h = \frac{1}{m} R_0 + \frac{2}{m} \sum_{p=1}^{m-1} R_p \cos \frac{ph\pi}{m} + \frac{1}{m} R_m \cos h\pi, \quad 0 < h < m \qquad \Bigg\} \quad (4.6)$$

$$L_h = \frac{1}{2m} R_0 + (-1)^m R_m + \frac{1}{m} \sum_{p=1}^{m-1} (-1)^p R_p, \quad h = m$$

where

L_h = the apparent line power at frequency h.

$$U_0 = 0.54 L_0 + 0.46 L_1$$

$$U_1 = 0.54 L_1 + 0.23(L_0 + L_2)$$

$$U_2 = 0.54 L_2 + 0.23(L_1 + L_3)$$

$$\cdot$$
$$\cdot$$
$$\cdot$$

$$U_{m-1} = 0.54 L_{m-1} + 0.23(L_{m-2} + L_m) \qquad \Bigg\} \quad (4.7)$$

$$U_m = 0.54 L_m + 0.46 L_{m-1}$$

where

U_m = the power spectrum estimate at frequency m.

The equality of the power spectrum estimates U_m is measured by the number of degrees of freedom associated with each estimate. The degrees of freedom is a measure of the number of effective frequencies associated with a Chi-square distribution (χ^2/f) and, according to Blackman and Tukey (29), the higher the degrees of freedom the greater the precision. Since the X_N's are normally or Gaussian distributed, the autocorrelation coefficients are distributed according to the Chi-square distribution

law. The degrees of freedom for the lagged products are calculated by the following equation:

$$\text{Degrees of Freedom} = \frac{2N - \frac{3m}{2}}{m} \qquad (4.8)$$

where

N = the total number of observations;

m = the number of lags.

The number of degrees of freedom for each portion of the spectrum along with the frequency range and the number of lags used are summarized in Table V.

Once the number of degrees of freedom is known, confidence limits can be calculated in order to portray the statistical significance of the major peaks and dips of the spectrum estimate. To obtain the confidence limits, recall that the spectrum is the distribution of the variance of the variable over the various frequencies. Since the spectrum estimates are distributed according to Chi-square χ^2/f (where f is the degrees of freedom as defined by Equation 4.8), the confidence limits can be calculated to obtain the 95% confidence interval for the variance σ^2. That is, since the variance is distributed Chi-squared, we can use the formula

$$\text{Pr } (\frac{nS^2}{b} < \sigma^2 < \frac{nS^2}{a}) = 0.95 \qquad (4.9)$$

where

S^2 = the sample variance;

n = the degrees of freedom;

Pr = probability; and

a and b = constants determined from probability tables.

TABLE V

DATA FOR VARIOUS PARTS OF HORIZONTAL WIND VELOCITY SPECTRUM OF FIGURE 14

Date and Time	Source of Data	Height of Anemometer	Total Time of Samples	Sample Average	N=No. of Samples	Frequency Range Cycles/Hour	No Lags	Degrees of Freedom
1 Jan., '62-6 Nov., '62	Oklahoma City	55 ft.	310 Days	5-Day	62	0.0007-0.0042	6	19
1 Jan., '62-19 July, '62	Oklahoma City	55 ft.	200 Days	1-Day	200	0.0035-0.021	6	65
1 Jan., '62-9 Feb., '62	Oklahoma City	55 ft.	40 Days	5-Hrs.	192	0.01 -0.1	10	38
1900 2100 28 May, '66-30 May, '68	Stillwater	23 ft.	50 Hrs.	30 Min.	149	0.1 -1.0	10	28
1900 2000 28 May, '66-31 May, '68	Stillwater	23 ft.	75 Hrs.	10 Min.	447	0.5 -3.0	10	87
1900 2100 28 May, '66-20 May, '68	Stillwater	23 ft.	50 Hrs.	75 Sec.	1500	0.8 -24	30	98
1200 1300 29 May 29 May	Stillwater	23 ft.	1 Hr.	2 Sec.	1800	30 -900	30	118

The constants a and b are determined from probability tables (32) to obtain the random interval $(nS^2/b, nS^2/a)$ having a probability 0.95 of including the fixed but unknown parameter σ^2.

Results of Spectrum Estimate

Results of the power spectrum estimates shown in Figure 14 were obtained by the reduction of data taken at Stillwater, Oklahoma, and Oklahoma City, Oklahoma. Two locations were used because time did not permit taking data samples for a long enough period to calculate the estimates for the one and five day averages at Stillwater.

The data for the high frequency part of the spectrum was taken from a Gill propeller anemometer mounted on a 20 foot platform located at the South end of the Stillwater Airport. See Appendix C for a description of the Gill propeller anemometer. The data for the low frequency part was taken from standard meteorological data taken at the Will Rogers International Airport in Oklahoma City. At Will Rogers the anemometer was a Bendix Friez Aerovane located 55 feet above the ground on Page Hanger No. 3. Figure 14 depicts the total spectrum of the horizontal wind velocity for heights near the ground. The legend indicates the type of samples required to generate the various parts. The frequencies at which the estimates occurred were determined using Equation 4.3. The spectrum estimates presented in the figure were modified to eliminate the effects of averaging and the last 20 per cent of each spectral estimate was excluded to reduce the effects of aliasing.

Figure 14 is plotted on a logarithmic frequency scale since the meteorological turbulence covers such a wide range of frequencies. Also according to Panofsky and McCormick (27) the area between two frequencies
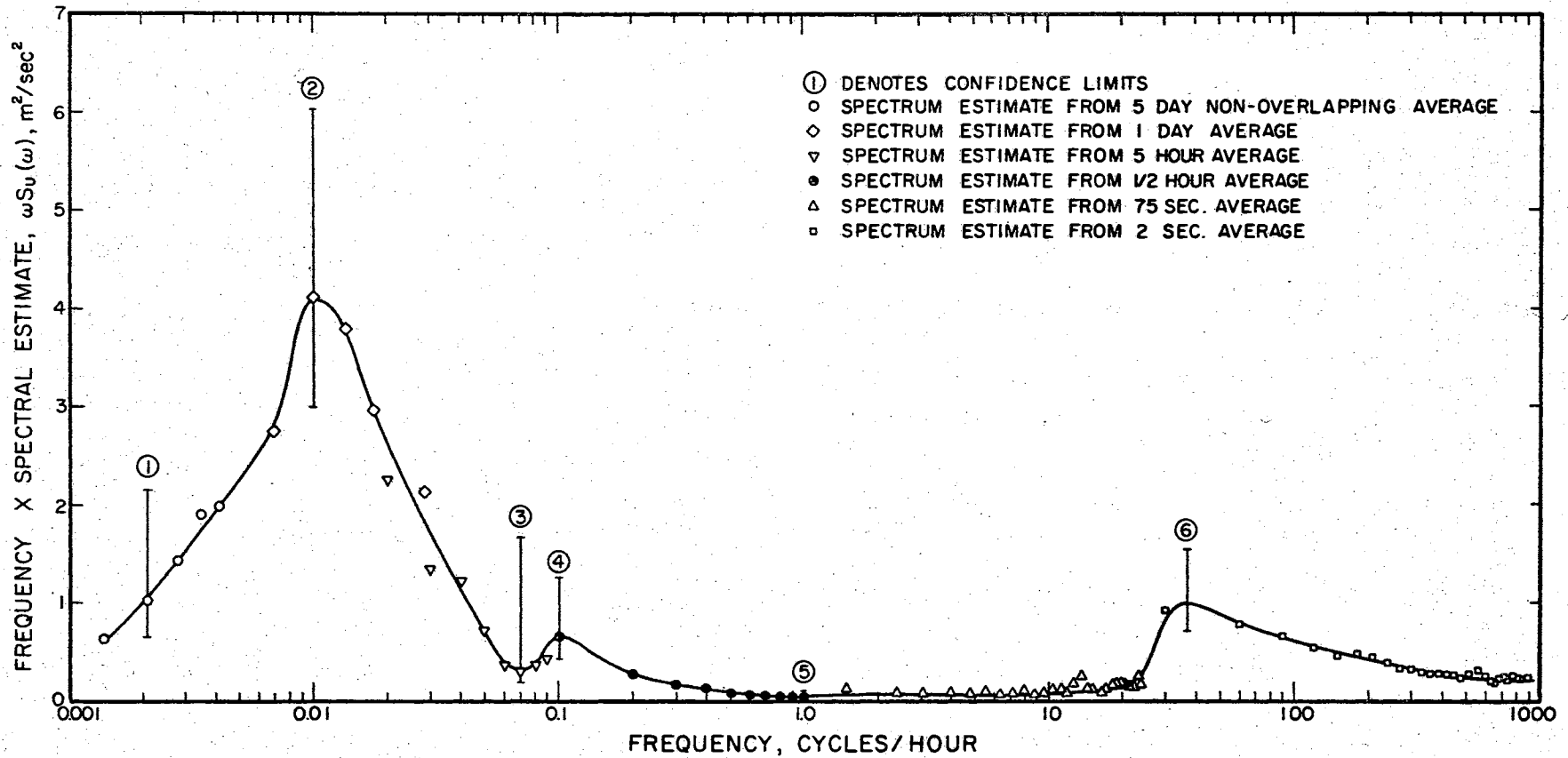
Figure 14. A Spectrum of Horizontal Wind Velocity at Heights Applicable to Wind Power Generation

under the spectral estimates represents the variance contributed in this frequency interval only if the spectral estimates are multiplied by the frequency. Therefore, the frequency times the spectral estimates are plotted along the ordinate. Each spectral estimate was multiplied by a conversion factor shown in Table VII in order to allow the complete spectrum to be plotted on the same scale.

Table VII provides a summary of the results obtained for the spectral estimates plotted on Figure 14. Table VI is a summary of the confidence limits that appear on the figure.

TABLE VI

Confidence Limits for Spectral Estimates

Confidence Limit No.[*]	Sample Var. S^2	Degrees of Freedom	a	b	Confidence Interval
1	1.0	19	8.91	32.85	(0.58,2.14)
2	4.12	65	44.3	89.2	(3.00,6.04)
3	0.3	38	22.65	56.0	(2.00,1.68)
4	0.68	28	15.31	44.46	(0.43,1.24)
5	1.0	87	63.0	104.3	(0.59,0.97)
6	1.0	58	38.2	81.0	(0.72,1.54)

[*]Corresponds to numbers on Figure 14.

Approximately 90 per cent of the area is in the frequency range 0.0007 cycles/hour to 1 cycle/hour and approximately 10 per cent is in the range 1 cycle/hour to 900 cycles/hour. This would indicate that the four day energy peak contains most of the energy in the variations of the wind velocity.

TABLE VII

SUMMARY OF RESULTS OF SPECTRUM CALCULATIONS

Spectrum Estimate No.	No. of Lags m	Sample Average ΔT	Frequency $fr=\dfrac{r}{2m\Delta T}$	Spectrum Estimates U_r	$\omega S_u(\omega)$ $\dfrac{meter^2}{sec^2}$	Degrees of Freedom $(2N-\dfrac{3m}{2})/m$	Conversion Factor
1	6	5 Days	0.000695	0.229	1.0	19	100.0
2			0.00139	0.07	0.611		
3			0.00208	0.091	1.03		
4			0.00278	0.084	1.47		
5			0.00347	0.087	1.9		
6			0.00417	0.0746	1.95		
1	6	1 Day	0.00347	0.871	1.9	65	100.0
2			0.00695	0.6328	2.76		
3			0.0104	0.636	4.15		
4			0.0139	0.435	3.8		
5			0.01735	0.253	2.98		
6			0.0208	0.162	2.12		
1	10	5 Hours	0.01	6.2	4.2	38	10.0
2			0.02	1.8	2.26		
3			0.03	0.695	1.31		
4			0.04	0.481	1.21		
5			0.05	0.224	0.712		
6			0.06	0.0958	0.361		
7			0.07	0.0725	0.319		
8			0.08	0.0766	0.386		
9			0.09	0.074	0.417		
10			0.10	0.05	0.314		
1	10	30 Min.	0.1	1.088	0.68	28	1.0
2			0.2	0.304	0.38		
3			0.3	0.109	0.205		
4			0.4	0.0669	0.168		
5			0.5	0.0428	0.134		
6			0.6	0.0254	0.096		
7			0.7	0.0159	0.070		
8			0.8	0.00932	0.068		
9			0.9	0.00986	0.051		
10			1.0	0.00876	0.055		
1	30	75 Sec.	0.8	0.199	0.101	98	0.1
2			1.6	0.132	0.1306		
3			2.4	0.0632	0.0951		
4			3.2	0.0394	0.0788		
5			4.0	0.0311	0.078		
6			4.8	0.0319	0.0957		
7			5.6	0.0258	0.0905		
8			6.4	0.0182	0.0732		
9			7.2	0.0184	0.0836		
10			8.0	0.0199	0.1002		
11			8.8	0.0167	0.0927		
12			9.6	0.0150	0.0904		
13			10.4	0.0163	0.1068		
14			11.2	0.0149	0.1052		
15			12.0	0.0131	0.0992		
16			12.8	0.0149	0.120		
17			13.6	0.0148	0.126		
18			14.4	0.0122	0.110		
19			15.2	0.0113	0.1084		
20			16.0	0.00959	0.0964		
21			16.8	0.00856	0.0904		
22			17.6	0.00939	0.104		
23			18.4	0.01006	0.116		
24			19.2	0.00885	0.117		
25			20.0	0.00926	0.1165		
26			20.8	0.00901	0.118		
27			21.6	0.00798	0.108		
28			22.4	0.00778	0.1095		
29			23.2	0.00851	0.1245		
30			24.0	0.00765	0.1156		
1	30	2 Sec.	30	0.427	0.918	118	0.01
2			60	0.210	0.791		
3			90	0.118	0.668		
4			120	0.0705	0.531		
5			150	0.0477	0.448		
6			180	0.0418	0.473		
7			210	0.0336	0.443		
8			240	0.0254	0.382		
9			270	0.0189	0.322		
10			300	0.0163	0.309		
11			330	0.0144	0.298		
12			360	0.0119	0.270		
13			390	0.0110	0.270		
14			420	0.0100	0.264		
15			450	0.00877	0.248		
16			480	0.00724	0.218		
17			510	0.00684	0.2185		
18			540	0.00838	0.284		
19			570	0.00860	0.308		
20			600	0.00703	0.265		
21			630	0.00517	0.205		
22			660	0.00468	0.189		
23			690	0.00510	0.221		
24			720	0.00530	0.239		
25			750	0.00491	0.231		
26			780	0.00506	0.248		
27			810	0.00485	0.246		
28			840	0.00434	0.229		
29			870	0.00420	0.229		
30			900	0.00409	0.231		

Comparison With Previous Spectrum Estimates

The results of the horizontal wind velocity spectrum are comparable

with those obtained by Van der Hoven (30) in New York in 1956. Van der

Hoven used the same procedure to obtain the horizontal wind velocity

spectrum for heights of 91, 108, and 125 meters at the Brookhaven National

Laboratory, New York. His results showed peaks and valleys at the same

frequencies as appear in Figure 14. He concluded that there were two

major energy peaks, one at a period of 4 days attributed to the passage

of frontal systems and one at one minute which he attributed to mechanical

and convective type of turbulence. He concluded that the energy peak at

one minute was unusually high because he used data obtained from very

high winds during a hurricane to obtain that particular part of the spec-

trum. Figure 15 is a reproduction of Van der Hoven's results.
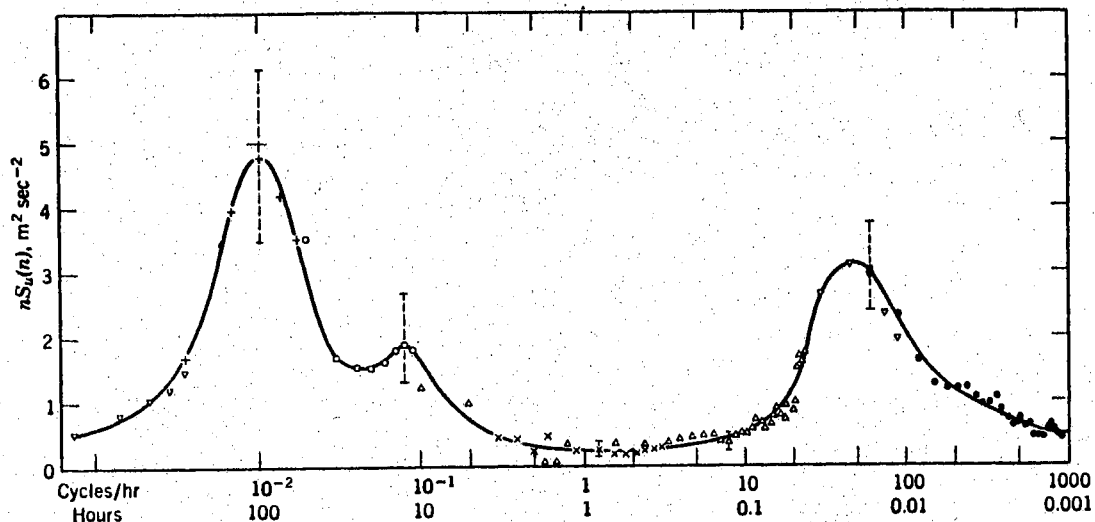
Figure 15. Schematic Spectrum of Wind Velocity Near the Ground
Estimated From a Study of Van der Hoven (1957)

Even though Van der Hoven had previously obtained the complete spectrum of the horizontal wind velocity, it was thought desirable to obtain the spectrum at heights that would be more representive of the heights that a small or medium size wind generator would operate. The spectrum estimate for Oklahoma had a major peak at 4 days as did Van der Hoven's; however the energy peak at 1 minute was not as pronounced.

Both energy peaks can be readily seen in actual wind recordings. The four day energy peak or four day cycle can be seen in Figure 16 which is a plot of the hourly wind velocities for Oklahoma City. There are definite peaks that occur at period of approximately four days. The one minute peaks can be seen in Figure 17 which represents an actual wind record for a twenty minute period using two second samples.

Importance of Spectrum to Energy Conversion

The results of the horizontal wind velocity spectrum are significant when considering energy conversion and storage systems for two reasons. First, the designer of the storage part of the system must design the storage large enough to extract the maximum amount of energy available in the four day energy peak. Second, the designer of the electro-mechanical (propeller, gears, and generator) system should attempt to optimize the design in order for the system to utilize the energy in the one-minute energy peak. As the size of the wind generator increases, less energy will be extracted from the one-minute energy peak because the increased inertia of the system would prevent the output from following the fluctuations of the input.

One additional factor about the horizontal wind which was not re-vealed in the spectrum should be considered as important. This is the
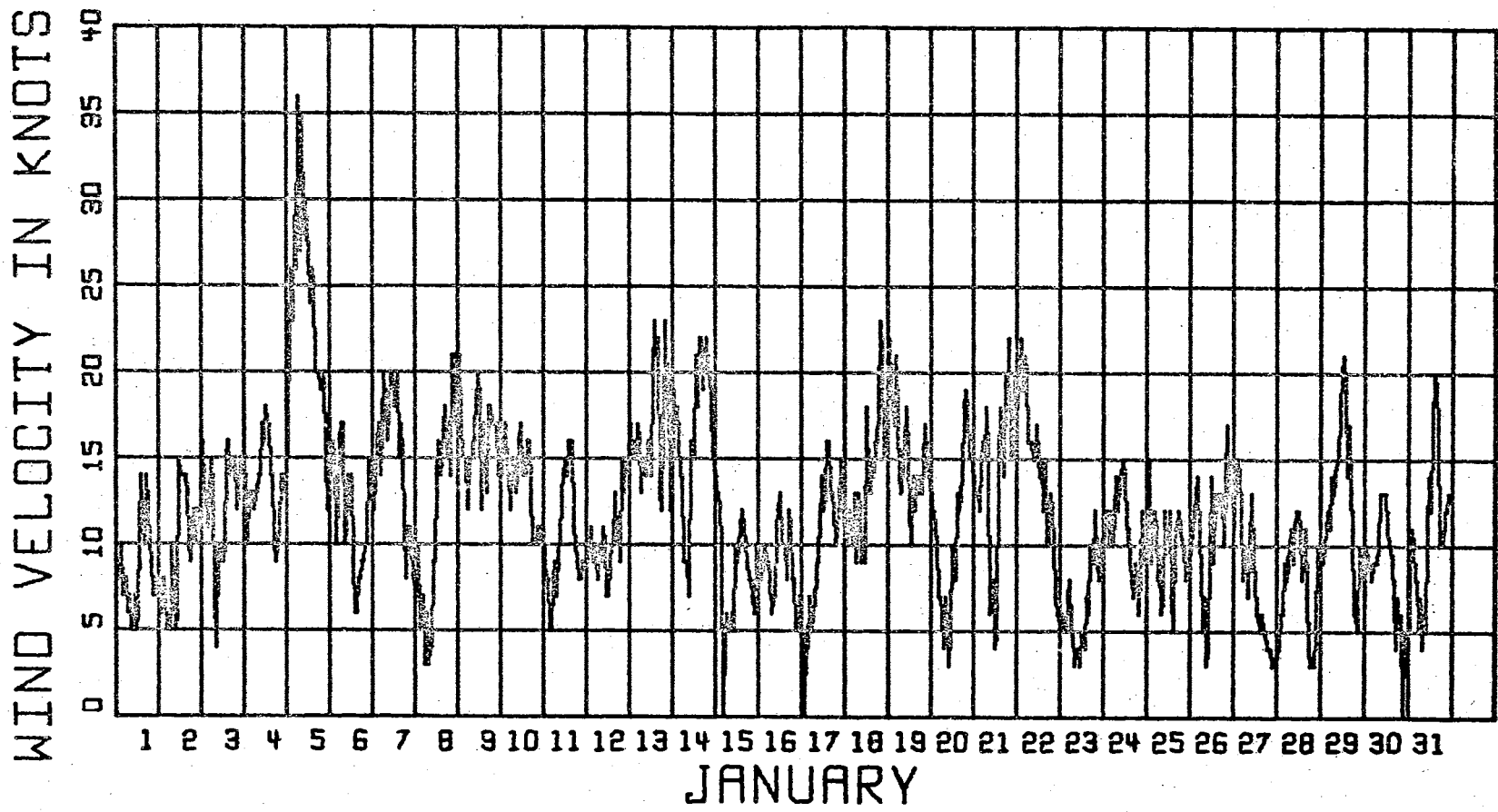
Figure 16. Wind Velocity for January, 1962, Using One-Minute Hourly Averages Showing Apparent 4 Day Cycles
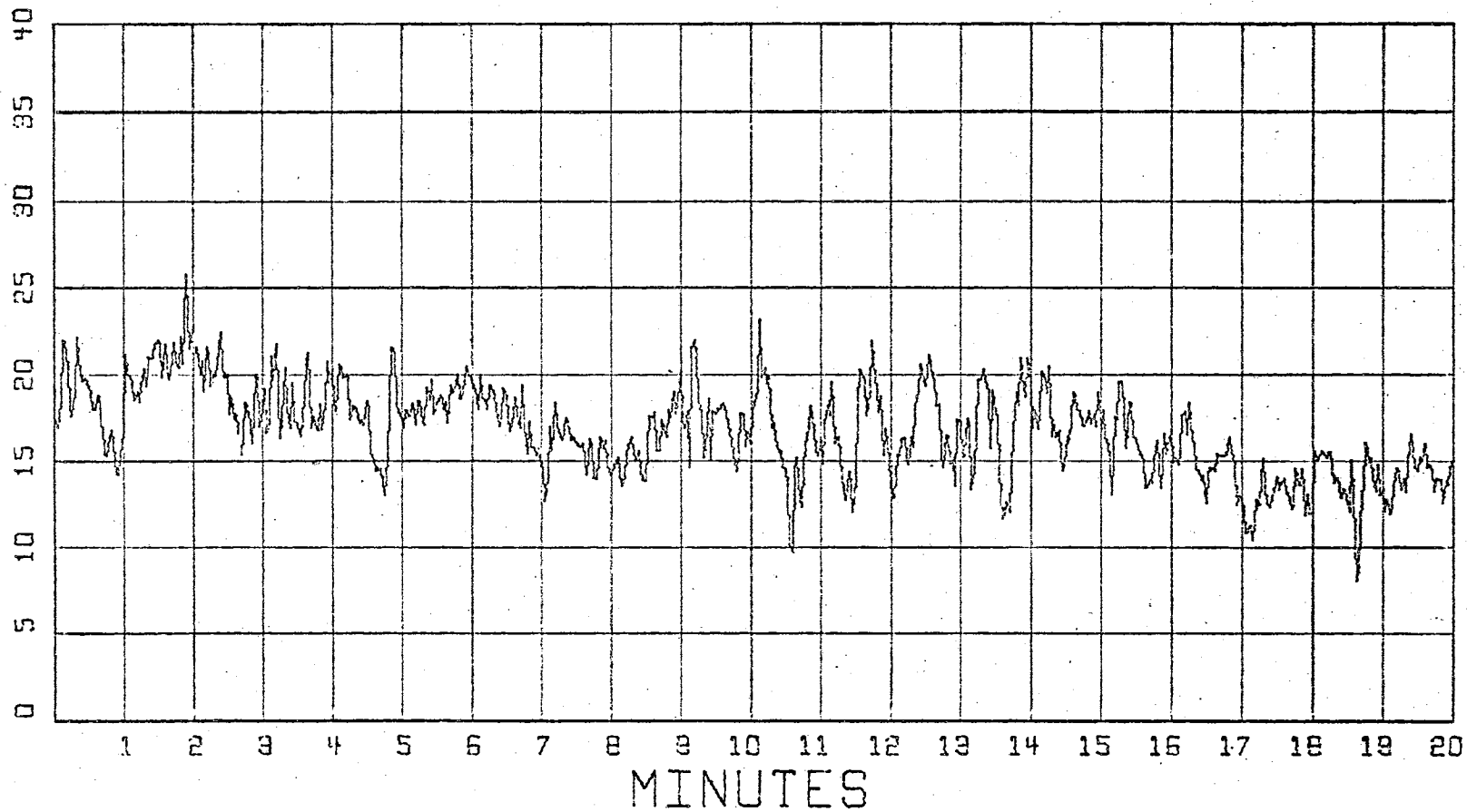
Figure 17. Actual Wind Velocity for Twenty Minutes Showing Apparent One-Minute Peaks

cyclical nature of the wind from month to month. Figure 18 represents

the average monthly wind velocities for Oklahoma City for four years.

The monthly average wind velocities have peaks and dips with a frequency

of oscillation of 12 months. The wind speed reaches a peak every twelve

months during April and dips to a low during the months of July and

August. Therefore, it might be possible for the storage system to be

built large enough to store energy during the high energy producing

months so that energy will be available during the low energy producing

months.

Estimated Spectrum of Simulated Data vs Estimated Spectrum

From Actual Data

As shown in the previous chapter, by comparisons of power calcula-

tions the simulated wind velocity model compared quite favorably with

actual wind velocity data. Another comparison of the horizontal wind

velocity would be to compare the estimated spectrum of the simulated

data and actual data. Results of spectrum comparisons are shown in

Figure 19. The estimated spectrum for the simulated data was approxi-

mately half-way between the estimate obtained by Van der Hoven and the

estimate obtained at Stillwater. All three estimates peaked at about

the same place, i.e. all three have energy peaks occurring at about one

minute. The simulated curve drops off much faster than the other two

because the simulated record is devoid of very high frequencies. This

can be seen in Figure 9. Data for curves B and C of Figure 19 are pre-

sented in Table VIII.

The difference in the heights of the peaks is attributed to the

average velocity of the data being used to obtain the spectral estimate.
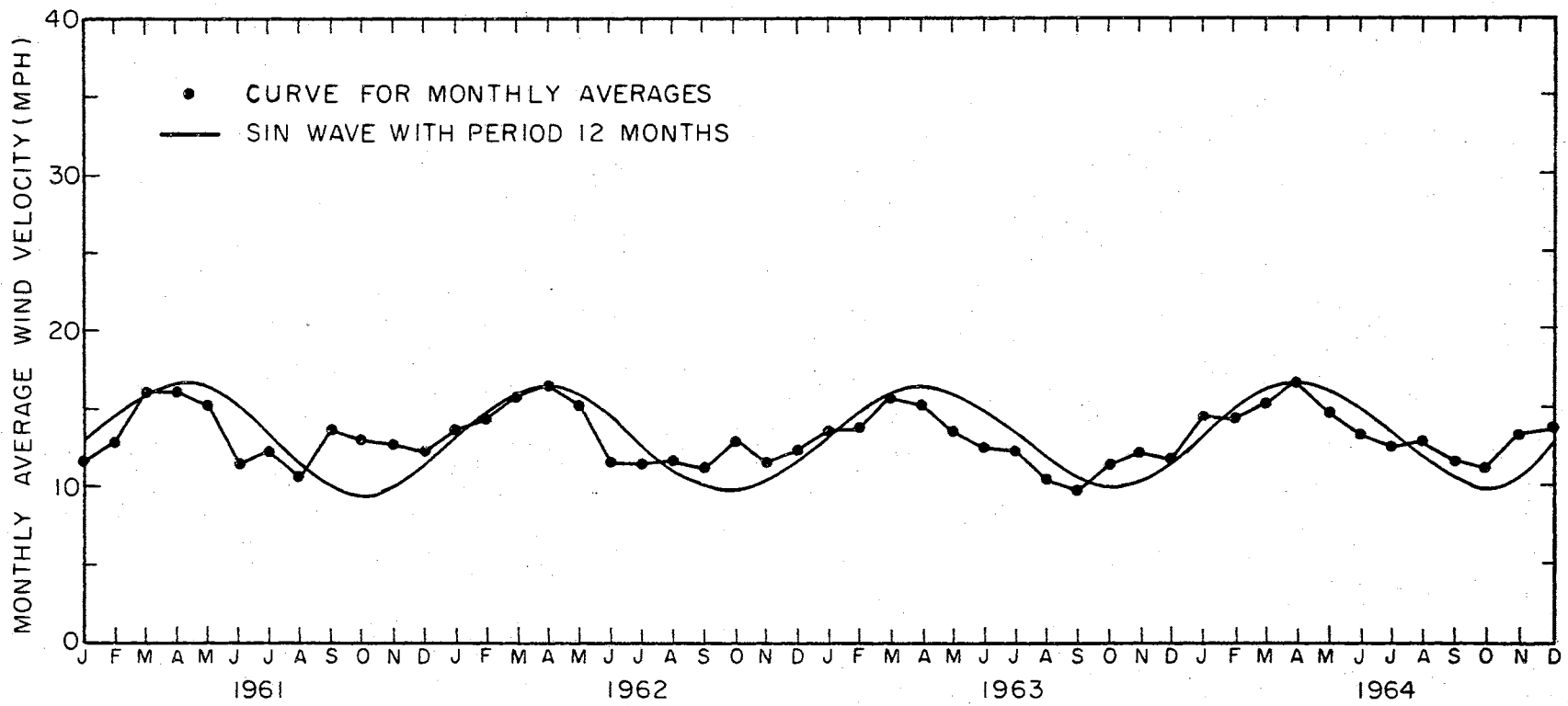
Figure 18. Monthly Average Wind Velocities for Will Rogers Field, Oklahoma City, From 1961 to 1964

TABLE VIII

SUMMARY OF SPECTRAL ESTIMATES FOR SIMULATED AND ACTUAL DATA
(ACTUAL DATA FOR STILLWATER, OKLAHOMA)

f_r	U_r^*	$U_r'^{**}$	ωU_r	$\omega U_r'$
0	0.597	0.96	0	0
30	0.426	0.821	80.3	155.0
60	0.210	0.426	79.2	161.0
90	0.118	0.158	66.8	89.6
120	0.070	0.068	52.8	51.3
150	0.0477	0.030	45.0	28.3
180	0.0418	0.0146	47.1	16.5
210	0.0336	0.008	44.3	5.27
240	0.0253	0.00426	38.2	3.81
270	0.0189	0.00184	32.2	3.21
300	0.0163	0.000935	30.9	3.07
330	0.0143	0.000916	29.8	2.97
360	0.0119	0.000920	27.0	2.69
390	0.0110	0.000921	27.0	2.70
420	0.0100	0.000926	26.4	2.45
450	0.00877	0.000860	24.8	2.48
480	0.00725	0.000747	21.8	2.21
510	0.00683	0.000619	21.8	1.98
540	0.00838	0.000508	28.4	1.72
570	0.00859	0.000415	30.4	1.49
600	0.00703	0.000320	26.5	1.20
630	0.00517	0.000333	20.5	1.32
660	0.00458	0.000352	18.9	1.39
690	0.00510	0.000382	22.1	1.58
720	0.00530	0.000387	23.9	1.75
750	0.00491	0.000362	23.1	1.71
780	0.00506	0.000351	24.8	1.72
810	0.00485	0.000334	24.6	1.03
840	0.00434	0.000325	22.9	0.885
870	0.00419	0.000276	22.9	0.727
900	0.00409	0.000200	23.1	1.13

$^*U_r$ is the spectral estimate for actual data.

$^{**}U_r'$ is the spectral estimate for simulated data.
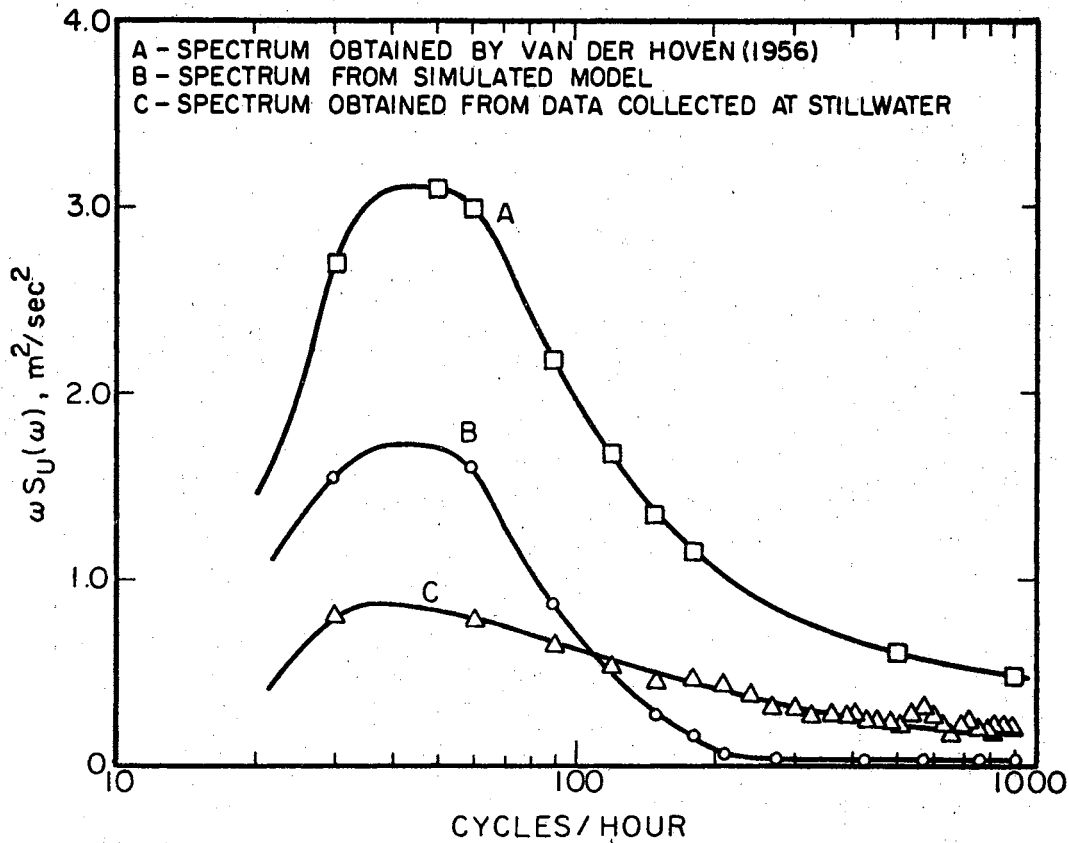
Figure 19. Horizontal Wind Velocity Power Spectrum Comparisons

The average velocity for the curves was: 44.5 miles per hour for curve

A, 25.0 miles per hour for curve B and 19.3 miles per hour for curve C.

If all three had the same average velocity, the simulated curve would be

very close to the other two except it would still drop off faster because

of the void in very high frequencies.

CHAPTER V

COMPARATIVE ANALYSIS OF VELOCITY AND POWER CURVES

In most wind studies for wind power applications completed in the
past, the wind velocity duration curves were obtained by counting the
number of times that the hourly wind measurements were between pre-
determined velocity levels. This method of obtaining the velocity dura-
tion curves is tedious because of the long wind records that must be
reduced by manual means. Therefore, an automatic method for accumulating
the velocity duration curves was provided and the information obtained
was used to determine the validity of using the one-minute hourly
averages for power estimates for potential sites.

The automatic method for obtaining the velocity duration curves
uses a series of detectors (windows or slices) that will record the
total time the wind velocity is within each window or slice. That is,
the velocity duration curves can be obtained directly without tedious
hand reduction. This is accomplished by letting a mechanical counter be
operated by a motor whenever the velocity of the wind is within the
range set on the counter. For example, one counter would be used for
each velocity range desired, 0-6 mph, 6-12 mph, 12-18 mph, etc.

A crude detector similar to this was built by Jensen (2) in Denmark
which had a series of pressure plates that were adjusted to cause several
counters to operate whenever the pressure on the plates exceeded a pre-
determined setting. One pressure plate was used for each velocity

window. This detector was large and bulky but it did provide sufficient information to obtain the velocity duration curve which in turn provided the necessary information to obtain the power duration curves and finally to estimate the amount of extractable power for a given location.

Velocity Distribution Analyzer Circuit

Because the velocity duration curves are essential in making adequate estimates of power, it was thought desirable to design a small, easily constructed and economical detector to obtain these curves. Such a detector was designed and built as part of this study. Figure 20 is a photograph of the detector and Figure 21 is a circuit diagram of the system designed to obtain the amplitude distribution of the horizontal wind velocity.

The Amplitude Distribution Analyzer (Slicer) is driven by a standard four-cup anemometer which produces an a-c voltage proportional to the wind velocity. The a-c voltage signal increases in both frequency and amplitude as the wind velocity increases; therefore, the amplitude distribution analyzer could have been built to switch either when the amplitude changed or when the frequency changed. It was decided to let the amplitude changes cause the switching. The circuit components convert the varying a-c voltage signal into a d-c voltage in a multiplier circuit. The d-c voltage signal is then used as an input to six parallel Schmitt trigger circuits which are coupled to relay drivers, relays, and running time meters. Two typical a-c voltages and their respective d-c voltages are shown in Figure 22.

The theory of operation of the slicer is quite simple; 1.0 K ohm potentiometers are set to switch each successive slice level at a
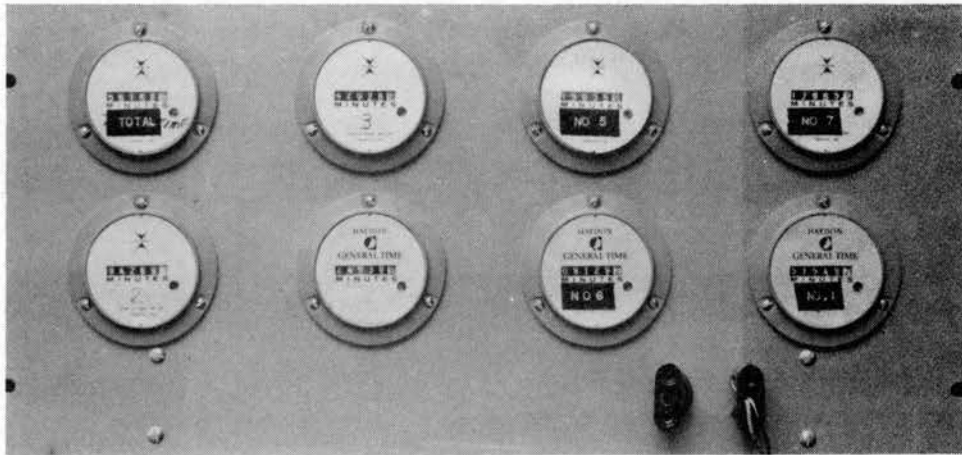
(a) Front View
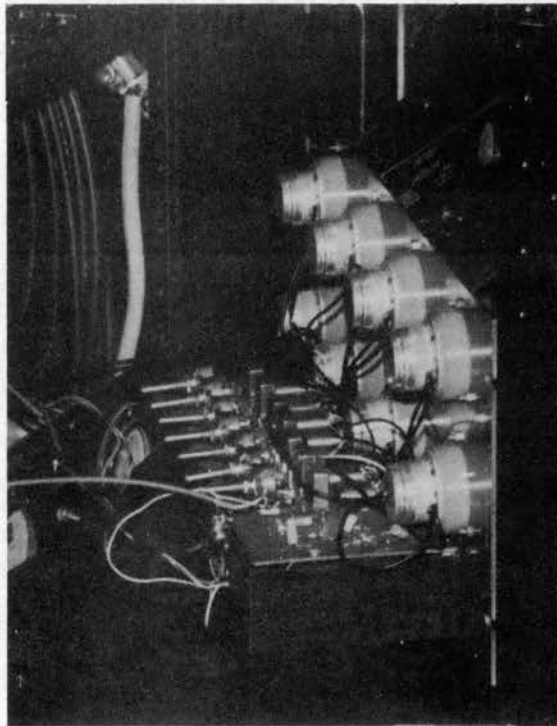
(b) Side View

Figure 20. Velocity Distribution Analyzer

Figure 21. Circuit Diagram of Velocity Amplitude Distribution
Analyzer
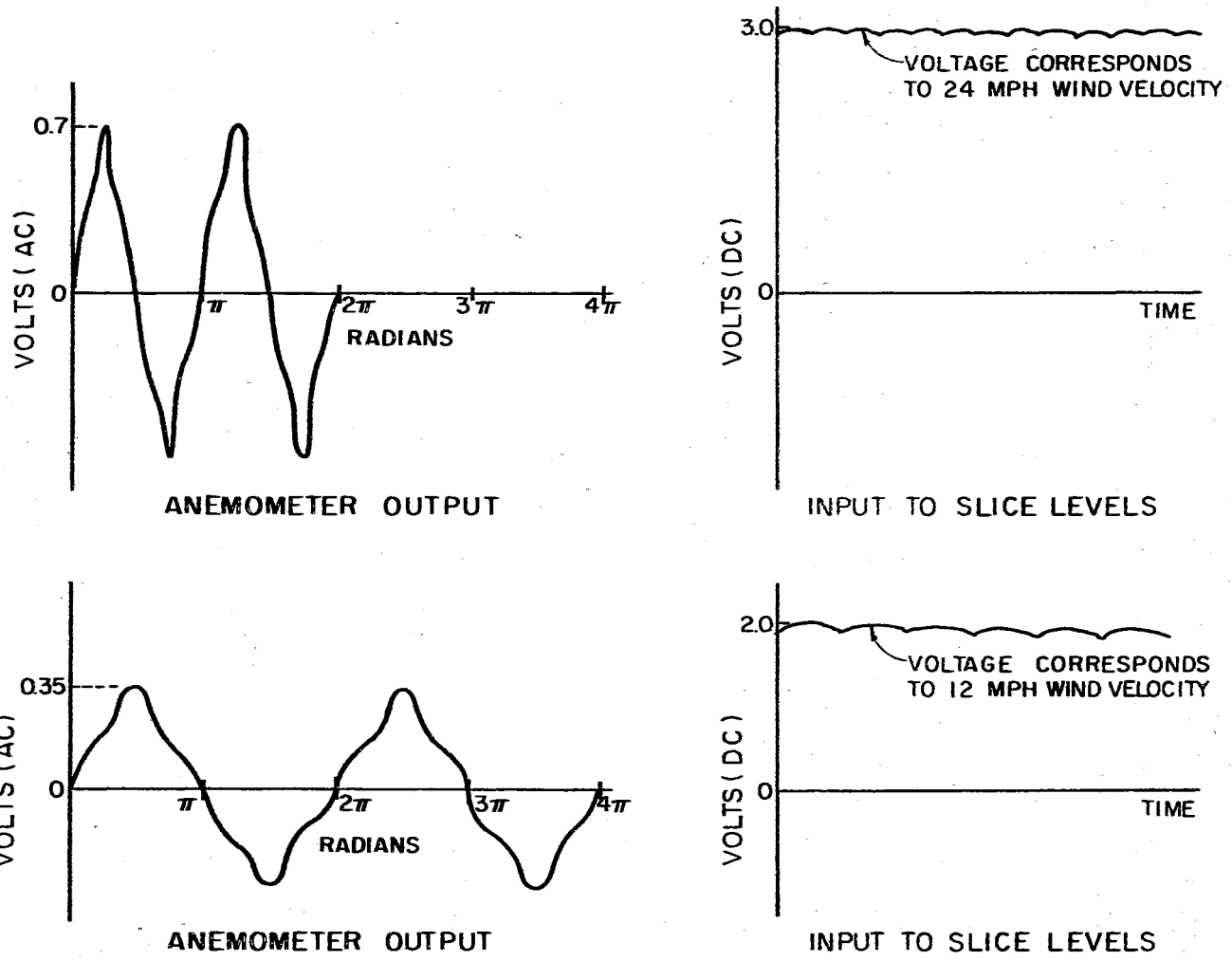
Figure 22. Typical Voltages for Velocity Distribution Analyzer

different d-c voltage level. As the velocity increases or decreases, a given threshold level is passed and causes a particular running time meter to turn on and another one to turn off. Logic for the analyzer is accomplished by using the output of the relay driver and both sides of a double action relay. For example, when the input to relay driver No. 1 reaches a plus reference, relay No. 1 operates and causes meter No. 1 to turn off and meter No. 2 to turn on. Meter No. 1 will remain off as long as the velocity is above the first slice level. When the input increases above the setting for slice two, relay driver No. 2 receives a plus reference causing relay No. 2 to operate which in turn stops meter No. 2 and starts meter No. 3.

The slicer circuit was calibrated in the Oklahoma State University Agriculture Engineering wind tunnel. Results of the calibration are shown in Appendix E. The calibration was verified by comparing the output of the fast response Gill propeller anemometer to the cup anemometer output feeding the slicer circuit. Figure 23 is a plot of the calibration wind tunnel results. This calibration curve can be used to determine the proper voltage setting for a desired switching level. Voltage levels for obtaining the velocity duration curves were set as shown in Table IX, i.e. the first slice level included all velocities from 0 to 6 mph, the second from 6 to 12 mph, etc.

As a check on accuracy of the velocity distribution analyzer, hourly comparisons were made between data obtained from the circuit and data obtained from two second samples of the actual wind velocity. Table X is a summary of four such comparisons. Based on these comparisons, it was felt that the analyzer was satisfactory in obtaining the velocity distribution curves.
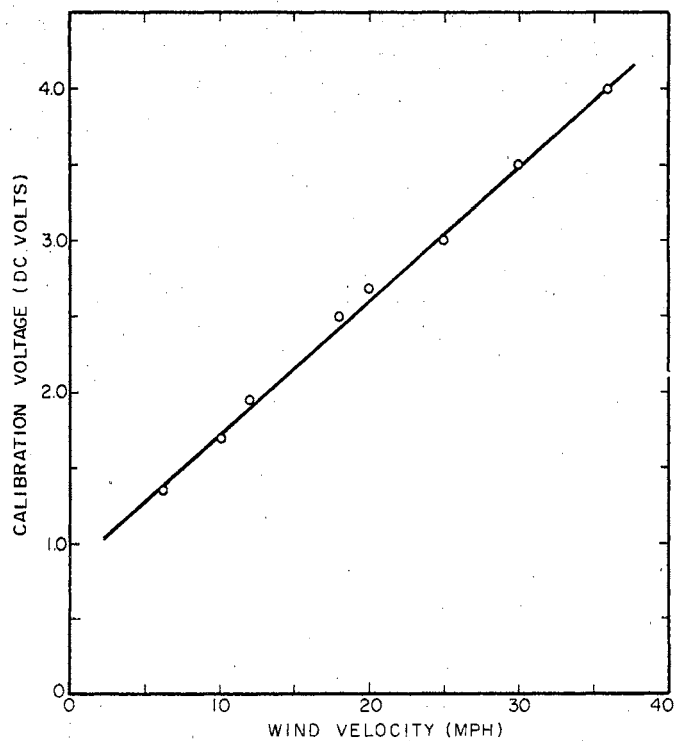
Figure 23. Calibration Curve for Velocity
Distribution Analyzer

TABLE IX

VOLTAGE LEVEL SETTINGS FOR SLICE LEVELS

Slicer Number	Velocity Width (mph)	Voltage Width (Volts)	Voltage Switch Level (Volts)
1	0-6	0-1.35	----
2	6-12	1.35-1.95	1.35
3	12-18	1.95-2.5	1.95
4	18-24	2.5 -3.0	2.5
5	24-30	3.0 -3.5	3.0
6	30-36	3.5 -4.0	3.5
7	36-	4.0 -	4.0

TABLE X

COMPARISON OF VELOCITY DISTRIBUTION ANALYZER DATA TO DATA OBTAINED FROM TWO SECOND SAMPLES

Date and Time	Source of Data	Total Time Minutes	Time in Velocity Level in Minutes						
			0-6 MPH	6-12 MPH	12-18 MPH	18-24 MPH	24-30 MPH	30-36 MPH	36- MPH
1306 to 1406 26 May	Circuit	60.0	0.8	5.8	35.4	17.5	0.5	0	0
	Two Sec. Samples	60.0	1.0	5.8	35.6	17.2	0.4	0	0
1300 to 1400 28 May	Circuit	60.0	0	4.1	23.1	27.8	5.0	0	0
	Two Sec. Samples	60.0	0	4.0	23.0	28.0	5.0	0	0
1220 to 1330 30 May	Circuit	60.0	0	1.3	23.0	30.4	5.4	0	0
	Two Sec. Samples	60.0	0	1.6	22.8	31.0	4.6	0	0
1603 to 1703 14 June	Circuit	60.0	0	0	2.4	31.9	23.6	2.1	0.1
	Two Sec. Samples	60.0	0	0	2.6	32.0	23.0	2.4	0

Comparison of Velocity Distribution Curves

There were two purposes for building the slicer; the first, as previously stated was to provide an economical method to obtain velocity duration curves. The second was to compare simultaneously the data obtained from the slicer circuit and the data obtained from one-minute hourly averages. The second purpose was to provide some indication as to how reliable the one-minute hourly averages are in predicting energy estimates for a given location.

In order to accomplish the second objective, it was necessary to group data from the one-minute hourly averages into the same velocity levels as set on the slicer circuit. Table XI is a summary of the day to day distribution of one-minute hourly averages. The values listed in the table represent the total hours that the wind velocity was in the slice level. Table XII is a summary of the total time spent in each slice level from both the slicer and the hourly averages. The hourly averages were manually counted to obtain the total hours that the wind velocity was within the specific interval.

The data of Table XI were plotted in Figure 24 to obtain the velocity duration curves which were then used to obtain the power duration curves shown in Figure 25. The extractable power is determined by finding the area under the power duration curves for velocities above the cut-in velocity of the wind generator.

The power extractable for the resulting power duration curve using the one-minute hourly averages is slightly larger than the power extractable from the slicer power duration curve as seen by the shaded areas of Figure 25. The one-minute hourly average extractable power is larger by

TABLE XI

SUMMARY OF ONE-MINUTE HOURLY AVERAGES 0800 23 MAY TO 0800 5 JULY

Date		0-6MPH	6-12MPH	12-18MPH	18-24MPH	24-30MPH	30-36MPH	36-MPH
				Velocity Level				
May	23	-	11	3	3			
	24	7	15	1	-	1		
	25	1	9	4	4	1		
	26	3	12	7	-	-	-	2
	27	9	9	6				
	28	6	11	4	3			
	29	11	12	1				
	30	-	13	8	3			
	31	4	19	1				
June	1	12	11	1				
	2	11	13					
	3	17	7					
	4	13	8	3				
	5	6	9	8	1			
	6	-	8	10	6			
	7	-	11	8	5			
	8	1	12	7	2	2		
	9	-	8	9	6	-	1	
	10	2	8	8	3	2	1	
	11	17	7					
	12	12	12					
	13	2	9	5	6	2		
	14	-	1	6	18	4		
	15	7	8	6	2	-	1	
	16	14	10					
	17	12	12					
	18	9	10	4	1			
	19	9	13	2				
	20	9	6	9				
	21	4	17	3				
	22	6	6	11	1			
	23	1	5	11	4	3		
	24	6	12	5	1			
	25	8	9	5	2			
	26	4	5	9	5	1		
	27	7	7	7	3			
	28	-	5	3	8	3	5	
	29	-	-	1	6	10	6	1
	30	1	1	2	12	6	1	1
July	1	15	3	4	-	1	1	
	2	8	6	10				
	3	8	16					
	4	17	6	1				
	5	6	1					
TOTALS		285	395	193	105	36	16	4

TABLE XII

COMPARISON OF SLICER DATA WITH ONE-MINUTE HOURLY AVERAGES - TIME 1034 HOURS

Velocity Level	Total Hours in Velocity Level From Slicer	Total Time Minus Hours in Lower Level	Per Cent of Time Above Lower Limit of Slice Level	Total Hours in Velocity Level From One-Min. Hourly Averages	Total Time Minus Hours in Lower Level	Per Cent of Time Above Lower Limit of Slice Lever
0-6	301	1034	100	285	1034	100
6-12	396	733	71.0	395	749	72.3
12-18	180	337	32.6	193	354	34.2
18-24	103	157	15.2	105	161	15.6
24-30	40	54	5.22	36	56	5.4
30-36	10	14	1.35	16	20	1.93
36-	4	4	0.39	4	4	0.39
TOTALS	1034	----	------	1034	----	------
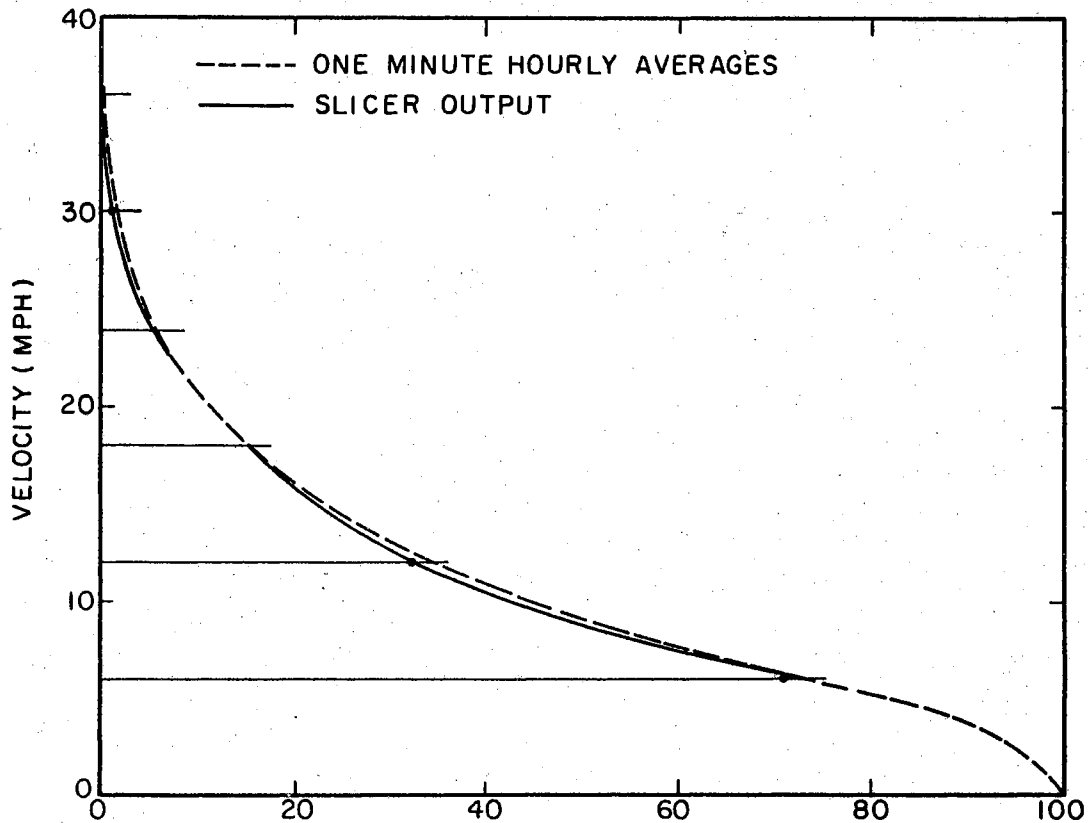
Figure 24. Velocity Duration Curves for Stillwater, Oklahoma, (0800 23 May to 0800 5 July, 1968)

the amount shown by the dark shaded area of the figure. This difference, however, is not significant and appears to approach zero as the interval of time for comparison of the two sources of data increases.

A daily comparison of the slicer data with the one-minute hourly data, reveals that large differences occur in the two velocity duration curves. A comparison of longer time periods again indicates much smaller differences. For example, from 0900 27 May to 0900 28 May, the two sources differed significantly. See Table XIII. Table XIII reveals that the wind velocity exceeded level three for 64 minutes while the one-minute hourly averages did not indicate any wind velocities above
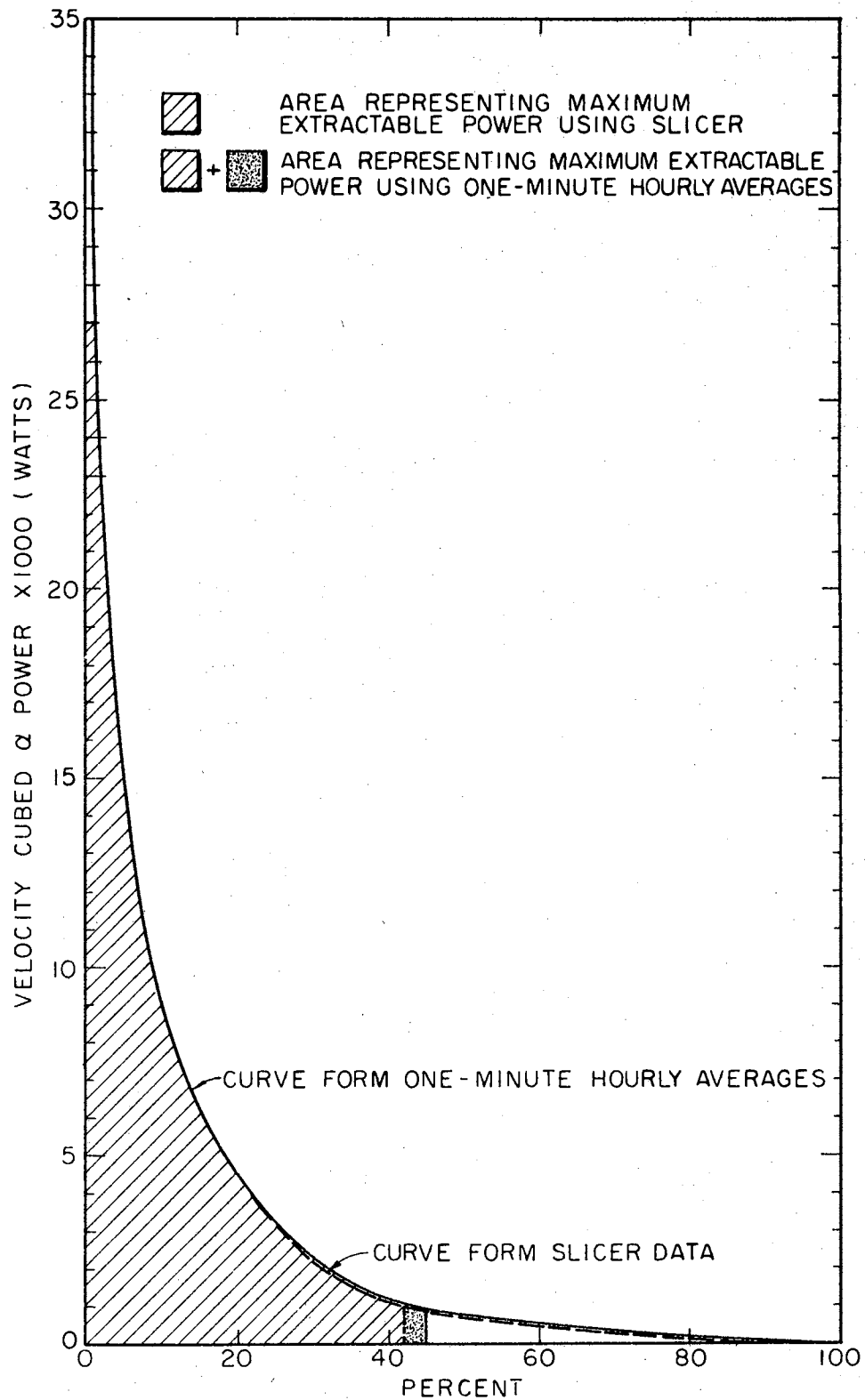
Figure 25. Power Duration Curves Corresponding to Velocity Duration Curves in Figure 25

TABLE XIII

COMPARISON OF SLICER DATA WITH ONE-MINUTE HOURLY AVERAGES
0900 27 MAY TO 0900 28 MAY

Velocity Level	Total Min. in Velocity Level (Slicer)	Total Min. in Velocity Level (One-Min.)
1	237	300
2	760	780
3	279	360
4	145	0
5	17	0
6	2	0
7	0	0
Total Time	1440	1440

that level. If one were to take another day at random, just the opposite indication might occur.

Comparisons of velocity duration curves for relatively calm periods and for periods of high winds were made to further verify the dependability of the one-minute hourly averages for use in energy estimates. Figure 26a through 26d shows that the one-minute hourly averages result in higher readings part of the time and lower readings part of the time. Over a longer time, say two months or more, the two curves are approximately the same. This was shown in Figure 24.

Linear Regression Analysis

In an attempt to further verify how close the one-minute hourly averages compare with the true wind velocity averages, linear regression analysis techniques were used. That is, the hourly one-minute averages
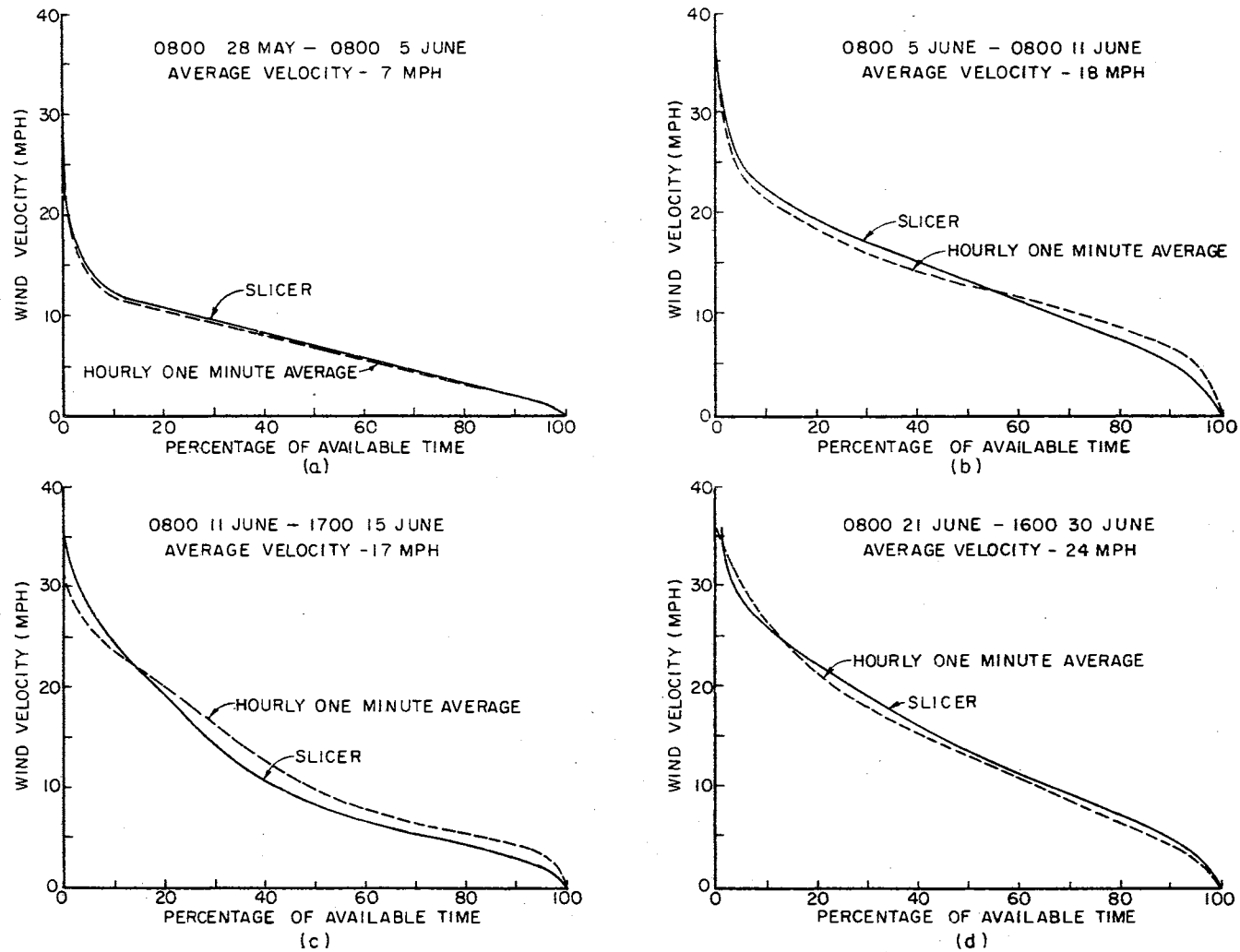
Figure 26. Velocity Duration Curves for Short Time Periods for Stillwater, Oklahoma

were compared to the true velocity averages determined by sampling the wind velocity at a rate of one sample every 15 seconds. A scatter diagram was plotted for the data and a straight line curve was fit to the data. Scatter diagrams and straight line approximations were obtained for the wind velocity and the corresponding extractable powers.

Figure 27 is the scatter diagram for the wind velocities. The horizontal axis represents the true wind velocity average derived from the 15 second data samples and the vertical axis is the one-minute hourly averages taken at the beginning of each hour. A least square straight line approximating curve was obtained by applying standard curve fitting methods.

The least square regression line of Y(one-minute hourly average) on X(time average) can be assumed with a form $Y = X$, $Y = aX$, or $Y = a_0 + a_1X$. The test hypothesis $Y = X$ was selected.

The qualitative manner in how well the line describes the relationship between the variables can be determined by direct observation of the scatter diagram. However, if a quantitative comparison is desired, measures of correlation must be considered. These measures of correlation are the standard error of the estimate and the coefficient of correlation. The standard error of the estimate is a measure of the scatter about the regression line and is found by the equation

$$S_{Y,X} = \sqrt{\frac{(Y - Y_{est})^2}{N}} \tag{5.5}$$

where

Y_{est} = the estimated value for Y; and

N = the number of observations.

The correlation coefficient is defined as the covariance of X and Y
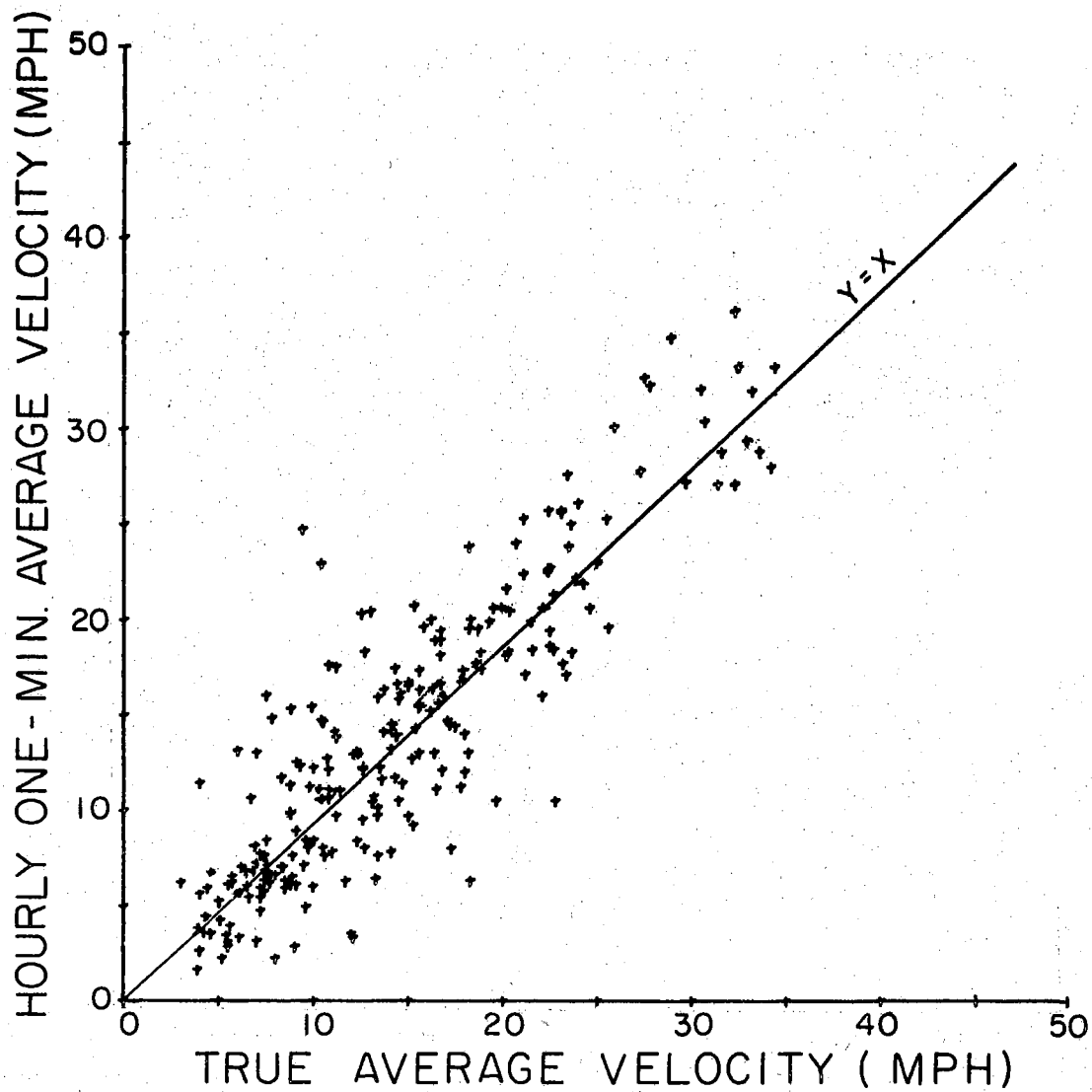
Figure 27. Velocity Scatter Diagram Comparing One-Minute Hourly
Average Velocities Obtained at the Beginning of
Each Hour With True Average Velocities Obtained

divided by the product of the standard deviations of the variables X and Y. That is,

$$r = \frac{S_{XY}}{S_X S_Y} \qquad (5.6)$$

where

r = correlation coefficient;

$S_{XY} = \frac{\sum XY}{N}$ = covariance of X and Y;

$S_X = \sqrt{\frac{\sum X^2}{N}}$ = standard deviation of X; and

$S_Y = \sqrt{\sum \frac{Y^2}{N}}$ = standard deviation of Y.

If the standard error of the estimate is small the points are close to the regression line and if the correlation coefficient r is close to unity there is good correlation between the two variables.

The regression lines, Y = X and X = Y, are the regression lines of Y on X and X on Y respectively. The regression line of X on Y is used for estimating true hourly averages from the one-minute averages obtained at the beginning of the hour. The standard error of the estimate for X on Y is 3.49 and the correlation coefficient is 0.879.

Since the power is proportional to the velocity cubed, it was thought desirable to obtain a scatter diagram and linear regression curve for the power data. Figure 28 is the scatter diagram of the power using 189 samples. The linear regression line, standard error of the estimate and correlation coefficient, are found in Table XIV. Table XIV is a summary of regression analysis between: the one-minute hourly averages and the true velocity averages, between the estimated extractable powers, between velocity and estimated power averaged over 12 hours and between velocity and estimated power averaged over 24 hours.
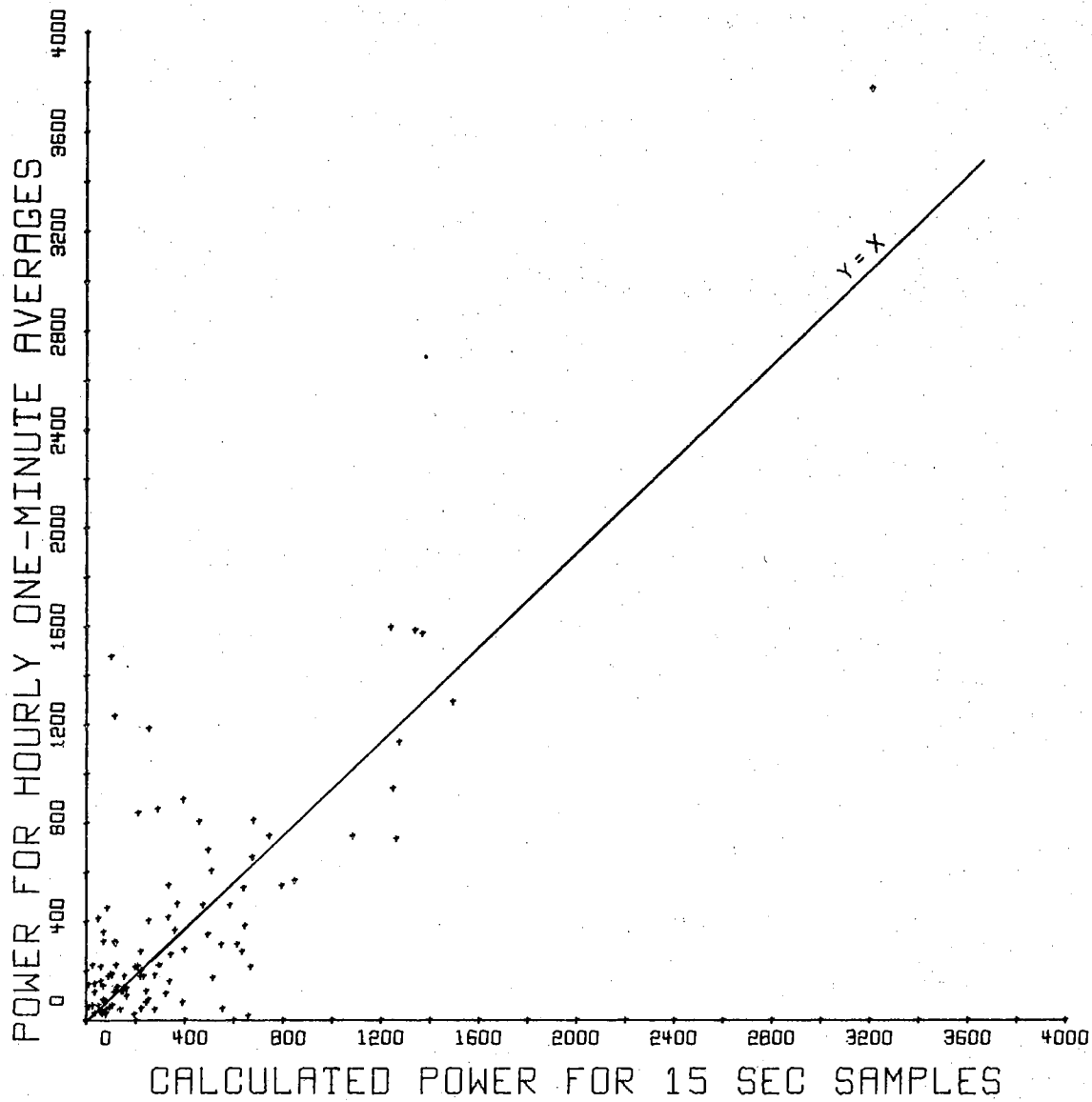
Figure 28. Power Scatter Diagram for Power Calculations for One-Minute Hourly Averages and True Averages

TABLE XIV

SUMMARY OF REGRESSION ANALYSIS FOR VELOCITY AND POWER COMPARISONS

Regression	Variable Compared	No. Samples Used	Correlation Coefficient	Standard Error of Estimate
X on Y	Velocity (1 Hr. Data)	249	0.879	3.71
	Velocity (12 Hr. Ave.)	20	0.979	1.26
	Velocity (24 Hr. Ave.)	10	0.980	1.07
	Power (1 Hr. Data)	189	0.878	453.9
	Power (12 Hr. Ave.)	16	0.977	156.7
	Power (24 Hr. Ave.)	8	0.975	144.0
Y on X	Velocity (1 Hr. Data)	249	0.879	3.48
	Velocity (12 Hr. Ave.)	20	0.979	1.28
	Velocity (24 Hr. Ave.)	10	0.980	1.13
	Power (1 Hr. Data)	189	0.878	431.2
	Power (12 Hr. Ave.)	16	0.977	121.8
	Power (24 Hr. Ave.)	8	0.975	111.9

Summary of Comparisons

As a result of the comparisons between the velocity duration curves and the linear regression analysis, it appears that the one-minute hourly averages are quite suitable for use in predicting energy estimates for

potential wind power sites. This is true, even though there are extreme inaccuracies in an hour by hour comparison of the velocity measurements. This conclusion contradicts the idea that the energy estimates have large errors because data are ignored for 59 out of every 60 minutes when the one-minute hourly averages are used. This result could be attributed to the fact that there is no apparent difference between the probability of obtaining a high one-minute average or a low one-minute average when compared to the true velocity average within the hour.

The amplitude velocity distribution analyzer designed as part of this study is adequate for obtaining the velocity duration curves for potential wind power locations whenever the standard meteorological data are not available.

CHAPTER VI

CONCLUSIONS AND RECOMMENDATIONS

Summary and Conclusions

The objective of this study was to make a detailed analysis of the wind to provide information that could be used to aid in the optimization of wind power systems. Three major areas of interest were considered. The first was the development of a suitable model of the horizontal wind velocity that could be used to simulate the wind. The second was to apply spectrum analysis techniques to the time series representing the horizontal wind velocity to find the power spectrum of the horizontal wind. The third was to determine how useful the one-minute hourly averages obtained at standard meteorological stations were in making energy estimates for potential wind power sites. To aid in this determination, a velocity amplitude distribution analyzer was designed and constructed.

The simulation model presented in Chapter II simulates the wind for applications to wind power generation better than previous models. The model could be used to simulate the wind velocity for only a few minutes or it could be used to simulate the wind for one hour or longer. It is easily generated and can be used to optimize the wind conversion equipment and the energy storage equipment. This conclusion was based on the fact that the simulated model for a given wind velocity accurately predicted the estimated energy. This was shown by making comparisons to

the actual energy for the same value of wind velocity.

The horizontal wind velocity spectrum obtained and discussed in Chapter III reveals that there is a four day energy peak which can be attributed to the passage of major frontal systems. The designer of the energy storage sub-system should take into account this four day energy peak when determining the size of storage required. The horizontal wind speed spectrum also contained a small peak at one minute which is attributed to convective turbulence. This one minute peak may be of little importance to designers of large systems where the inertia is so large that the system cannot follow the fluctuations of the input. However, the energy in the one minute peak may result in an increased power output of approximately 10 per cent for small wind energy systems if the system is small enough to allow the system to follow the one minute fluctuations.

The one-minute hourly averages obtained at standard meteorological stations are suitable for use in making energy estimates. This is the case even though 59 out of every 60 minutes of hourly wind velocity data are ignored.

The velocity distribution analyzer designed as part of this study is a good and economical method for obtaining velocity duration curves at potential wind power sites where sufficient wind data are not normally available and for making comparisons with data collected at meteorological stations.

Recommendations for Further Study

There are a number of investigations that would be desirable to continue the work in the wind energy area. A few of the more important

investigations are:

Further comparisons of the velocity duration curves obtained from the one-minute hourly averages and the distribution analyzer would be useful. That is, month by month, semi-annual, and annual comparisons could be made to further verify results obtained in this study.

Comparisons between the distribution analyzer data and data obtained at several standard meteorological stations should be made to obtain comparative velocity duration curves for a number of different locations. This could be accomplished quite easily since data is presently being taken for the one-minute hourly average velocities and since the velocity distribution analyzer would be relatively easy to relocate.

Refinements to the distribution analyzer could be made to provide convenient calibration checks or automatic adjustments. Also additional distribution analyzers could be built to allow data collection at several different locations simultaneously.

The different model of the horizontal wind which could possibly be investigated is a model using two jointly normal random variables with means V_0, with variances σ^2 as obtained in this study and with the exponential function of time determined as shown in Appendix B.

Other extensions to this study can use the simulated wind velocity model to optimize design of the wind energy conversion equipment. This would entail varying the parameters of the system while using the simulated wind velocity as an input. A family of curves can be obtained for different values of the parameters. Before the family of curves can be obtained, it is necessary to relate the input velocity for a wind energy system to the input torque on the propeller and to the angular velocity. The development of this relationship between input velocity and torque

and angular velocity would be a most important extension of this work.

As in most research projects, the theoretical and estimated results should be verified by actual data. Therefore, small energy systems should be paired with a cup anemometer feeding the velocity distribution analyzer. This would allow comparison of actual extractable energy with estimated extractable energy determined from the power duration curve derived from the velocity distribution analyzer.

BIBLIOGRAPHY

1. Energy Storage (Key to Our Economic Future). The Office of Engineering Research, Oklahoma State University, Stillwater, Oklahoma, 1963.

2. Proceedings of the United Nations Conference on New Sources of Energy, Rome, 21-31, Aug., 1961, Vol. 7, United Nations, New York (1964).

3. Research Proposal, Developing Unconventional Energy Sources for use in Developing Countries. The Office of Engineering Research, Oklahoma State University, Stillwater, Oklahoma (1967).

4. Energy Conversion and Storage. Annual Report for the year ending June 30, 1965, School of Electrical Engineering, Oklahoma State University, Stillwater, Oklahoma (1965).

5. Betz, A. "Windmills in the Light of Modern Research." Tech. Memo. No. 474., National Advisory Committee for Aeronotics (1927), 29-47.

6. Putnam, P. C. Power From the Wind. New York: Van Nostrand, 1948.

7. Golding, E. W. The Generation of Electricity by Wind Power. New York: Philosophical Library, Inc., 1956.

8. Venkiteshwaran, S. P., K. R. Sivaraman, and C. G. Gupte. "A Note on the Feasibility of Wind Generation of Electric Power for Communication Links in India." National Aero. Lab., Bangalore, Tech. Note No. TN-WP-36-65, NASA Accession No. N65-33046, (1965), 1-16.

9. Venkiteshwaran, S. P., and K. R. Sivaraman. "Utilization of Wind Power in Arid and Semi-Arid Areas in India." National Aero. Lab., Bangalore, Tech. Note No. TN-WP-22-63, NASA Accession No. N63-22524, (1963).

10. Rao, M. S. P., and S. R. Radhakrishnan. "Velocity Measurements for Converting Wind Energy to Power for Wind Electric Generator Operation." National Aero. Lab., Bangalore, Tech. Note No. TN-WP-17-62, NASA Accession No. N66-19213, 1962.

11. Rao, D. V. L. N., K. N. Narasimhaswamy, and S. R. Radhakrishnan. "A Study of Hourly Wind Speeds at Jogdalpur and Jamshedpur From the Point of View of Wind Power Utilization." National Aero. Lab., Bangalore, Tech. Note No. TN-WP-34-64, NASA Accession No. N65-22054, 1964.

12. Manual of Surface Observations (WBAN), Circular N. U. S. Department of Commerce, April (1966), Chapter 8.

13. Proceedings of the United Nations Conference on New Sources of Energy. Rome, 21-31, Aug., 1961, Vol. 7, United Nations, New York (1964), 137-146.

14. Davenport, A. G. "Rationale for Determining Design Wind Velocities." ASCE Proceedings (Structure Division), Vol. 86 (1960), 39-68.

15. Sherlock, R. H. "Variations of Wind Velocity and Gusts With Height." ASCE Trans., Vol. 118 (1953), 463-488.

16. Davenport, A. G. "The Application of Statistical Concepts to the Wind Loading of Structures." Proc. Inst. Civ. Engrs., Vol. 19 (1961), 458.

17. Scrase, F. J. "Some Characteristics of Eddy Motion in the Atmosphere." Geophysical Memoirs, No. 52, London Meteorological Office (1930).

18. Frenkiel, J. "Wind Profiles Over Hills (in Relation to Wind Power Utilization)." Quar. J. R. Met. Soc., Vol. 88 (1962), 156.

19. Davenport, A. G. "The Spectrum of Horizontal Gustiness Near the Ground in High Winds." Quar. J. R. Met. Soc., Vol. 87 (1961), 194-211.

20. Merchant, D. A. "Stochastic Model of Wind Gusts." (unpub. Ph.D. thesis, Stanford University, 1965, 55-70).

21. Parzen, E. Stochastic Processes. San Fransisco: Holden-Day, 1962, 313.

22. Tukey, J. W. "The Sampling Theory of Power Spectrum Estimates." Symp. on Applic. of Autocorr. Analysis to Phys. Probl., Washington, Office Naval Res. (1949), 47-67.

23. Jones, Richard H. "Spectral Analysis and Linear Prediction of Meteorological Time Series." J. Applied Meteor., Vol. 3 (1964), 45-52.

24. Snyder, Russell L. "A Partial Spectrum Approach to the Analysis of Quasi-Stationary Time Series." IEEE Trans. on Info. Theory, Vol. IT-3, No. 4 (1967), 579-587.

25. Griffith, H. L., H. A. Panofsky, and I. Van der Hoven. "Power Spectrum Analysis Over Large Ranges of Frequency." J. Meteor., Vol. 13 (1956), 279-282.

26. Bendat, J. S., A. G. Piersol. Measurement and Analysis of Random Data. New York: John Wiley and Sons, Inc., 1958.

27. Panofsky, Hans A., Robert A. McCormick. "Properties of Spectra of Atmospheric Turbulence at 100 Metres." Quar. J. R. Meteor. Soc., Vol. 80 (1954), 546-564.

28. Gentleman, W. M., and G. Sande. "Fast Fourier Transforms - For Fun and Profit." Proc. Fall Joint Computer Conference, AFIPS Proc. Washington, D. C.: Spartan, Vol. 29 (1966), 563-578.

29. Blackman, R. B., and J. W. Tukey. The Measurement of Power Spectra. New York: Dover Publications, 1958.

30. Van der Hoven, I. "Power Spectrum of Horizontal Wind Speed in the Frequency Range From 0.0007 to 900 Cycles per Hour." J. Meteor., Vol. 14 (1956), 160-164.

31. Pearson, E. S., and H. O. Hartley. Biometrika Tables for Statisticians. New York: Cambridge University Press, Vol. 1 (1956), 130-131.

32. Lee, L. "Sample Rate Required to Estimate Energy in Wind Speed Record." (unpub. report, Oklahoma State University, 1967).

33. Spiegel, M. R. Schaum's Outline of Theory and Problems of Statistics. New York: Schaum Pub. Co., 1961.

APPENDIX A

DEFINITIONS

Because this study considers concepts from unrelated areas, defini-
tions of some of the more important terms are included. Numbers beside
the term correspond to the reference where the definition was obtained.
No number indicates that it is a definition peculiar to this study.

Aliasing (29). That property that removes energy from a high fre-
quency and makes it appear at a lower frequency. The aliasing effect is
due to the finite spacing between observations which make it impossible
to observe higher frequency oscillations than twice the period between
oscillations.

Amplitude Distribution Analyzer. A device to obtain an estimate of
the distribution function of the amplitude of a signal.

Autocorrelation Function (29). The normalized autocovariance func-
tion (normalized so that its value for lag zero is unity), or $R(\tau)$ =
$E X(t) \cdot X(t + \tau)$ = expected value of the product of random variable
$X(t)$ and $X(t + \tau)$.

Autocovariance Function (29). The covariance between $X(t)$ and
$X(t + \tau)$ as a function of the lag T. If the averages of $X(t)$ and
$X(t + \tau)$ is zero, it is equal to the average value of $X(t) X(t + \tau)$.

Chi-Square Random Variable (29). A random variable distributed as
$X_1^2 + X_2^2 + \ldots + X_k^2$ with X_1, X_2, $\ldots$, X_k independent and Gaussian and
have average zero and variance unity.

Covariance (29). A measure of common variation between two quanti-ties, equal to the average product of deviations from averages.

Cube Factor (7). The cube root of the energy pattern factor.

Correlation Coefficient (29). A measure of the correlation between two or more variables.

Degrees of Freedom (29). As applied to chi-square distributions arising from quadratic forms in Gaussian variables, the number of linearly independent squared terms of equal size into which the form can be divided.

Energy Pattern Factor (7). The total energy in the wind divided by the energy calculated by cubing the average wind velocity.

Fast Fourier Transform (28). An algorithmic process for calculating with great computational efficiency the Fourier coefficients of a given series.

Folding (Nyquist) Frequency (29). The lowest frequency which "is its own alias", that is, is the limit of both a sequence of frequencies and the sequence of their aliases. The reciprocal of twice the time interval between sample values.

Gaussian (29). A single quantity, or a finite number of quantities distributed according to a probability density representable by e to the power minus a quadratic form.

Gust (7). A sudden deviation of the horizontal component of the velocity from the average wind velocity.

Hamming (29). The operation of smoothing with weights 0.23, 0.54, and 0.23. (After R. W. Hamming).

Lag (29). A difference in time of two events or values considered together.

Lagged Product (29). The product of two values corresponding to different times.

Least Square Curve (Line) (33). A curve having the property that the sum of the squared distances from the estimation curve to the actual data points is a minimum.

Line Power (29). A finite contribution associated with a single frequency.

Mean Lagged Products (29). The mean of products of equally spaced lagged products.

One-Minute Hourly Averages. The velocity obtained by averaging the wind velocity each hour for a duration of one minute. Reported as the average wind velocity for the entire hour by standard meteorological stations.

Power Duration Curve (7). A curve obtained by cubing the values of velocity of a corresponding velocity duration curve.

Power Spectrum (Spectral Density) (29). A value of a function or the entire function whose integral over any frequency interval represents the contribution from that frequency interval.

Regression Curve (33). A least squares curve which fits the sample data and is used to estimate the value of one variable from a given value of another. To estimate X from a given value of Y we would use a regression curve of X on Y.

Resolution (33). A measure of the concentration of a spectral estimate expressed in frequency units.

Scatter Diagram (33). A plot of two variables say X and Y on a rectangular coordinate system. If all points on the scatter diagram seem to lie near a straight line, the correlation between X and Y is linear.

Spectral Density Estimates (29). Estimates of the spectral density, termed raw when obtained from equispaced mean lagged products by cosine series transformation, refined when hanned or hammed from raw estimates or obtained by an equivalent process.

Stationary (29). An ensemble of time functions or random process is stationary if any translation of the time origin leaves its statistical properties unchanged.

True Hourly Average. The average wind velocity for an hour obtained by sampling actual wind velocity data every two seconds.

Velocity Duration Curve (7). A curve showing the range of the wind velocity per given time for which the wind speed equals or exceeds each ordinate value of velocity. Also known as velocity distribution curve.

Variance (29). A quadratic measure of variability of the average squared deviation from the average.

Wind Velocity. Refers to the magnitude of the wind speed in the direction of the horizontal component.

APPENDIX B

GENERATION OF EXPONENTIAL RANDOM VARIABLES

The exponential random variables were generated by a method based on the probability integral transformation. The probability integral transformation is the transformation of a random variable X into a uniformly distributed random variable $U = F_X(X)$. Parzen (21) in effect shows that a continuous distribution function of a random variable is uniformily distributed over an interval 0 to 1. Therefore, since there is a one-to-one correspondence between a random variable and its distribution function, a group of random numbers may be used to calculate a group of independent and identically distributed random variables. For the exponential distribution with unit parameter, the random variable may be expressed as:

$$X = -(\frac{1}{\lambda}) \log_e \left[1 - F_X(X) \right]$$ (B.1)

where

$F_X(X)$ is uniformily distributed over the interval 0 to 1; and

λ = the exponential parameter.

If the generation of exponentially distributed random variables are considered in more detail, the following results would be obtained. If a density function

$$f(x) = \begin{cases} e^{-\lambda x} & \text{for } x > 0 \\ 0 & \text{otherwise,} \end{cases}$$ (B.2)

is given, the distribution function can be found by taking the integral

from $-\infty$ to x, i.e.

$$F(x) = \int_{-\infty}^{x} \lambda e^{-\lambda T} dT = \int_{0}^{x} \lambda e^{-\lambda T} dT \qquad . \qquad (B.3)$$

Performing the integration results in $F(x) = 1 - \lambda e^{-\lambda x}$ which can be

written as

$$e^{-\lambda x} = \frac{1 - F(x)}{\lambda} \qquad . \qquad (B.4)$$

Now if we take the logarithm of both sides of B.4, which is possible

since $F(X)$ is single valued, the following equation is obtained:

$$x = -(\tfrac{1}{\lambda}) \log_e \left[1 - F(x) \right] \qquad . \qquad (B.5)$$

The new variable is exponentially distributed with parameter λ. Figure

29 is a histogram of three hundred exponential numbers generated in this

manner with parameter $\lambda = 1$. Other types of random variables can also

be generated by this method.
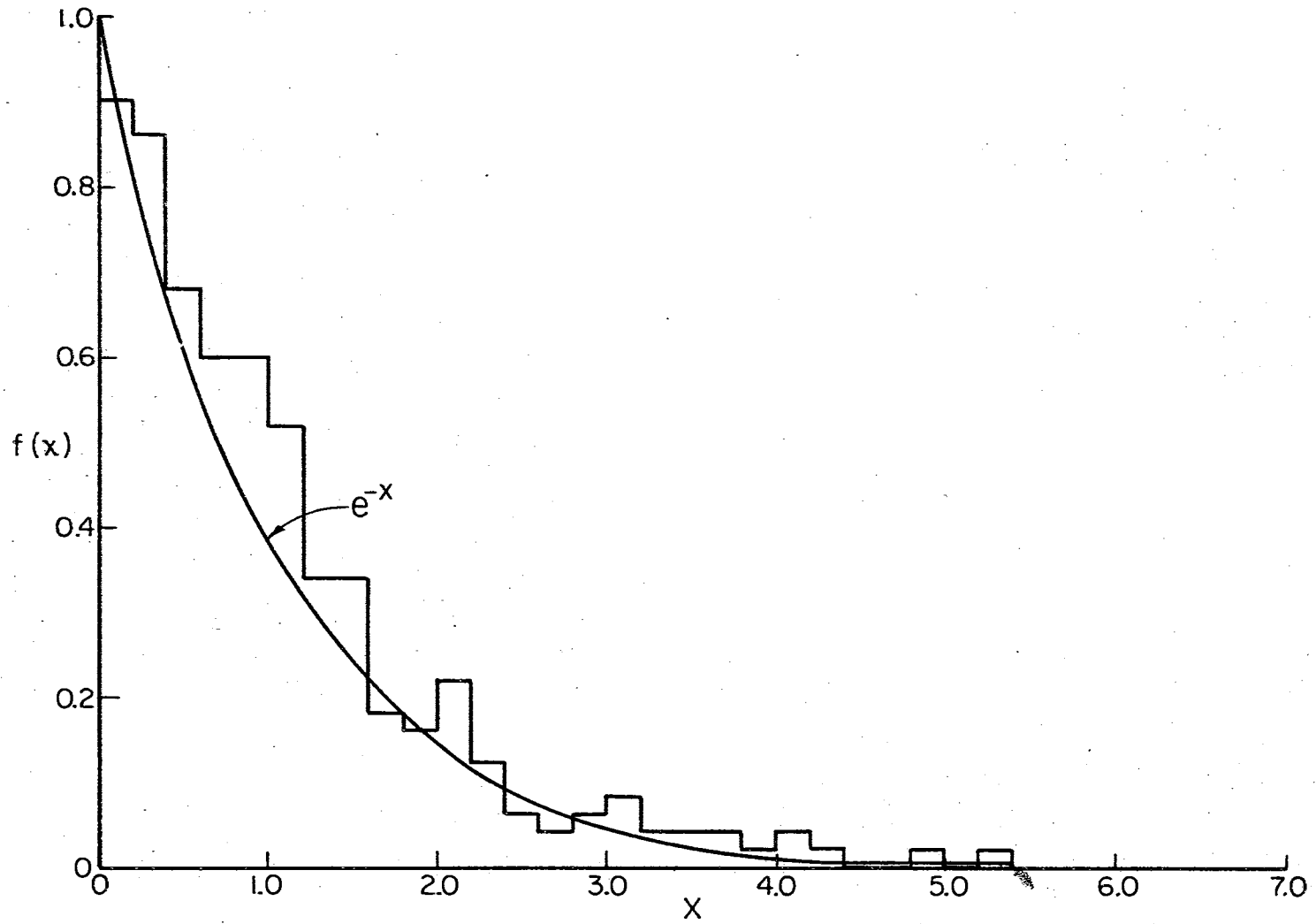
Figure 29. Histogram for Exponentially Distributed Random Numbers

APPENDIX C

TEST EQUIPMENT

A brief description of the test equipment used and the type of data
collected are discussed in this Appendix. The equipment used consisted
of an analog to digital coverter, a fast response anemometer, a standard
4-cup anemometer and an amplitude distribution analyzer (slicer circuit).
Figures a and b of Figure 30 are photographs of the equipment used and
Figure 31 is a block diagram of the data flow. The block diagram shows
the flow of data from the wind source to the computer output.

A-D Converter

Analog or continuous signals were converted to digital voltages and
punched on paper tape by the A-D conversion system designed by Honeywell.
The system consisted of:
1. A power supply which provided regulated power to the other
    units of the system.
2. A model 620 digital voltmeter which encoded and converted the
    voltage reading to a binary number which is then punched on a
    paper tape.
3. A model 700-40 scanner which is a multi-position signal switch
    that can select any one of forty three wire-inputs and route
    the inputs to a single three-wire output.
4. A model 825B output control unit which converts parallel input

(a) Internal Equipment
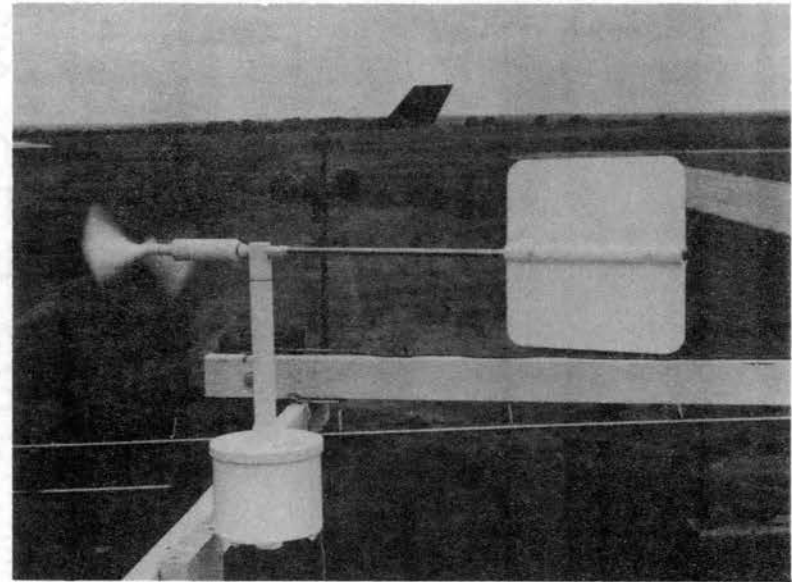
(b) External Equipment

Figure 30. Test Equipment Used to Obtain Wind Velocity Data, (a) Honeywell A-D Equipment (Left), Gill Propeller Anemometer Power Supply and Indicators (Upper Right), Amplitude Distribution Analyzer (Center Right), (b) Gill Propeller Anemometer and 4-cup Anemometer.
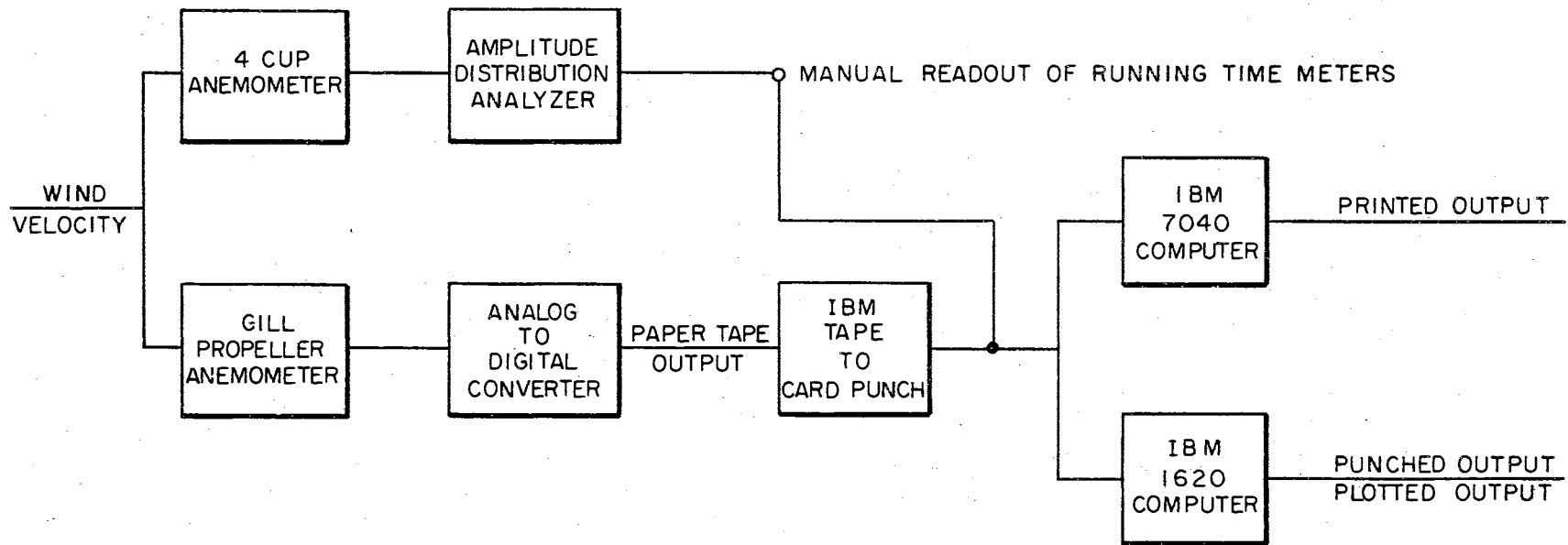
Figure 31. Block Diagram of Data Flow

data from the digital voltmeter to serial output data which is routed to the teletype paper tape punch machine.

5. A Teletype BPRE-11 paper tape perforating machine that receives commands from the digital voltmeter, the scanner and the output control unit to punch a ten character message each time a channel is selected. The message includes the channel number and the digital reading.

Gill Propeller Vane, Model 35001

The Gill Propeller Vane was designed and developed by Gerald C. Gill, Professor of Meteorology of the University of Michigan. The propeller vane provides sensitive measurements of the horizontal wind direction and wind velocity. It was built by the R. M. Young Co., of Ann Arbor, Michigan.

The wind speed sensor section of the vane employs a foamed polystyrene two blade propeller molded in the form of a generated helicoid. The propeller rotates 0.96 revolutions per foot of wind for all speeds above four feet/second (2.7 MPH). The propeller drives a miniature D.C. tachometer generator through a flexible coupling. The wind speed signal is connected through an adjustable resistor to the power supply translator to allow for calibration. The signal is unipolar and adjustable from zero to about $+5\frac{1}{2}$ volts (for 50 MPH full scale). The voltage signal is calibrated to 0.50 volts at 50 MPH and there is a voltage change of 10 millivolts per MPH. The wind speed is directly related to the output voltage, i.e. 0.010 volts represents 10 MPH and 0.020 volts represents 20 MPH.

The propeller specification as taken from the instruction manual

are as follows:

Blades	2
Diameter	9 inches
Range	75 MPH
Threshold	0.3-0.5 MPH
Distance Constant	3.4 feet

In addition to the wind speed sensor there is a wind direction sensor to provide accurate azimuth information and a power supply translator to provide a regulated power supply for the wind direction potentiometers and to provide the necessary calibration adjustments for the wind speed and wind direction signals.

4-Cup Anemometer

The 4-cup anemometer is a non-totalizing anemometer which has 2 3/4 inch cups on a rotor with a turning diameter of 10 inches. It has an alternating current output with the cup wheel starting speed at approximately two MPH. Its output voltage is directly proportional to the cup wheel rotation.

Amplitude Distribution Analyzer

The velocity amplitude distribution analyzer circuit used for data reduction was designed to record the number of hours that the wind velocity was within each of seven velocity levels. Details of the design and theory of operation are presented in Chapter V.

Computers

The IBM 7040 and IBM 1620 were used for data reduction, generation

of models and plotting of data.

Wind Tunnel

The Agricultural Engineering Department's wind tunnel was used for testing and calibration of the amplitude distribution analyzer.

Data Requirement

Information desired from the equipment consisted of values of velocity at sample rates varying from two second samples to samples taken for a duration of one minute each hour. The two second, 20 second, 75 second, 10 minute, and one-half hour samples were necessary data used to calculate parts of the power spectrum described in Chapter IV. The samples taken each hour for a duration of one minute were used to obtain the velocity duration curves. If additional time had been available, hourly averages would have been used for the generation of the remainder of the power spectrum. The hourly samples were also used to make comparisons with the true velocity average for the hour.

APPENDIX D

USEFUL RESULTS AND DATA FOR ANALYSIS

Sampling of Horizontal Wind Records

In order to analyze the horizontal wind velocity, it was necessary
to convert the continuous wind record to a discrete digital record by
sampling. The sampling rate for data used in this study varied from two
second samples to samples taken each hour. The two second, 20 second,
75 second, 10 minute, and one-half hour samples were used to obtain
parts of the spectral estimate.

The sample rate used to estimate the extractable energy in the wind
for comparisons with the simulated model was one sample every two sec-
onds. The sample rate used to obtain the "true" hourly mean velocity
which in turn was compared with the one-minute hourly averages was one
sample every 15 seconds. According to L. Lee (32) the sample rate of
$H = 2$ seconds would introduce an error of 0.74 per cent in the total
energy while the sample rate of $H = 15$ seconds would introduce an error
of less than five per cent.

Power vs. Velocity Curves

Power calculations were made by assuming a six foot diameter propel-
ler. The six foot propeller was assumed because it is a typical size
for many small scale wind generators and because Equation 2.1, $P = KAV^3$,

103

reduces to a simple function of velocity: $0.0001V^3$ kilowatts or $0.1V^3$ watts. Figure 32 depicts power curves plotted as a function of velocity. These curves could be used to obtain an estimate of the power for any length of propeller by multiplying $P = 0.1V^3$ by the necessary factor to change the diameter of the propeller. That is, the maximum theoretical power that could be extracted from a twelve foot diameter propeller would be twice the power values plotted on the figure. This figure is presented to provide a convenient method for relating velocity in miles per hour to power in watts.

Data

The data used in this study to obtain the velocity duration curves are presented. The meter readings at the start and end of data on the distribution analyzer are listed in Table XV. The data for the hourly one-minute averages are presented in Table XVI.
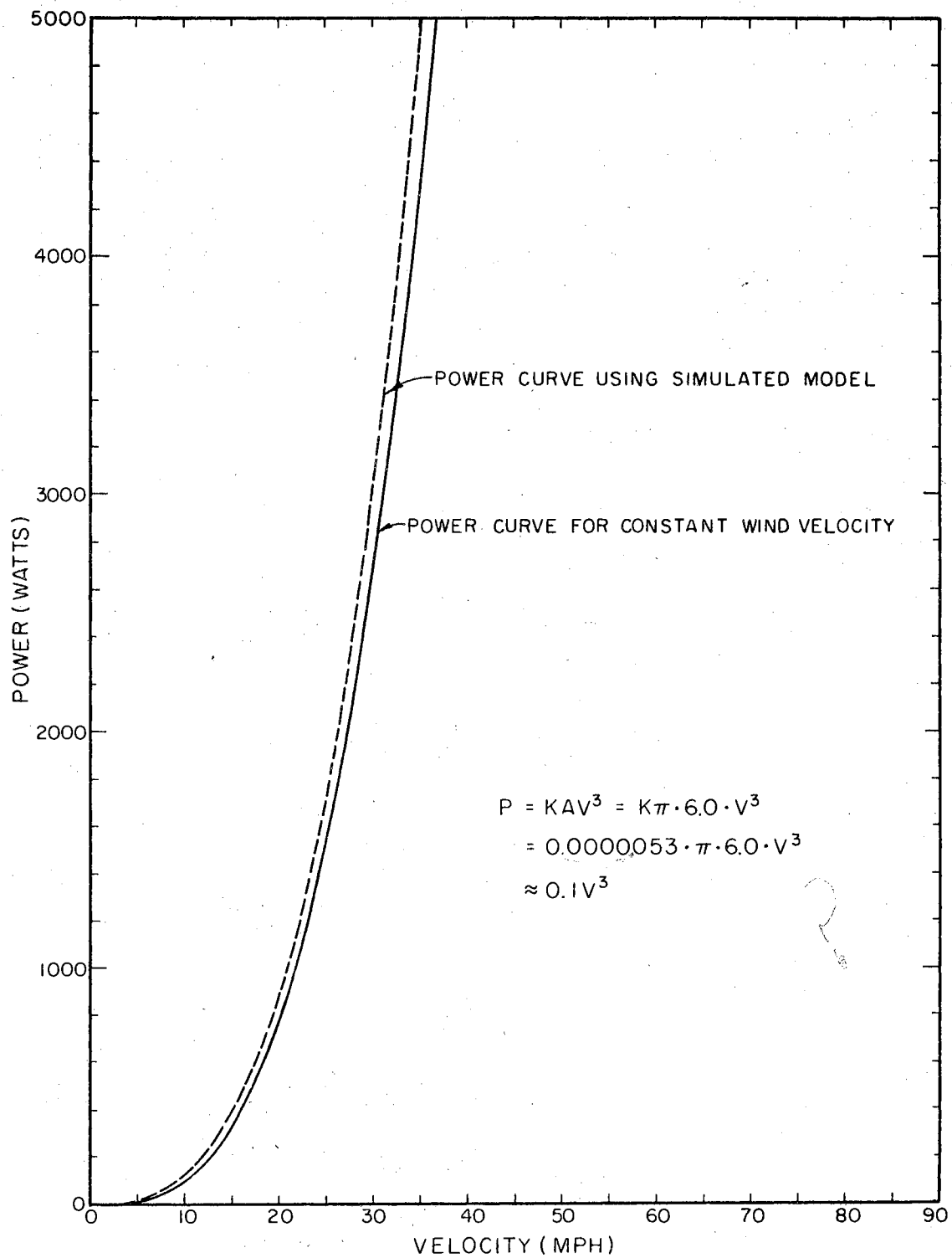
Figure 32. Estimated Power for Given Wind Velocities Using Six
Foot Diameter Propeller

TABLE XV

DATA FROM VELOCITY DISTRIBUTION ANALYZER

Date	Total Time	Meter Number						
		No. 1 0-6MPH	No. 2 6-12MPH	No. 3 12-18MPH	No. 4 18-24MPH	No. 5 24-30MPH	No. 6 30-36MPH	No. 7 36-MPH
Start 0800 23 May, 1968	183,020.6	27,962.2	66,078.0	29,888.5	18,249.2	13,438.2	8,557.9	17,612.6
End 0800 5 July, 1968	244,570.0	46,669.4	89,205.0	40,656.3	24,387.4	15,824.7	9,129.5	17,865.3
Total Time (Minutes) on Each Meter	61,449.4	18.707.2	22,127.0	10,767.8	6,138.2	2,386.5	571.6	252.7
Total Time (Hours) on Each Meter	1,024.1	311.8	368.6	179.5	102.3	39.8	9.5	4.2

TABLE XVI

ONE-MINUTE HOURLY AVERAGES FOR STILLWATER, OKLAHOMA - 0800 23 MAY TO 0800 5 JULY, 1968

	May									June																														July				
Hour	23	24	25	26	27	28	29	30	31	1	2	3	4	5	6	7	8	9	10	11	12	13	14	15	16	17	18	19	20	21	22	23	24	25	26	27	28	29	30	1	2	3	4	5
0100		9.2	20.5	13.3	3.7	4.4	0.4	9.8	7.1	5.2	6.7	2.0	3.4	3.3	8.4	23.2	14.6	10.6	22.1	8.2	4.0	9.5	16.1	33.6	5.1	8.0	3.7	5.9	14.8	7.7	11.8	19.5	5.3	2.4	25.4	0.4	7.0	18.6	22.9	7.3	7.1	7.5	10.1	9.9
0200		1.5	8.2	45.2	4.1	4.1	3.0	8.5	10.8	4.4	9.2	0.3	3.2	3.8	8.6	13.9	10.4	13.9	28.6	6.8	2.2	7.1	20.7	19.6	4.9	4.2	3.8	2.6	17.9	14.3	16.6	25.8	4.0	3.5	15.6	0.4	7.8	17.8	18.5	5.9	7.0	4.1	3.6	10.8
0300		2.8	9.3	12.5	7.7	8.4	4.0	23.1	8.1	9.6	6.6	2.3	2.2	3.9	8.7	10.2	10.5	11.9	20.1	6.1	5.5	7.6	19.8	16.8	2.8	5.4	4.1	1.7	17.2	10.8	12.3	25.9	4.9	2.3	9.9	7.9	8.3	18.5	25.5	4.5	6.1	5.4	6.1	10.6
0400		0.2	10.3	12.0	4.8	6.1	6.2	12.4	14.8	1.5	7.4	3.1	2.7	4.0	6.6	9.7	10.8	15.3	17.6	6.0	1.7	6.5	16.3	10.8	6.5	4.9	3.6	4.2	29.8	11.1	13.3	19.7	5.8	2.8	12.1	4.8	8.2	18.8	21.7	2.3	5.1	5.4	4.8	12.8
0500		6.0	19.4	9.4	2.4	7.1	7.1	11.3	10.7	3.0	6.9	6.7	3.2	6.3	7.7	7.7	5.2	18.9	16.8	8.2	1.1	6.5	16.2	10.2	7.3	6.0	2.6	4.0	8.8	11.8	13.1	19.1	4.3	2.4	19.5	4.6	8.7	25.9	18.8	0.6	3.9	5.6	2.4	7.1
0600		9.5	27.6	10.4	2.7	6.9	6.2	11.4	7.5	4.0	4.4	3.0	4.1	3.3	7.3	11.4	7.1	13.4	22.1	13.1	1.5	3.3	18.3	12.2	6.3	6.1	3.0	6.1	7.2	7.1	12.9	14.5	4.4	7.	16.7	5.9	14.5	19.8	25.9	3.5	3.9	7.1	3.0	5.2
0700		8.7	13.5	13.6	4.2	6.8	5.4	13.2	8.8	2.6	3.9	1.7	3.6	5.2	7.1	9.1	7.9	20.9	16.5	8.9	1.8	3.7	13.2	12.2	7.5	9.7	2.1	9.8	13.8	6.9	12.3	16.8	0.8	5.4	11.4	6.2	13.7	27.3	19.8	1.8	4.8	4.9	2.2	5.1
0800	23.7	9.9	19.6	8.1	0.4	4.5	6.5	8.1	7.2	8.1	7.3	0.3	2.5	6.0	10.8	11.4	6.9	14.4	30.7	9.8	2.6	8.8	14.9	6.8	6.6	6.8	3.8	2.8	14.2	6.6	6.9	12.3	2.0	21.1	21.5	0.7	13.3	29.6	27.3	5.6	9.6	4.2	2.5	
0900	23.2	7.3	8.2	9.0	6.4	8.6	4.6	8.5	6.7	7.3	8.1	2.4	4.6	7.0	17.0	7.6	6.1	18.3	26.5	8.6	7.6	10.8	18.9	12.0	11.0	5.6	5.5	7.8	9.9	5.9	4.3	11.2	3.9	8.6	20.7	5.1	21.2	36.4	29.6	5.9	7.7	2.6	0.6	
1000	11.0	5.7	7.8	10.3	5.4	18.5	4.6	15.4	7.7	3.1	6.0	2.5	7.3	7.8	14.3	6.1	24.4	10.0	16.6	9.4	6.3	9.7	23.8	4.2	5.9	4.3	18.1	8.9	9.9	6.3	4.8	7.2	13.2	6.1	19.6	10.1	23.6	32.2	36.4	5.7	10.8	2.9	0.2	
1100	9.1	8.0	6.1	16.7	16.9	10.8	0.5	7.9	8.5	2.6	5.1	1.1	7.2	13.2	14.0	6.2	86	11.2	15.6	2.9	2.5	15.2	21.6	5.7	2.9	0.4	11.0	9.5	8.2	12.5	6.5	7.8	12.8	2.2	19.8	7.3	22.1	27.2	32.2	3.8	16.8	2.6	0.6	
1200	12.4	8.7	7.9	15.0	17.3	9.3	2.8	6.4	7.1	7.5	7.2	5.3	10.3	13.3	18.9	9.4	10.7	19.7	13.9	4.9	3.6	17.6	19.2	10.1	4.0	8.3	13.9	10.6	7.0	9.4	13.2	6.4	7.9	7.4	16.5	10.2	23.5	33.5	27.2	13.8	15.3	4.6	2.4	
1300	11.6	8.1	8.8	36.7	17.6	12.3	5.8	14.6	10.9	8.0	5.9	3.8	9.1	16.2	20.2	8.6	16.9	20.7	14.4	7.8	9.4	21.9	20.8	17.8	11.1	5.5	9.9	7.1	6.4	6.5	11.3	6.5	12.9	7.7	16.2	12.8	31.7	27.2	19.0	14.5	15.2	3.1	2.5	
1400	11.1	6.4	10.3	16.0	11.6	14.2	1.2	20.2	9.4	8.3	8.0	3.6	14.3	17.1	15.1	13.6	17.6	15.1	7.4	5.9	6.1	22.0	29.6	19.8	10.7	11.9	12.0	6.8	5.9	6.0	6.9	8.3	8.1	6.3	16.9	17.6	28.2	28.2	17.3	32.0	15.5	1.2	3.7	
1500	11.2	5.3	18.4	7.4	14.5	20.8	6.8	20.5	10.6	11.9	10.0	9.6	13.0	21.4	21.4	13.7	22.2	15.2	5.7	7.6	4.2	24.3	24.7	6.5	6.5	7.7	12.9	7.5	7.3	1.7	24.9	5.5	9.0	9.0	15.8	12.6	24.9	33.5	16.2	26.9	17.7	0.3	2.0	
1600	19.0	6.1	11.3	8.4	16.5	18.3	3.2	16.1	5.3	6.1	4.9	8.3	12.7	15.5	16.2	13.2	24.4	19.8	4.5	5.3	5.6	21.8	26.9	7.2	4.1	9.2	6.2	13.4	5.8	0.5	11.6	7.8	6.5	6.0	14.7	17.8	31.9	32.2	24.1	16.1	13.2	1.9	2.2	
1700	15.4	24.1	7.6	15.5	16.4	14.9	7.8	16.2	6.5	6.3	8.9	8.4	6.0	8.3	15.3	13.6	18.7	15.3	4.4	2.8	6.0	23.3	23.5	15.4	3.5	8.7	11.4	4.7	4.1	2.3	13.2	15.3	10.6	13.2	11.8	18.3	32.4	29.0	18.5	17.8	17.3	0.6	1.7	
1800	15.8	6.9	17.1	12.5	10.9	16.1	6.2	10.0	1.3	6.9	4.2	6.8	6.5	14.7	16.0	16.3	14.5	15.2	2.9	2.9	10.1	27.7	22.5	6.3	5.7	11.4	13.3	4.9	8.4	5.8	17.5	20.1	17.6	11.2	16.5	17.5	32.8	30.5	18.2	6.6	10.2	1.1	1.3	
1900	10.6	8.1	12.1	10.7	8.4	8.4	10.0	14.2	8.7	3.5	7.9	4.9	7.2	10.1	18.2	20.4	16.3	31.5	3.0	4.4	10.7	20.8	25.1	4.5	4.3	8.9	7.6	9.7	12.7	6.6	16.7	9.6	10.5	19.1	8.1	21.4	30.3	34.9	23.9	3.9	5.5	0.3	6.8	
2000	8.3	7.7	8.9	10.9	7.9	5.8	13.3	10.9	11.5	2.9	2.0	6.6	6.3	12.1	17.3	13.2	13.1	17.7	2.4	5.6	8.4	22.0	21.2	4.1	4.9	4.7	8.9	9.4	11.7	6.8	17.6	12.6	4.5	14.0	6.6	18.8	20.7	25.2	15.6	5.2	4.7	1.8	5.0	
2100	9.6	5.6	13.9	5.9	7.6	3.5	7.5	14.8	8.4	3.5	5.2	4.8	7.1	6.4	20.9	20.5	11.3	10.7	5.0	6.3	9.4	17.5	18.8	2.1	6.5	4.1	7.8	12.8	10.5	12.3	14.5	6.9	3.6	6.2	3.9	14.9	20.2	20.6	5.0	3.5	6.7	3.3	12.6	
2200	10.5	5.0	3.8	6.1	9.4	6.3	7.7	11.5	6.0	3.6	2.8	6.1	4.0	8.8	23.6	15.8	11.3	10.7	1.8	7.4	4.8	11.3	9.2	1.2	4.6	3.3	7.9	14.6	11.5	14.1	20.1	6.3	3.5	3.6	4.4	12.2	22.1	22.3	9.9	5.0	6.5	3.4	6.9	
2300	8.6	11.0	7.8	4.8	9.2	6.2	7.3	8.5	4.9	4.0	1.1	4.0	3.6	9.0	18.8	19.2	10.3	11.1	1.8	5.4	7.0	13.5	22.9	2.4	3.6	2.9	6.9	15.5	15.3	20.5	17.9	6.4	2.9	14.8	1.7	9.9	27.9	27.7	17.7	4.3	4.1	4.7	5.2	
2400	8.3	14.9	9.4	2.3	5.4	1.6	6.7	10.7	4.2	6.3	3.8	3.6	4.8	13.1	15.3	19.3	12.3	8.2	3.8	6.9	6.0	13.7	15.7	1.0	4.8	4.7	9.3	13.4	10.8	15.9	17.6	6.0	3.2	17.2	1.2	8.9	20.1	26.2	6.3	8.0	4.9	3.6	11.8	

APPENDIX E

TESTING AND CALIBRATION OF VELOCITY DISTRIBUTION ANALYZER

Calibration of the velocity distribution analyzer was accomplished in the Agricultural Engineering Department's wind tunnel. The wind tunnel simulated wind velocities up to approximately 48 miles per hour. The velocity of the air in the wind tunnel was determined by using a static pitot tube which measures the velocity pressure head h. The pitot tube was located in the center of the four foot square tunnel with one opening in the tube in the direct air stream and another opening in the tube perpendicular to the air stream. Both openings are connected to bottles filled with water. As the velocity changes, the openings in the air stream displaces the water. The displacement by the direct air stream represents the head pressure in inches of water due to both velocity and static pressure. The second opening measures displacement of static pressure changes. The static pressures cancel and give a net effect of velocity head directly in inches of water. This velocity head h in inches of water was then converted to H in feet of air then the velocity of the wind tunnel in feet per second was obtained using Equation (E.1).

$$V = \sqrt{2gH} \tag{E.1}$$

where

    V = velocity in wind tunnel (feet per second);

    g = specific gravity (32.3 feet per second^2);

$$H = \frac{\text{density of water}}{\text{density of air} \times 12 \text{ inches/foot}} \times h \text{ inches of water}$$

$$= \frac{62.4 \text{ lb/ft}^3}{0.074 \text{ lb/ft}^3 \times 12 \text{ in/ft}} \times h \text{ in.}$$

$$= 70.25 \text{ h ft. of air.}$$

With the voltmeters connected as shown in Figure 33. The velocity was varied in the wind tunnel to obtain results shown in Table XVII. The values of the direct current voltage were then plotted on Figure 34, thus yielding a calibration curve for the distribution analyzer.

The analyzer circuit had to be recalibrated because a longer input cable from the cup anemometer was used and because the anemometer indicator caused erratic operation on the circuit. Table XVIII shows the results from the second calibration with longer input cable and with the anemometer indicator removed. These results are also plotted on Figure 34. Using the results of this second calibration, the d.c. voltage levels were set to cause switching of the various slices as shown in Table IX of Chapter V.

The switching levels on the analyzer were set in the following manner: the cup anemometer input was switched off; a d.c. power supply was connected to TP 1 in Figure 21, the d.c. power supply was set at the desired voltage setting as found from the calibration curve, Figure 23, and finally the proper potentiometer was adjusted to switch at the set voltage level. The lowest level was set first. Then each higher level was set until the settings were complete. Once each level was set, the procedure was repeated to make sure that the switch levels did not change. The calibration was checked daily to determine if the voltage switching levels were changing. Very few adjustments were required to
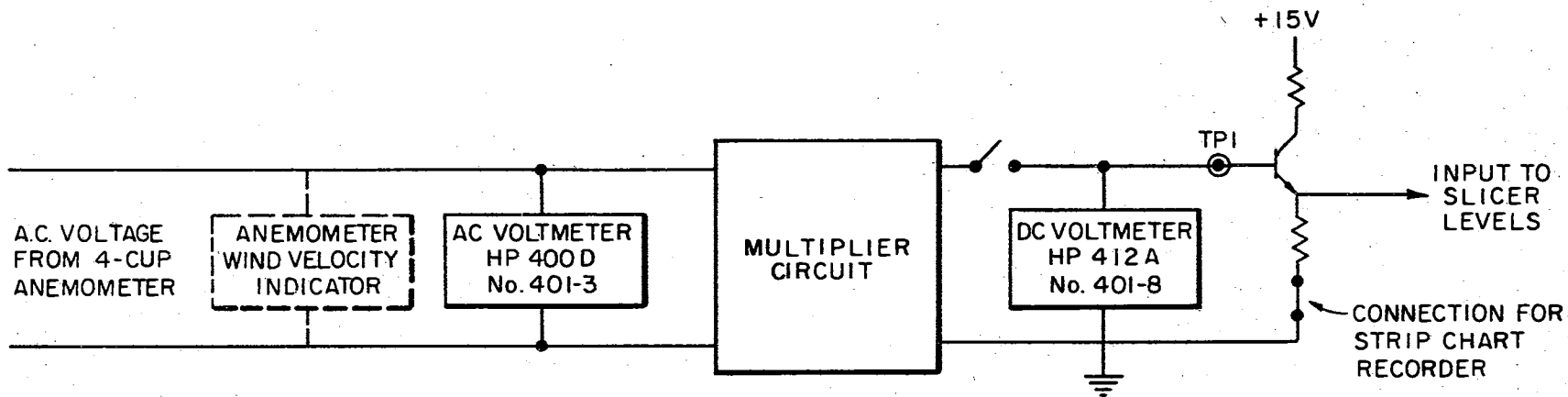
Figure 33. Interconnections of Equipment for Obtaining Calibration Curves of Velocity Distribution
Analyzer

TABLE XVII

TEST RESULTS OF CALIBRATION FOR VELOCITY DISTRIBUTION ANALYZER
(INPUT CABLE 30 FEET ANEMOMETER WIND VELOCITY
INDICATOR CONNECTED)

Run No.	Reading No.	Water Head Reading h	AC Voltage Reading Volts	DC Voltage Reading Volts	Wind Velocity Squared $2hH^*$	Velocity MPH	Anemometer Reading MPH
1	1	0	0.028	1.7	0	0	0
	2	0.040	0.15	2.8	180	9.14	7
	3	0.078	0.34	3.5	352	12.8	10
	4	0.168	0.57	4.6	758	18.75	15
	5	0.281	0.73	5.5	1270	24.3	20
	6	0.432	0.89	6.6	1950	30.1	25
	7	0.568	1.0	7.4	2560	34.6	30
	8	0.793	1.15	8.4	3580	40.9	35
	9	0.880	1.25	9.0	3970	43.0	38
2	1	0	0.028	1.7	0	0	0
	2	0.034	0.15	2.8	154	8.45	6
	3	0.077	0.36	3.5	348	12.8	10
	4	0.168	0.57	4.6	758	18.75	15
	5	0.276	0.72	5.5	1245	24.1	20
	6	0.420	0.88	6.5	1900	29.8	25
	7	0.566	1.0	7.4	2560	34.6	30
	8	0.775	1.15	8.5	3500	39.7	34

$$^*H(\text{ft. of air}) = \frac{62.4 \ \text{lb/ft}^3}{0.074 \ \text{lb/ft}^3 \times 12 \ \text{in/ft}} \times h(\text{in. of water}).$$
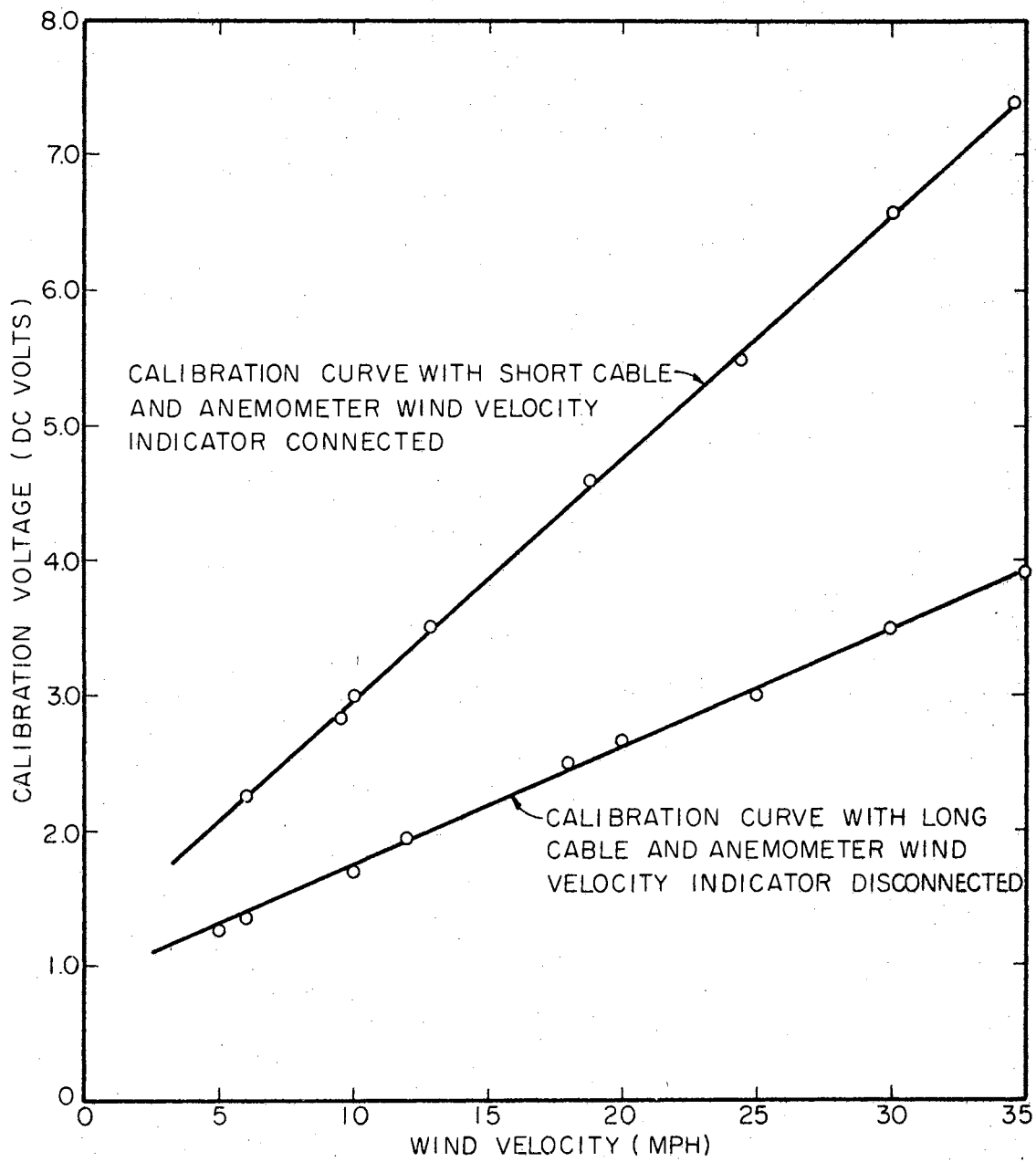
Figure 34. Calibration Curves for Velocity Distribution Analyzer

TABLE XVIII

TEST RESULTS OF CALIBRATION TESTS FOR VELOCITY DISTRIBUTION ANALYZER
(INPUT CABLE 150 FEET ANEMOMETER WIND VELOCITY
INDICATOR REMOVED)

Run No.	Reading No.	Water Head Reading h=in. of water	AC Voltage Reading Volts	DC Voltage Reading Volts	Wind Velocity Squared 2gH[*]	Wind Velocity in Tunnel MPH
1	1	0.049	0.26	1.65	222	10.01
	2	0.089	0.68	2.0	402	13.6
	3	0.123	0.85	2.23	556	16.1
	4	0.151	0.95	2.45	684	17.8
	5	0.185	0.98	2.6	836	19.7
	6	0.223	0.99	2.8	1008	21.6
	7	0.258	1.0	3.0	1168	22.3
	8	0.291	1.0	3.15	1315	24.7
	9	0.333	1.02	3.30	1504	27.1
2	1	0.046	0.25	1.67	208	9.75
	2	0.076	0.65	1.90	343	12.6
	3	0.100	0.80	2.12	450	14.48
	4	0.143	0.91	2.35	646	17.31
	5	0.215	0.98	2.77	971	21.3
	6	0.262	1.0	3.0	1165	23.35
	7	0.321	1.02	3.25	1450	26.0
	8	0.414	1.06	3.55	1860	29.3

$$^*H(\text{ft. of air}) = \frac{62.4 \text{ lb/ft}^3}{0.074 \text{ lb/ft}^3 \times 12 \text{ in/ft}} \times h(\text{in. of water}).$$

keep the switching levels constant.

Errors in the analyzer due to hysterisis are small. The switching circuits of the analyzer had very little hysterisis. Within the accuracy of the d.c. voltage meter used, the switching of the various slice levels occurred at approximately the same voltage level.

The analyzer does have a source of error however, and this source of error occurs whenever the velocity of the wind is blowing at the velocity level set on a slice level. When this occurs, switching from the lower level to the higher level and back to the lower level occurs many times. The running time meters connected to the switches are unable to stop and start as fast as the switching occurs so both meters tend to read slightly higher. This error is not excessive however, and can be neglected. For example in a five day period, the total minutes recorded on the total time meter was 7,167.5 minutes and the total time recorded on the seven slice levels was 7173.8 minutes which results in an error of less than 0.10 per cent.

APPENDIX F

AN APPLICATION FOR THE SIMULATED WIND MODEL

For the technical and economical evaluation of wind power plants,
the knowledge and relationship between wind speed and power output, the
power characteristics, is of great importance. These characteristics
vary according to the type and size of the wind power plant as well as
the rated output of the generator or alternator. Also the mode of oper-
ation has significant influence on the power characteristics. The power
characteristics are different for the system required to have synchronous
interaction with an existing electrical network as compared with the
system feeding a storage battery or a fuel cell.

Obtaining the power characteristics for a specific wind generator
system is relatively simple and can be accomplished by performing static
and dynamic tests on the system. However, optimization of the system is
more difficult because testing of many different propellers, gears, and
generators would be required. As in many other research programs, it is
easier and more economical to use computers as a tool for optimizing the
system. In order to use the computers, an adequate model of the input
must be available.

Once one has access to a suitable model of the input wind velocity,
the optimization of the wind energy system is one step closer. The simu-
lation model of the wind velocity developed in Chapter Three could be
used to determine design parameter curves or power characteristic curves.

The design parameter curves could in turn be used to determine the physical size of the propeller, gears, and other parts of the system. Figure 35 depicts a typical wind energy conversion system that would supply a load coupled through a fuel cell.
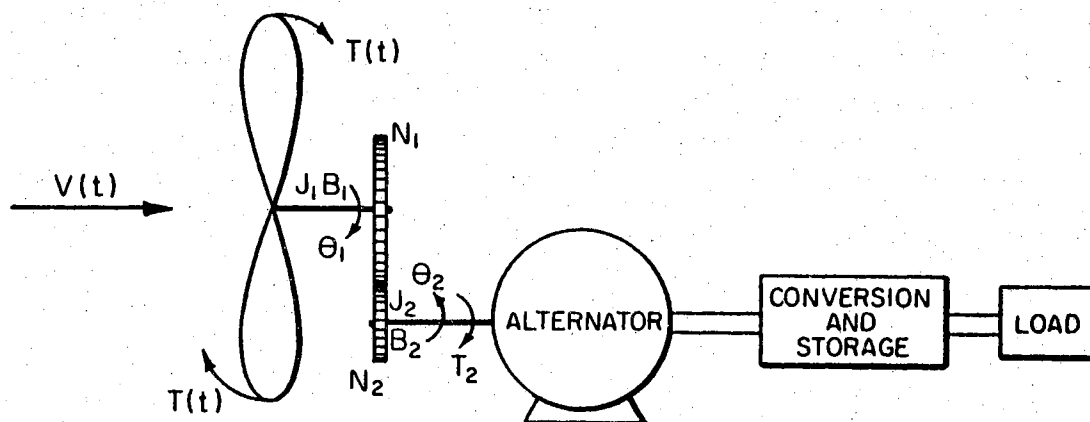

Figure 35. Wind Conversion System Showing Torques, Inertias, and Damping Terms

The input velocity $V(t)$ is simulated using the model in Chapter Three. The input torque $T(t)$ is a function of the input wind velocity and the angular velocity of the propeller shaft. The equations describing the system are obtained using standard control system techniques. Equation F.1 is for the input of the system to gear number one and Equation F.2 represents the system from gear number two to the output or load.

$$J_1 D\Theta_1^2 + B_1 D\Theta_1 + T_1(t) = T(t) \qquad (F.1)$$

$$J_2 D\Theta^2 + B_2 D\Theta + T_L = T(t) \qquad (F.2)$$

where

$D\Theta$ = derivative of $\underline{\Theta}$ with respect to time;

T_1 = load on gear one produced by the rest of the gear train;

T_2 = torque transmitted to gear one to drive the rest of the gear train;

T_L = load torque;

Θ_1 = angular position of shaft one;

Θ_2 = angular position of shaft two;

N = number of teeth of each gear;

$w_1 = D\Theta_1$ = angular velocity of gear one;

$w_2 = D\Theta_2$ = angular velocity of gear two;

$n = \dfrac{w_1}{w_2} = \dfrac{\Theta_1}{\Theta_2} = \dfrac{N_2}{N_1}$ = speed ratio of $\dfrac{\text{driving shaft}}{\text{driven shaft}}$; and

$T_2 = n_a T_1$.

By making the proper substitutions, Equations F.1 and F.2 can be reduced to a single differential equation relating the input torque to the output. Substituting for $T_1(t)$ in Equation F.1 we have:

$$J_1 D^2\Theta_1 + B_1 D\Theta_1 = \frac{1}{n_a} J_2 D^2\Theta_2 + B_2 D\Theta_2 + T_L = T(t)$$

which can be reduced to

$$J_{eq} D^2\Theta_1 + B_{eq} D\Theta_1 + \frac{T_L}{n_a} = T(t) \tag{F.3}$$

where

$$J_{eq} = J_1 + \frac{J_2}{n_a}{}^2$$

and

$$B_{eq} = B_1 + \frac{B_2}{n_a^2} .$$

Equation F.3 could be used for computer analysis by letting J_2 and B_2 include the inertia and friction respectively of the system from gear two to load. Equation F.3 could also be extended if desired to include the differential equations of the alternator or generator and the load.

The values of J_{eq}, B_{eq}, and T_L of a particular system could be determined experimentally then each could be varied individually in the computer analysis of the system. The input torque T(t) in Equation F.3 is the most difficult to determine because the torque is a function of both the input wind velocity and the angular velocity of the propeller shaft. Therefore, one must obtain a relationship between the torque and the input velocity and angular velocity in order to have a meaningful solution to Equation F.3 and in order to determine a relationship between wind speed and output power. Sufficient time was not available to obtain the desired relationship and to perform this very important analysis; however, a suitable model of the input wind velocity was developed for use in this analysis.

The simulated and actual wind velocities shown in Figures 9a and 9b respectively have definite peaks at a frequency of one cycle per minute; therefore one should try to optimize the system in such a way that the output is able to follow the input as closely as possible.

APPENDIX G

COMPUTER PROGRAMS

Two computer programs used in this study are presented in this
appendix. The first was used to simulate the model of the wind and the
second was used to obtain the power spectrum of the horizontal wind
velocity. Other programs were used to reduce and anlyze the data but
they were either simple programs or standard library programs. These
latter programs are not included as part of this report.

In order to use the program to simulate the horizontal wind, it is
necessary to obtain a program that will generate uniform random numbers
which will be used to generate the exponentially distributed random
numbers. The first DO loop must be indexed to yield the desired quantity
of the numbers. Data cards required consist of two cards; one card
Format (F10.0) which indicates the average velocity about which the
simulation is to be made and one card Format (I5) which tells how many
discrete velocities will be generated (usually 100 to 150 for a one hour
simulation). The main program would have card D1A=6.0 changed if one
desired to make calculations for propeller diameters larger or smaller
than six feet.

In order to use the program to calculate the spectrum estimate, the
data corresponding to the sampled velocities are read in with a Format
(24F3.1). The number of velocities is N and the number of lags is M.
If the spectrum is required for values of $m \neq 30$, modifications to ALO,

AL(I), and AL(M) should be made to correspond to the value of m desired.

TABLE XIX

PROGRAM TO SIMULATE HORIZONTAL WIND VELOCITY

```
$ID       A-0001 LEROY A GIBSON              2515-40044
$JOB             LEROY A GIBSON              2515-40044
$IBJOB NAMEPR  MAP
C     SIMULATION OF HORIZONTAL WIND VELOCITY FOR APPLICATIONS TO POWER
C     EXTRACTION FROM THE WIND
C     AMPLITUDE OF THE SIMULATED WIND IS THE SUM OF A CONSTANT PLUS A
C     NORMALLY DISTRIBUTED GUST VELOCITY
C     DURATION BETWEEN VELOCITY AMPLITUDES ARE EXPONENTIALLY DIS-
C     TRIBUTED
C     300 NORMALLY DISTRIBUTED RANDOM NUMBERS ARE READ IN AS Y
C     VARIANCE OF WIND VELOCITY IS A FUNCTION OF ROUGHNESS COEFFICIENT
C     AND INPUT AVERAGE VELOCITY
C     VELOCITIES ARE SIMULATED THEN POWER IS DETERMINED
C     NUMBR- REPRESENTS THE NUMBER OF NORMAL RANDOM NUMBERS TO BE USED
C     UNINUM IS A STANDARD LIBRARY PROGRAM TO CALCULATE UNIFORM RANDOM
C     NUMBERS
      DIMENSION Y(300),VELMAG(300),CUBMAG(300),EXPON(300),GUST(300)
      READ(5,100)Y
C
C     GENERATION OF EXPONENTIAL RANDOM NUMBERS
C
      DO 1 J=1,300
      CALL UNINUM(Z)
1     EXPON(J)=-ALOG(1.-Z)
      READ(5,117)VEL
      READ(5,116)NUMBR
      PI=3.14159
      DIA = 6.0
4     VAR = 6.6*0.005*VEL**2
      STDEV = SQRT(VAR)
      I = 1
      AVEVEL =0.0
      WRITE(6,108)VAR
      WRITE(6,111)
      GUST(I)=STDEV*Y(I)
      VELMAG(I)=VEL + GUST(I)
      CUBMAG(I)= VELMAG(I)**3
      AVEVEL = AVEVEL + CUBMAG(I)
      WRITE(6,113)J,I,K,VELMAG(I),CUBMAG(I),GUST(I),AVEVEL
      J=1
C
C     DETERMINE DURATION BETWEEN DATA SAMPLES
C
5     IF(EXPON(J).LE.0.5)GO TO 10
      IF(EXPON(J).LE.1.5)GO TO 20
      IF(EXPON(J).LE.2.5)GO TO 30
      IF(EXPON(J).LE.3.5)GO TO 40
      IF(EXPON(J).LE.4.5)GO TO 50
C
C     CALCULATE WIND VELOCITY AT NEXT SAMPLE WHEN DURATION IS ONE
C     SAMPLE PERIOD
C
      GO TO 50
10    K=I
      I=I+K
      GUST(I)=STDEV*Y(I)
      VELMAG(I)=VEL + GUST(I)
      CUBMAG(I)= VELMAG(I)**3
      AVEVEL = AVEVEL + CUBMAG(I)
      WRITE(6,110)J,I,K,VELMAG(I),CUBMAG(I),EXPON(J),GUST(I),AVEVEL
      IF(I.GE.NUMBR)GO TO 80
      J=J+1
```

```
      GO TO 5
C
C     CALCULATE WIND VELOCITY AT NEXT TWO SAMPLE PERIODS WHEN DURATION
C     IS TWO SAMPLE PERIODS
C
20    K=2
      N1= I+K/2
      L= I+K
      GUST(L)= STDEV*Y(L)
      VELMAG(L)=VEL + GUST(L)
      CUBMAG(L)= VELMAG(L)**3
      VELMAG(N1)= (VELMAG(I) + VELMAG(L))/2.0
      CUBMAG(N1)= VELMAG(N1)**3
      AVEVEL = AVEVEL + CUBMAG(N1)
      WRITE(6,112)J,N1,K,VELMAG(N1),CUBMAG(N1),AVEVEL
      AVEVEL = AVEVEL + CUBMAG(L)
25    WRITE(6,110)J,L,K,VELMAG(L),CUBMAG(L),EXPON(J),GUST(L),AVEVEL
      IF(I.GE.NUMBR)GO TO 82
      I=L
      J=J+1
      GO TO 5
C
C     CALCULATE WIND VELOCITY AT NEXT THREE SAMPLE PERIODS WHEN DUR-
C     ATION IS THREE SAMPLE PERIODS
C
30    K= 3
      N1= I+ 1
      N2= I+2
      L= I+3
      GUST(L)= STDEV*Y(L)
      VELMAG(L)= VEL + GUST(L)
      CUBMAG(L)= VELMAG(L)**3
      VELMAG(N1)=VELMAG(I) + (VELMAG(L) - VELMAG(I))/3.0
      VELMAG(N2)=VELMAG(I)+ 2.0*(VELMAG(L)-VELMAG(I))/3.0
      CUBMAG(N1)=VELMAG(N1)**3
      AVEVEL = AVEVEL + CUBMAG(N1)
      WRITE(6,112)J,N1,K,VELMAG(N1),CUBMAG(N1),AVEVEL
      CUBMAG(N2)= VELMAG(N2)**3
      AVEVEL = AVEVEL + CUBMAG(N2)
      WRITE(6,112)J,N2,K,VELMAG(N2),CUBMAG(N2),AVEVEL
      AVEVEL = AVEVEL + CUBMAG(L)
35    WRITE(6,110)J,L,K,VELMAG(L),CUBMAG(L),EXPON(J),GUST(L),AVEVEL
      IF(I.GE.NUMBR)GO TO 82
      J=J+1
      I=L
      GO TO 5
C
C     CALCULATE WIND VELOCITY AT NEXT FOUR SAMPLE PERIODS WHEN DUR-
C     ATION IS FOUR SAMPLE PERIODS
C
40    K=4
      N1= I + 1
      N2= I+2
      N3= I+3
      L= I+4
      GUST(L)= STDEV*Y(L)
      VELMAG(L)=VEL + GUST(L)
      CUBMAG(L)= VELMAG(L)**3
      VELMAG(N2)=(VELMAG(I)+VELMAG(L))/2.0
      VELMAG(N1)=(VELMAG(I)+VELMAG(N2))/2.0
      VELMAG(N3)=(VELMAG(L)+VELMAG(N2))/2.0
      CUBMAG(N1)=VELMAG(N1)**3
```

TABLE XIX (Continued)

```
        CUBMAG(N2)=VELMAG(N2)**3
        CUBMAG(N3)=VELMAG(N3)**3
        AVEVEL = AVEVEL + CUBMAG(N1)
        WRITE(6,112)J,N1,K,VELMAG(N1),CUBMAG(N1),AVEVEL
        AVEVEL = AVEVEL + CUBMAG(N2)
        WRITE(6,112)J,N2,K,VELMAG(N2),CUBMAG(N2),AVEVEL
        AVEVEL = AVEVEL + CUBMAG(N3)
        WRITE(6,112)J,N3,K,VELMAG(N3),CUBMAG(N3),AVEVEL
        AVEVEL = AVEVEL + CUBMAG(L)
   45   WRITE(6,110)J,L,K,VELMAG(L),CUBMAG(L),EXPON(J),GUST(L),AVEVEL
        IF(I.GE.NUMBR)GO TO 82
        J=J+1
        I=L
        GO TO 5
C
C       CALCULATE WIND VELOCITY AT NEXT FIVE SAMPLE PERIODS WHEN DUR-
C       ATION IS FIVE SAMPLE PERIODS
C
   50   K=5
        N1= I+1
        N2= I+2
        N3= I+3
        N4= I+4
        L= I+5
        GUST(L)= STDEV*Y(L)
        VELMAG(L)=VEL + GUST(L)
        CUBMAG(L)= VELMAG(L)**3
        VELMAG(N1)=VELMAG(I) +      (VELMAG(L)-VELMAG(I))/5.0
        VELMAG(N2)=VELMAG(I)+2.0* (VELMAG(L)-VELMAG(I))/5.0
        VELMAG(N3)=VELMAG(I)+3.0* (VELMAG(L)-VELMAG(I))/5.0
        VELMAG(N4)=VELMAG(I)+4.0* (VELMAG(L)-VELMAG(I))/5.0
        CUBMAG(N1)=VELMAG(N1)**3
        AVEVEL = AVEVEL + CUBMAG(N1)
        WRITE(6,112)J,N1,K,VELMAG(N1),CUBMAG(N1),AVEVEL
        CUBMAG(N2)=VELMAG(N2)**3
        AVEVEL = AVEVEL + CUBMAG(N2)
        WRITE(6,112)J,N2,K,VELMAG(N2),CUBMAG(N2),AVEVEL
        CUBMAG(N3)=VELMAG(N3)**3
        AVEVEL = AVEVEL + CUBMAG(N3)
        WRITE(6,112)J,N3,K,VELMAG(N3),CUBMAG(N3),AVEVEL
        CUBMAG(N4)=VELMAG(N4)**3
        AVEVEL = AVEVEL + CUBMAG(N4)
        WRITE(6,112)J,N4,K,VELMAG(N4),CUBMAG(N4),AVEVEL
        AVEVEL = AVEVEL + CUBMAG(L)
   55   WRITE(6,110)J,L,K,VELMAG(L),CUBMAG(L),EXPON(J),GUST(L),AVEVEL
        IF(I.GE.NUMBR)GO TO 82
        J=J+1
        I=L
        GO TO 5
   80   T=I
        GO TO 90
   82   T=L
C
C       CALCULATE EXTRACTABLE POWER USING SIMULATED VELOCITIES
C       CALCULATE POWER USING INPUT AVERAGE VELOCITY,POW1
C
   90   AVEVEL= (AVEVEL/T)
        POWER= 0.0000053*PI*DIA*AVEVEL
        POW1= 0.0000053*PI*DIA*VEL**3
        WRITE(6,103)POWER
        WRITE(6,104)POW1
        XVEL= 0.0
```

```
        DO 95 K=1,NUMBR
        XVEL = XVEL + VELMAG(K)
        T=K
C
C       DETERMINE AVERAGE VELOCITY OF SIMULATED WIND VELOCITY
C       CALCULATE POWER USING DERIVED AVERAGE VELOCITY,POW2
C       ADJUST POWER USING SIMULATED VELOCITIES BY THE RATIO=POW1/POW2
C
   95   XVELAV = XVEL/T
        WRITE(6,101)XVEL,XVELAV,T
        POW2= 0.0000053*PI*DIA*XVELAV**3
        RATIO=POW1/POW2
        ADJPOW = POWER*RATIO
        WRITE(6,114)
        WRITE(6,115)POW1,POW2,RATIO,POWER,ADJPOW
        READ(5,116)NUMBR
        IF(NUMBR.EQ.0)GO TO 98
        GO TO 4
   98   READ(5,117)VEL
        IF(VEL.EQ.0.0)CALL EXIT
        READ(5,116)NUMBR
        GO TO 4
   99   CONTINUE
  100   FORMAT(5F15.8)
  101   FORMAT(5XE15.8,5XE15.8,5XF6.0)
  102   FORMAT(11HXAVELVEL=  ,E15.8)
  103   FORMAT(11HXPOWER =   ,E15.8)
  104   FORMAT(10H XPOW1 =   ,E15.8)
  108   FORMAT(5XE15.8)
  110   FORMAT(1X,I4,I4,I4,2XE15.8,2XE15.8,2XE15.8,2XE15.8,2XE15.8)
  111   FORMAT(80HX    J   I   K      VELMAG(I)          CUBMAG(I)      EXPON(J)
        1      GUST(I)        AVEVEL)
  112   FORMAT(1X,I4,I4,I4,2XE15.8,2XE15.8,36XE15.8)
  113   FORMAT(1X,I4,I4,I4,2XE15.8,2XE15.8,19XE15.8,2XE15.8)
  114   FORMAT(92H      POW1                    POW2                    RATIO
        1          POWER                ADJPOW)
  115   FORMAT(5(5XE15.8))
  116   FORMAT(I5)
  117   FORMAT(F10.0)
        CALL EXIT
        END
$IBLDR UNINUM  06/26/67                                                        UNIN0001
$CDICT UNINUM                                                                  UNIN0002
*/ G(' O'  9*(P J *P*O  **)O  **)O  *(PO '                                     UNIN0003
$TEXT  UNINUM                                                                  UNIN0004
*O *(P*7V*7(*7-*(P76 75 74 7' 74 0  74'7' 749'4'0477' 758769'4'448'4 4 'UNIN0005
*O9'((*7(*7(*7-C '49+' =19 ' 91 '9 '7 '2 'E 77 '7T'' =9 '7 '7T7' =9 71 'UNIN0006
*X8PP(*7('7VX  9 '4 '' 61 '6 '94 5 9- 9     '     =-  9 '                       UNIN0007
$OKEND UNINUM                                                                  UNIN0008
$ENTRY
```

TABLE XX

PROGRAM TO CALCULATE SPECTRUM ESTIMATE FOR m = 30

```
$JOB    WATFOR      LEROY A GIBSON              2515-40044
C       PROGRAM TO CALCULATE SPECTRUM BY MEAN LAGGED PRODUCTS
C       NUMBER OF LAGS,M=30
C       LAG PRODUCTS=SUM OF N-P LAG PRODUCTS/N-P
C       CALCULATE LINE POWERS,(COSINE TRANSFORM OF AUTOCORRELATION
C       CALCULATE SMOOTHED SPECTRUM BY HAMMING
        DIMENSION R(30),X(1800),RR(1800),L(30),U(30),AL(30),RO(1800)
        DIMENSION W(1800)
        N=1800
        M=30
        PI=3.14159
        READ(5,100)(W(I),I=1,N)
        XVEL=0.0
        DO 1 I=1,N
        XVEL=XVEL+W(I)
1       XMEAN=XVEL/FLOAT(N)
        I=1
C       MULTIPLY BY 0.447 TO CONVERT VEL. FROM MPH TO METER/SEC
2       X(I)=0.4470*(W(I)-XMEAN)
        IF(I.EQ.N)GO TO 3
        I=I+I
        GO TO 2
3       WRITE(6,101)(X(I),I=1,N)
        RO=0.0
        DO 5 I=1,N
        RO(I)=X(I)*X(I)
5       RO= RO + RO(I)
        RO=RO/FLOAT(N)
        WRITE(6,105)RO
        RRR=0.0
        DO 20 K=1,M
        DO 10 I=1,N
        IK=I+K
        IF(IK.GT.N)GO TO 15
        RP(I)=X(I)*X(IK)
10      RRR=RR(I)+RRR
15      R(K)=RRR/(FLOAT(N)-FLOAT(K))
        WRITE(6,103)K,R(K)
20      RRR=0.0
C
C       CALCULATE LINE POWERS
C
        RX=0.0
        DO 25 K=1,29
25      RX=RX+R(K)
        ALO=(0.5/FLOAT(M))*(RO+R(M)))+ RX/FLOAT(M)
        N=M-1
        WRITE(6,104)ALO
        DO 30 I=1,N
        T=I
        Z=T*PI
        Y=(T*PI)/FLOAT(M)
        RSUM1=R(10)*COS(10.*Y)+R(11)*COS(11.*Y)+R(12)*COS(12.*Y)+R(13)*
       1COS(13.*Y)+R(14)*COS(14.*Y)+R(15)*COS(15.*Y)+R(16)*COS(16.*Y)+
       2RU(17)*COS(17.*Y)+R(18)*COS(18.*Y)+R(19)*COS(19.*Y)+R(20)*
       3COS(20.*Y)
        RSUM2=R(21)*COS(21.*Y)+R(22)*COS(22.*Y)+R(23)*COS(23.*Y)+R(24)*
       1COS(24.*Y)+R(25)*COS(25.*Y)+R(26)*COS(26.*Y)+R(27)*COS(27.*Y)+
       2RU28)*COS(28.*Y)+R(29)*COS(29.*Y)
        AL(I)=(RO+R(M)*COS(Z))/FLOAT(M)+ ((R(1)*COS(1.*Y)+R(2)*COS(2.*Y)+
       1RU3)*COS(3.*Y)+R(4)*COS(4.*Y)+R(5)*COS(5.*Y)+R(6)*COS(6.*Y)+
       2R(7)*COS(7.*Y)+R(8)*COS(8.*Y)+R(9)*COS(9.*Y)+RSUM1+
```

```
       3RSUM2)*2.0)/FLOAT(M)
30      WRITE(6,104)AL(I)
        AL(M)=0.5*(RO + R(M))/FLOAT(M) +(-R(1)+R(2)-R(3)+R(4)-R(5)+R(6)-
       1 R(7)+R(8)-R(9)+R(10)-R(11)+R(12)-R(13)+R(14)-R(15)+R(16)-R(17)+
       2R(18)-R(19)+R(20)-R(21)+R(22)-R(23)+R(24)-R(25)+R(26)-R(27)+R(28)-
       3R(29))/30.0
        WRITE(6,104)AL(M)
C
C       CALCULATE SMOOTHED SPECTRUM
C
        UO=0.54*ALO+0.46*AL(1)
        WRITE(6,105)UO
        DO 50 K=1,M
        IF(K.EQ.1)GO TO 45
        IF(K.EQ.M)GO TO 46
        UU(K)=0.54*AL(K)+.23*(AL(K-1) +AL(K+1))
        GO TO 50
45      U(K)=0.54*AL(K)+0.23*(ALO+AL(K+1))
        GO TO 50
46      U(K)=0.54*AL(K)+0.46*AL(K-1)
50      CONTINUE
        DO 60 K=1,M
60      WRITE(6,103)K,U(K)
100     FORMAT(24F3.1)
101     FORMAT(8(1XE15.8))
102     FORMAT(5XE15.8,5XE15.8)
103     FORMAT(I6,5XE15.8)
104     FORMAT(5XE15.8)
105     FORMAT(6HOUO,  ,E15.8)
        CALL EXIT
        END
$ENTRY
```

APPENDIX H

WIND VELOCITY PLOTS FOR WILL ROGERS INTERNATIONAL AIRPORT
FOR THE YEAR 1962

Daily variations of wind velocity obtained by averaging twenty four

one-minute hourly averages are presented for each month during the year

1962. These data are presented to provide a qualitative indication of

the wind characteristics for Oklahoma City. Results that one could

obtain from plots of this nature might be, the number of zero readings

or the number of days each month that the wind velocity was below some

desired velocity such as cut in velocity of a given generator. These

data were obtained from Local Climatological Data (Supplement) for Will

Rogers Airport, Oklahoma City, Oklahoma.
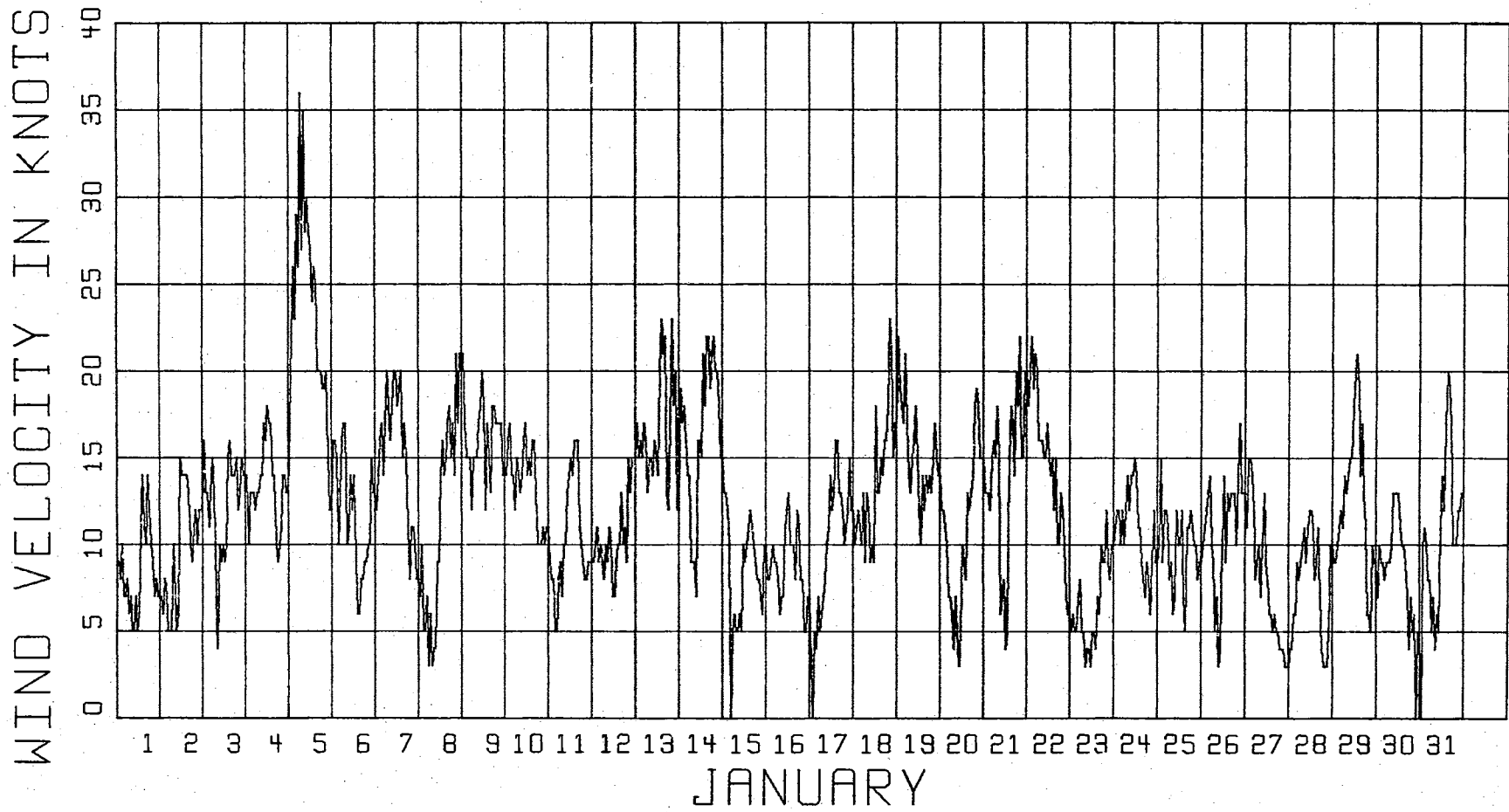
Figure 36. Wind Velocity for January, 1962, Using Standard Meteorological Data
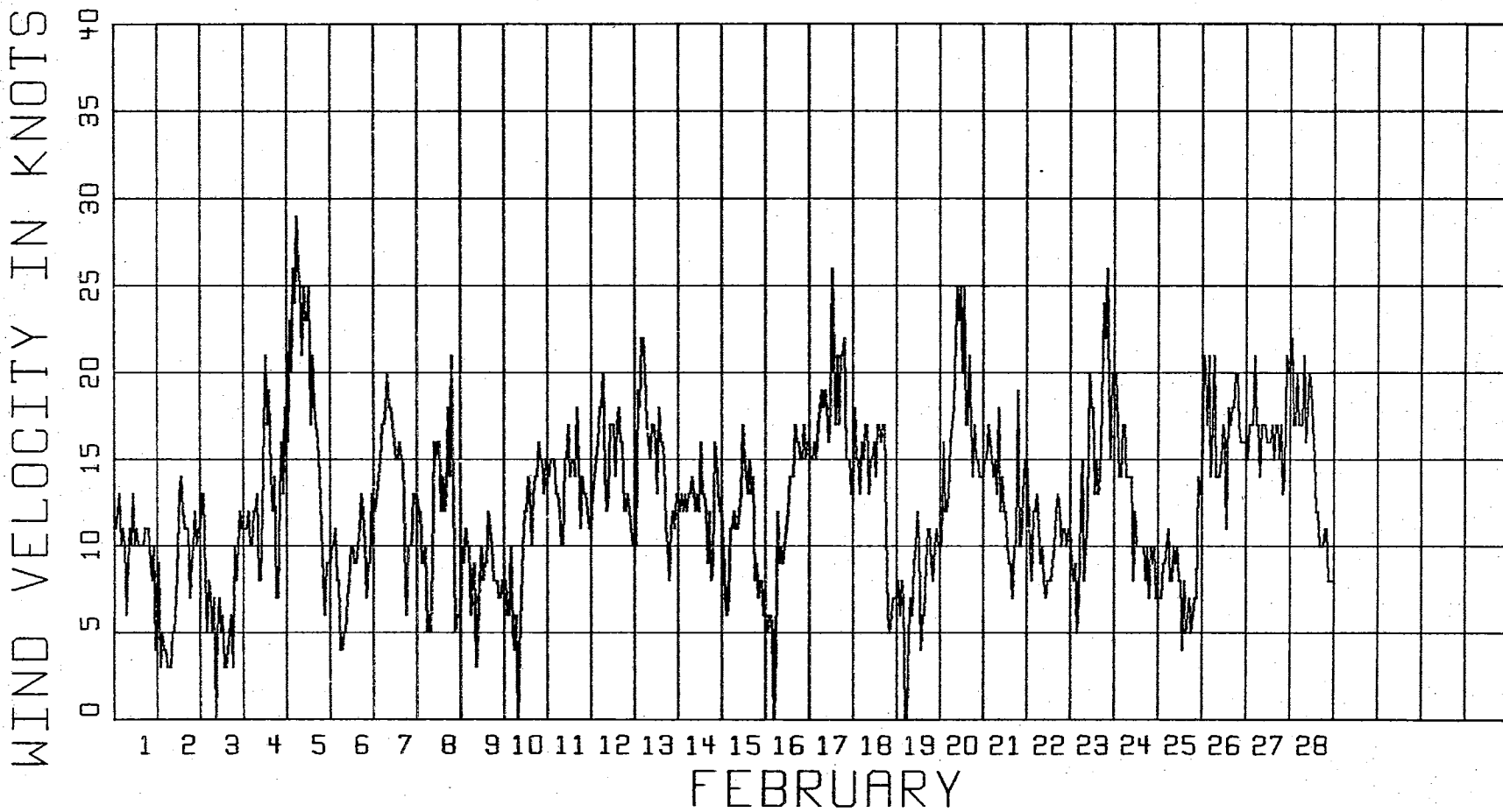
Figure 37. Wind Velocity for February, 1962, Using Standard Meteorological Data
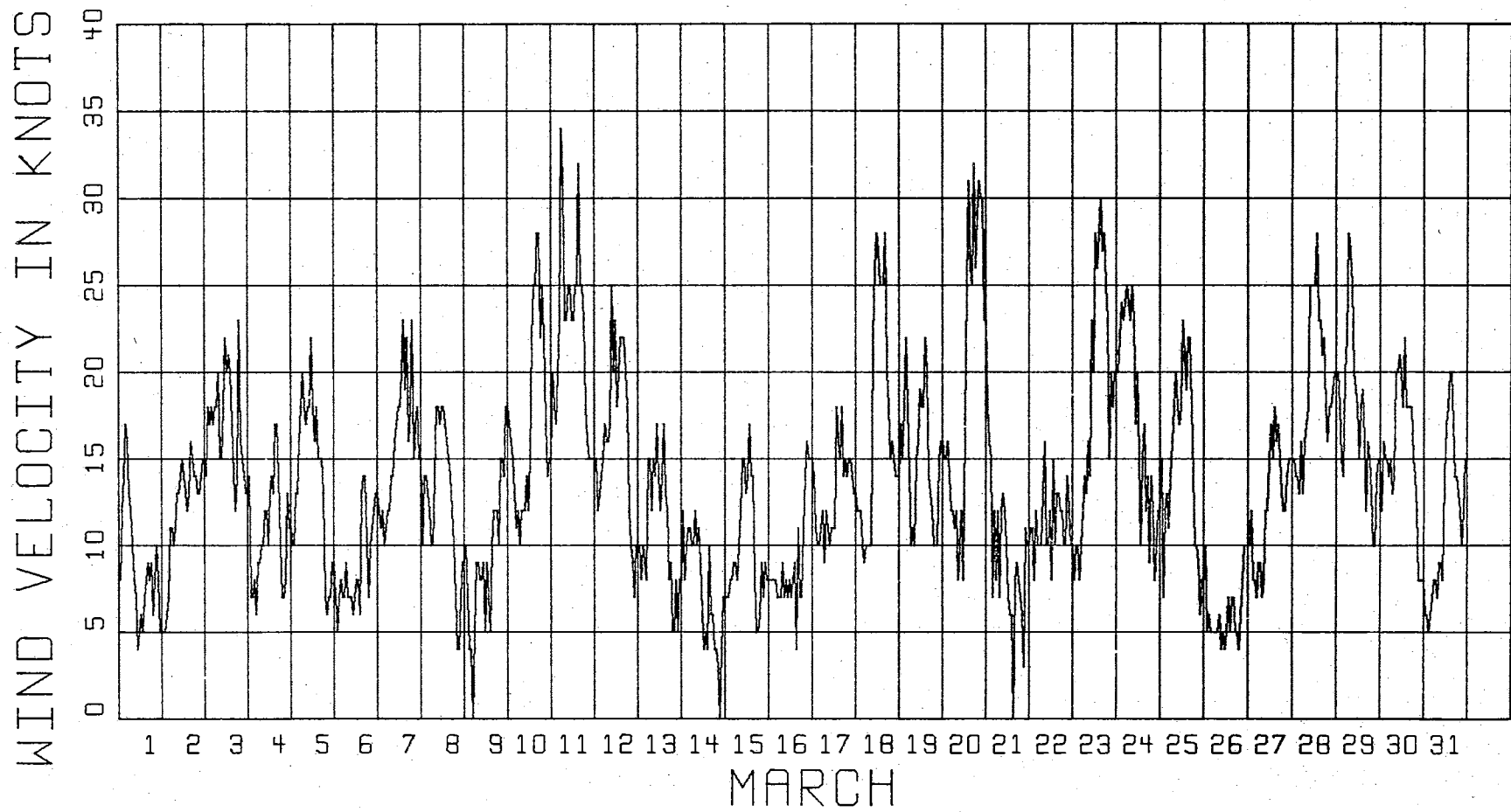
Figure 38. Wind Velocity for March, 1962, Using Standard Meteorological Data
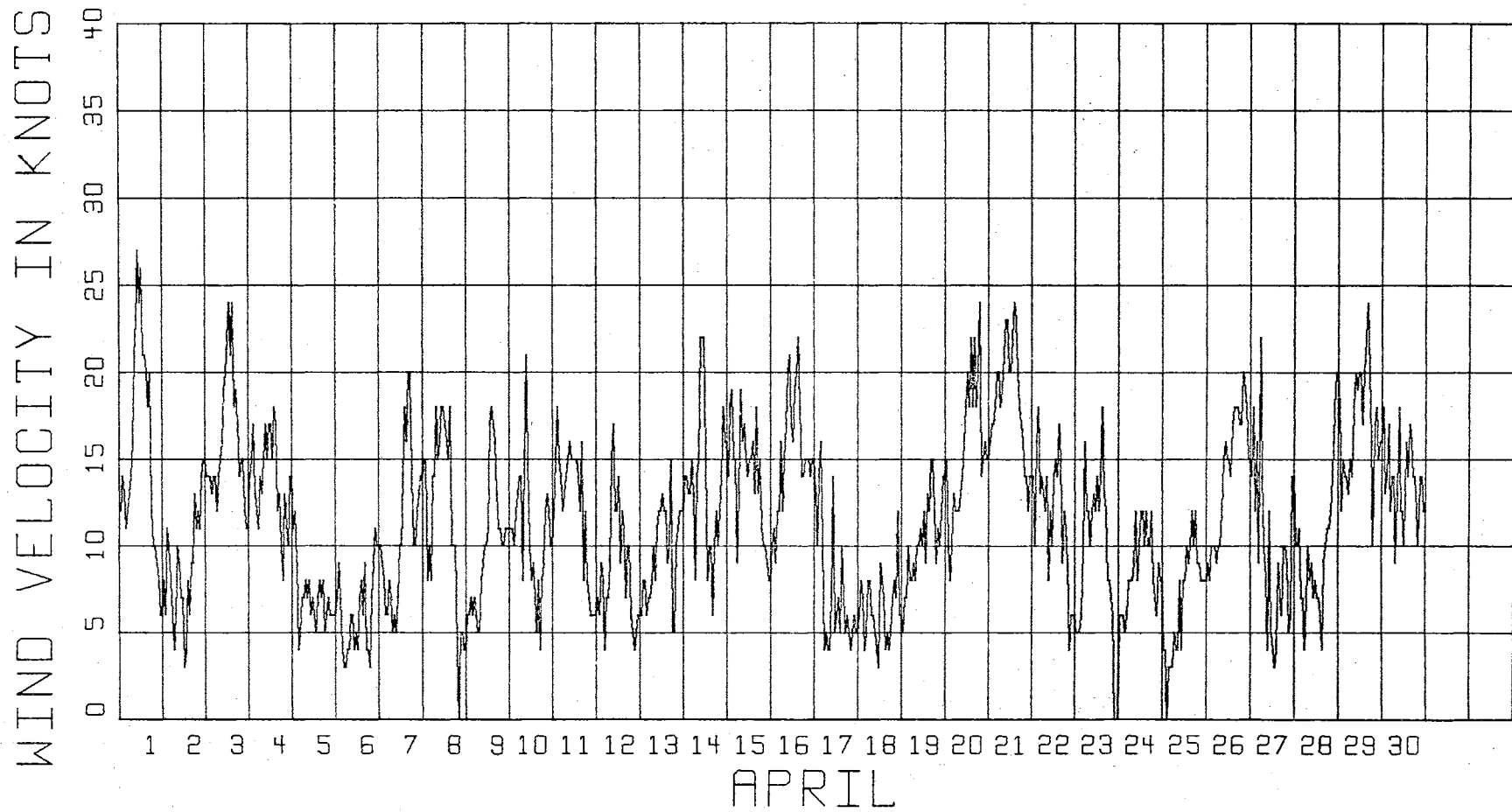
Figure 39. Wind Velocity for April, 1962, Using Standard Meteorological Data
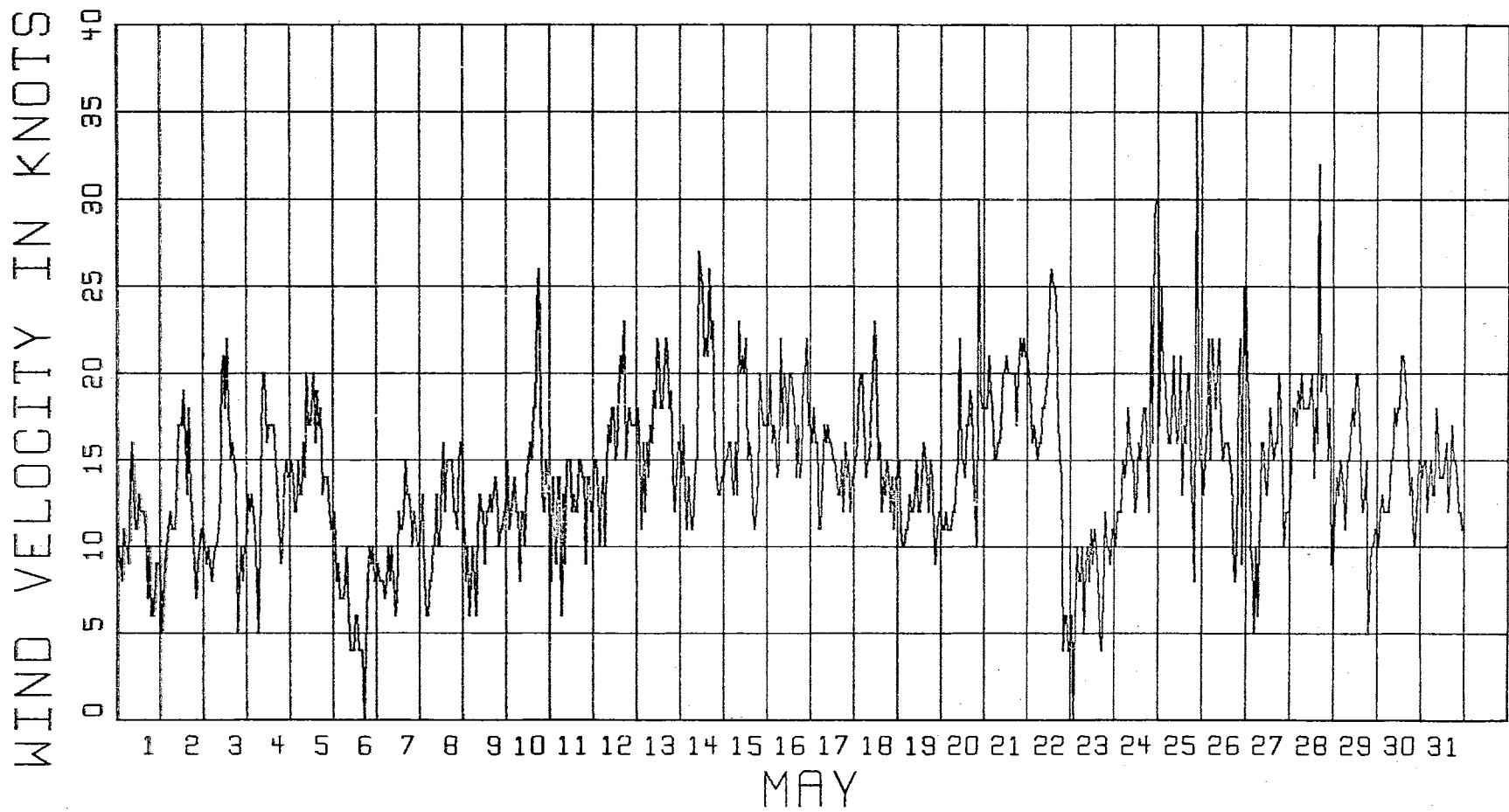
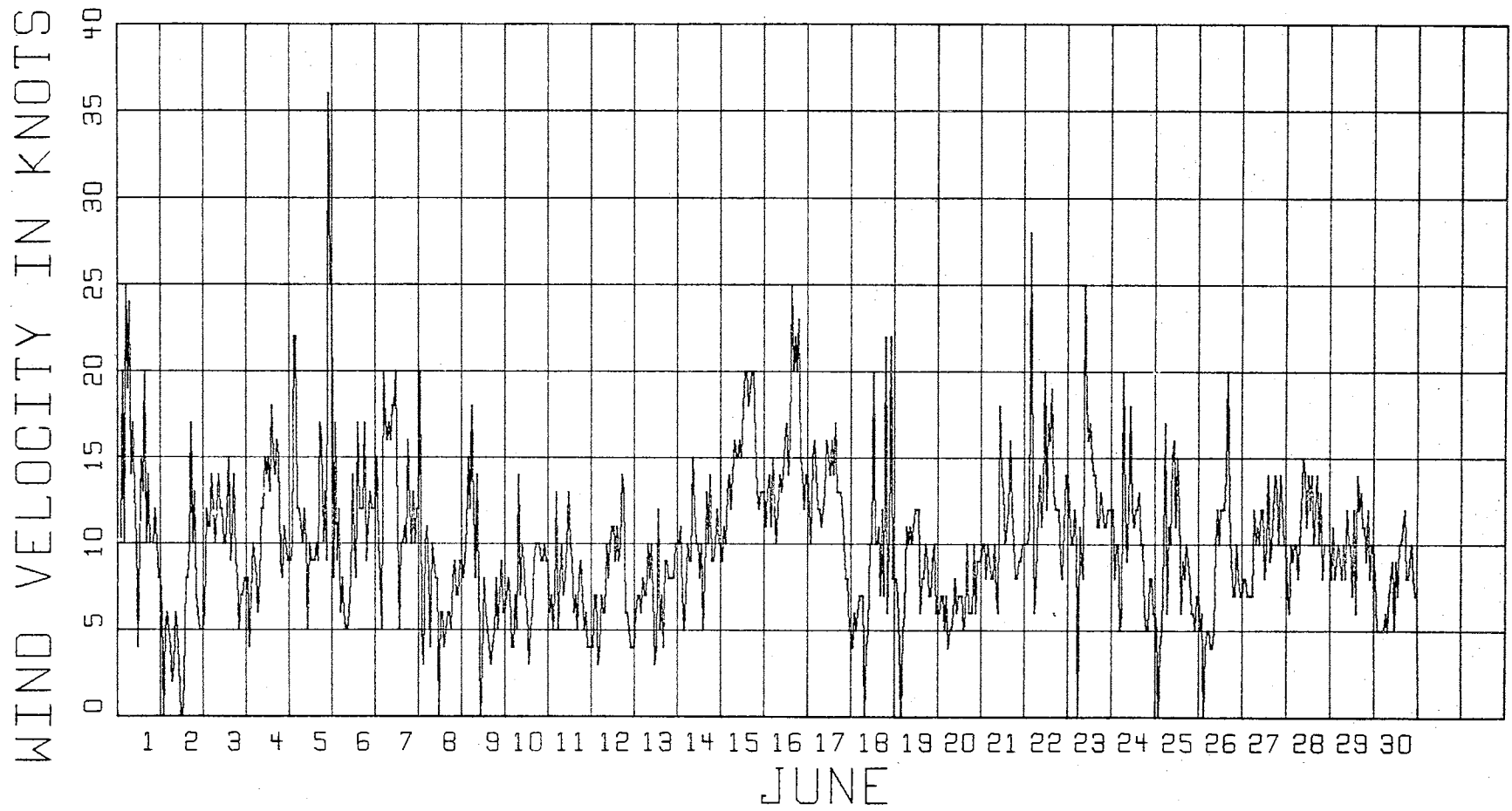Figure 40. Wind Velocity for May, 1962, Using Standard Meteorological Data

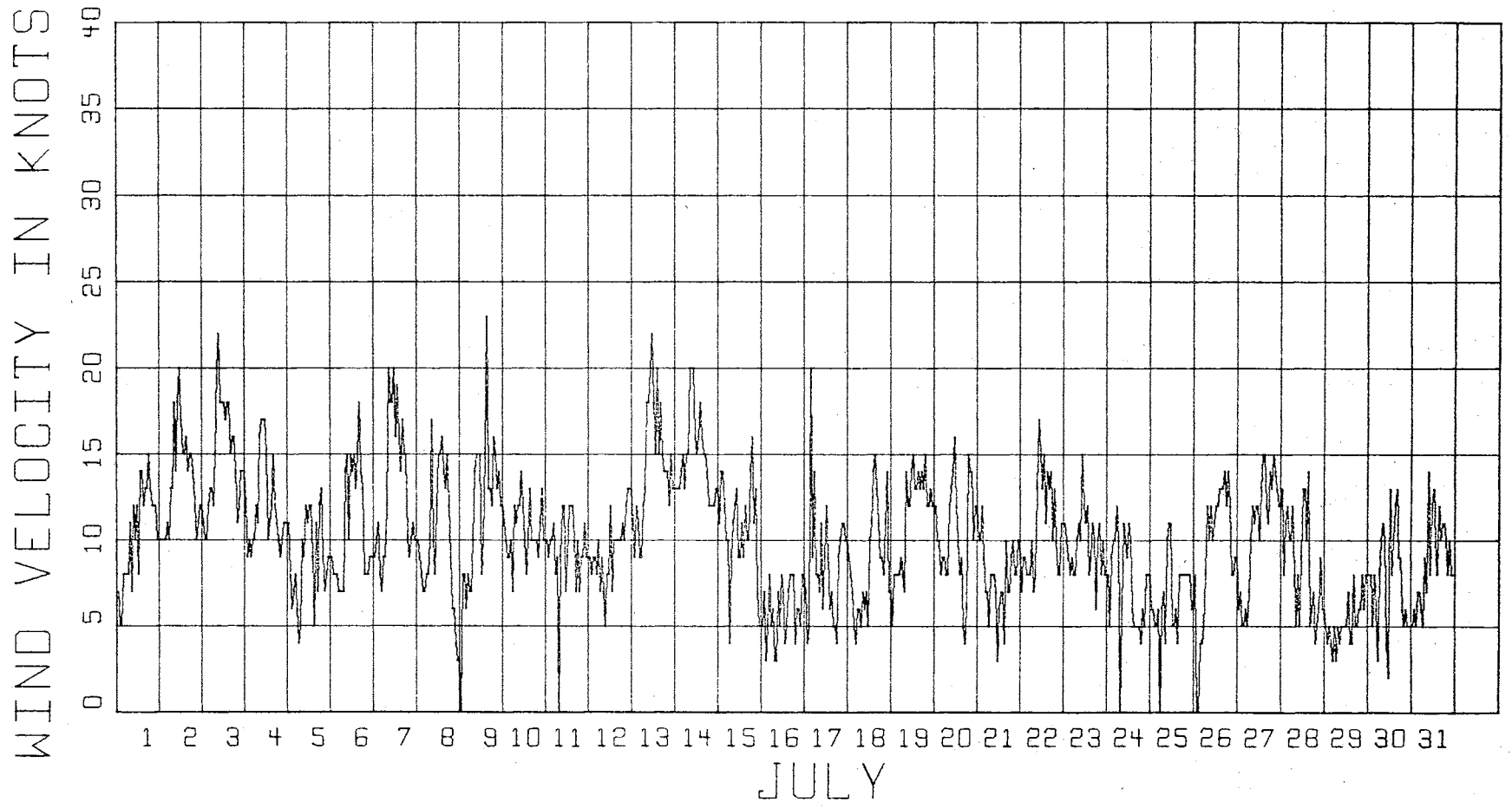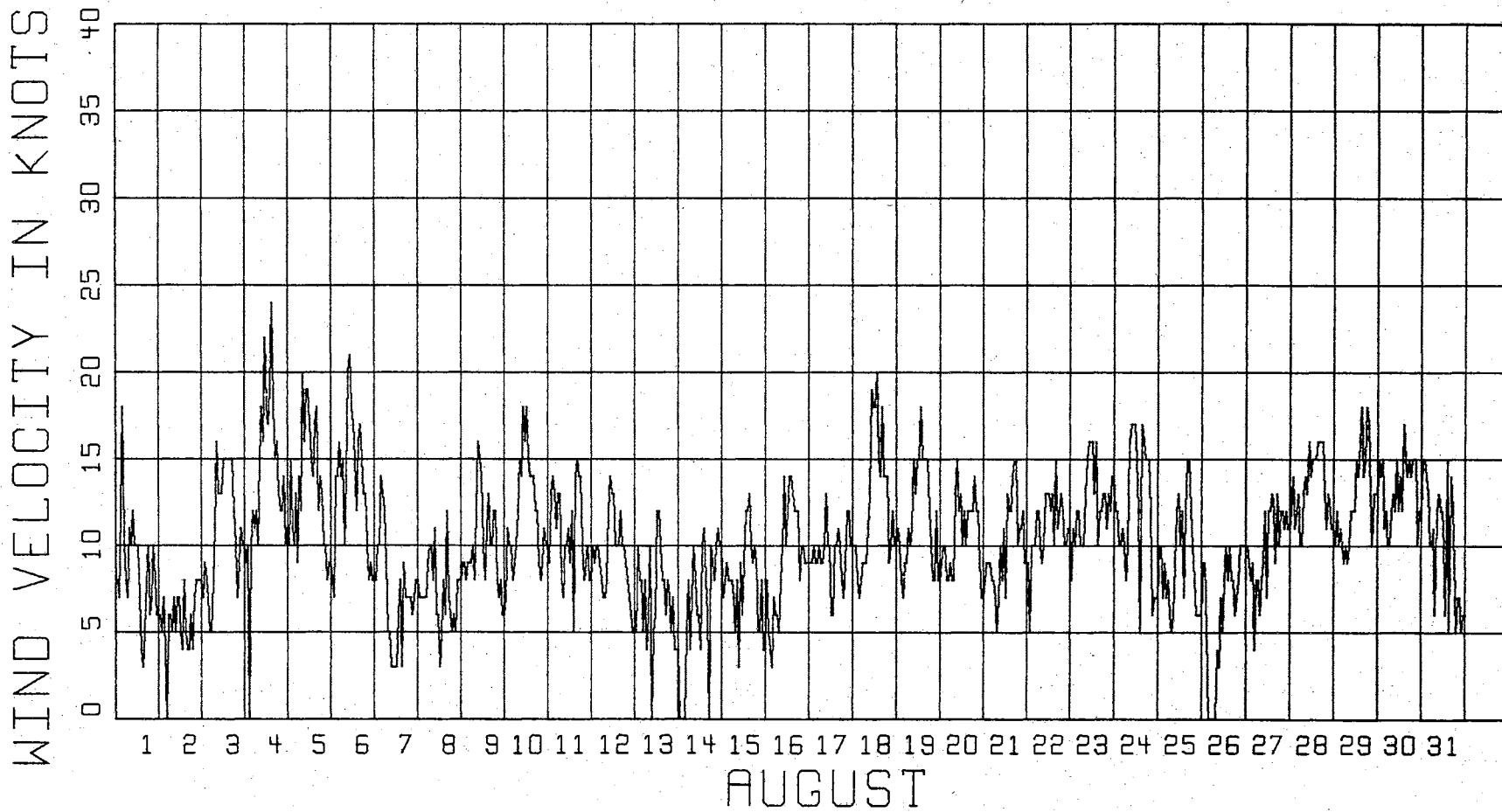Figure 41. Wind Velocity for June, 1962, Using Standard Meteorological Data

Figure 42. Wind Velocity for July, 1962, Using Standard Meteorological Data

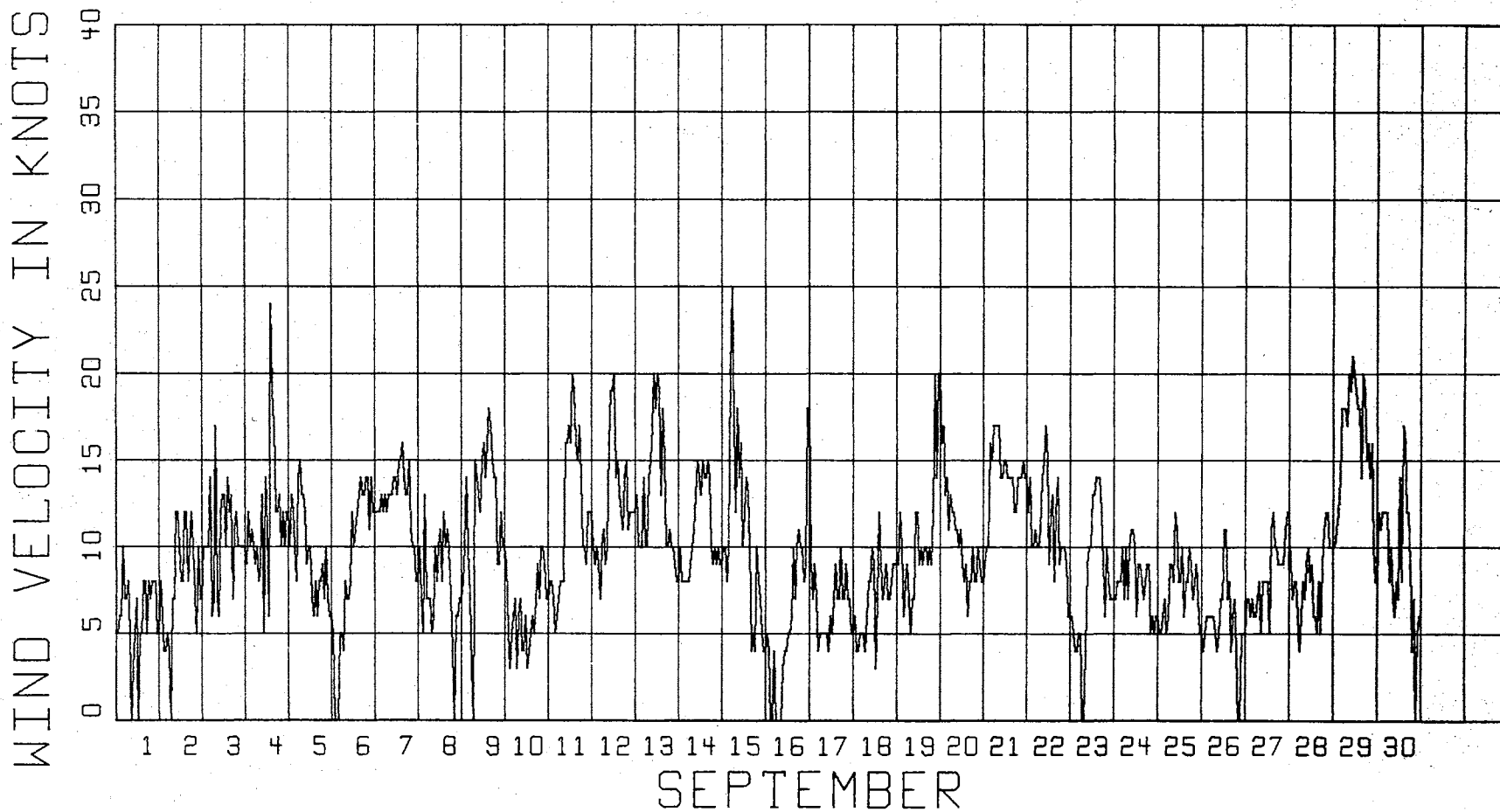Figure 43. Wind Velocity for August, 1962, Using Standard Meteorological Data

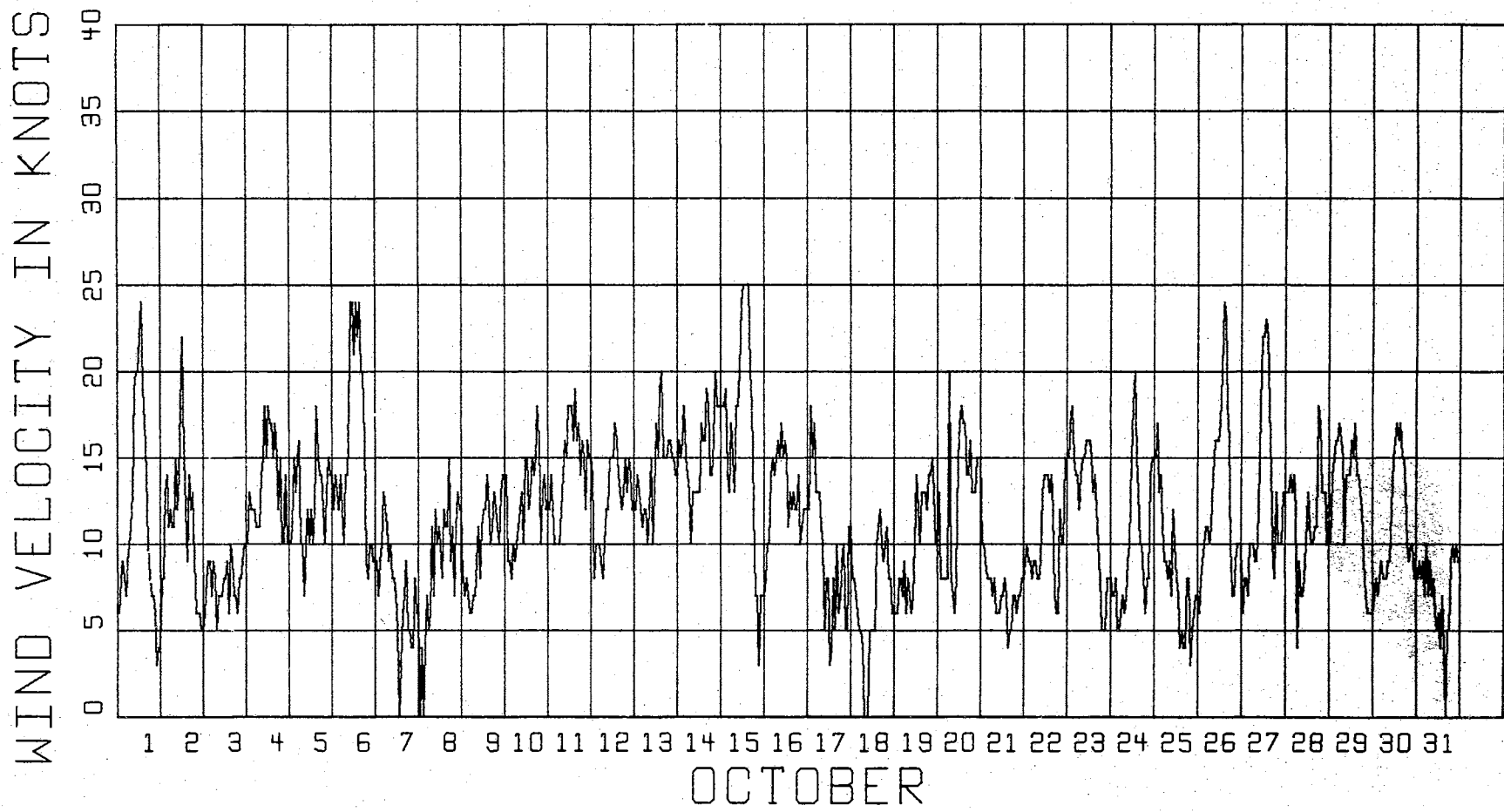Figure 44. Wind Velocity for September, 1962, Using Standard Meteorological Data

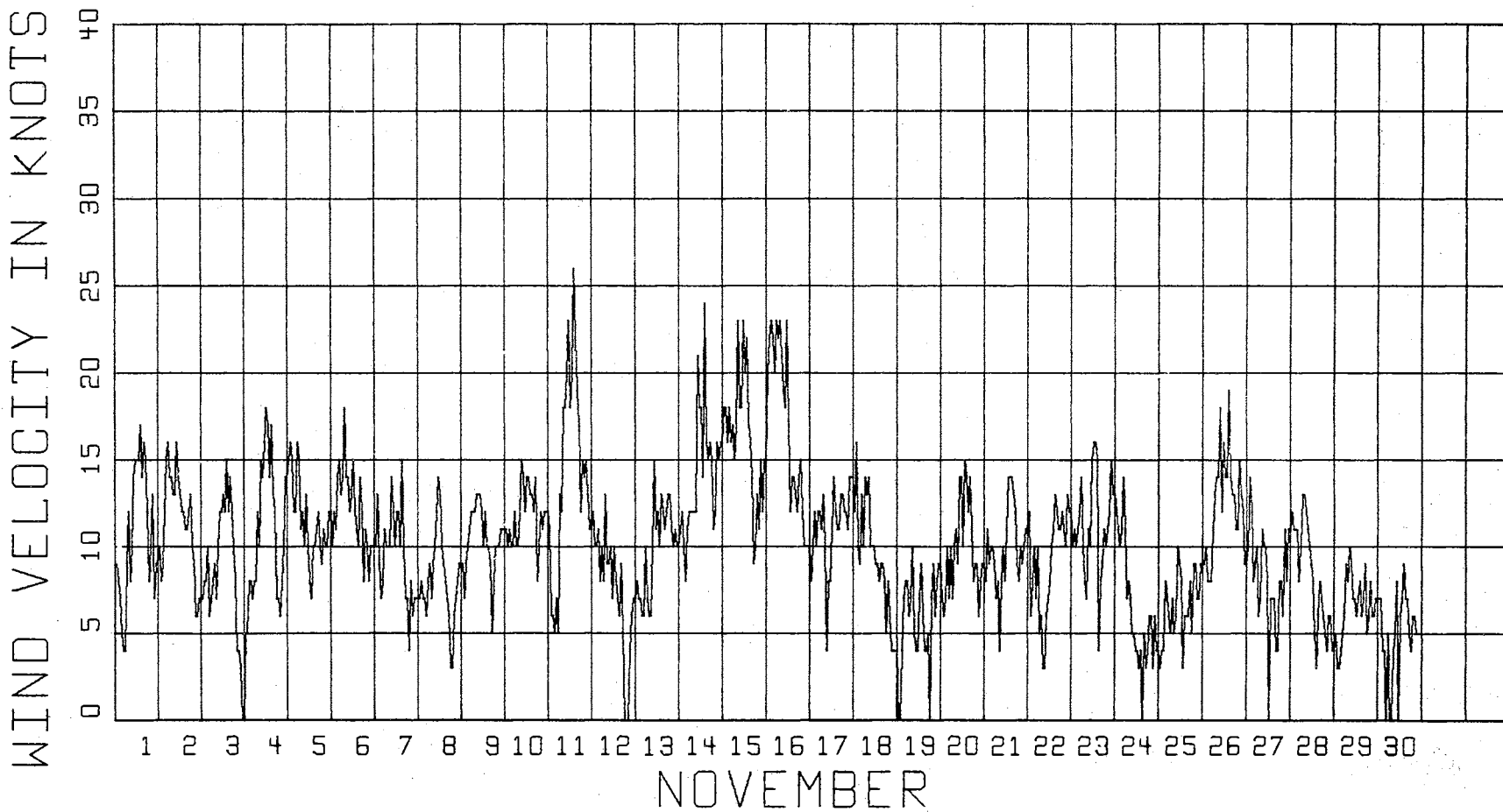Figure 45. Wind Velocity for October, 1962, Using Standard Meteorological Data

Figure 46. Wind Velocity for November, 1962, Using Standard Meteorological Data
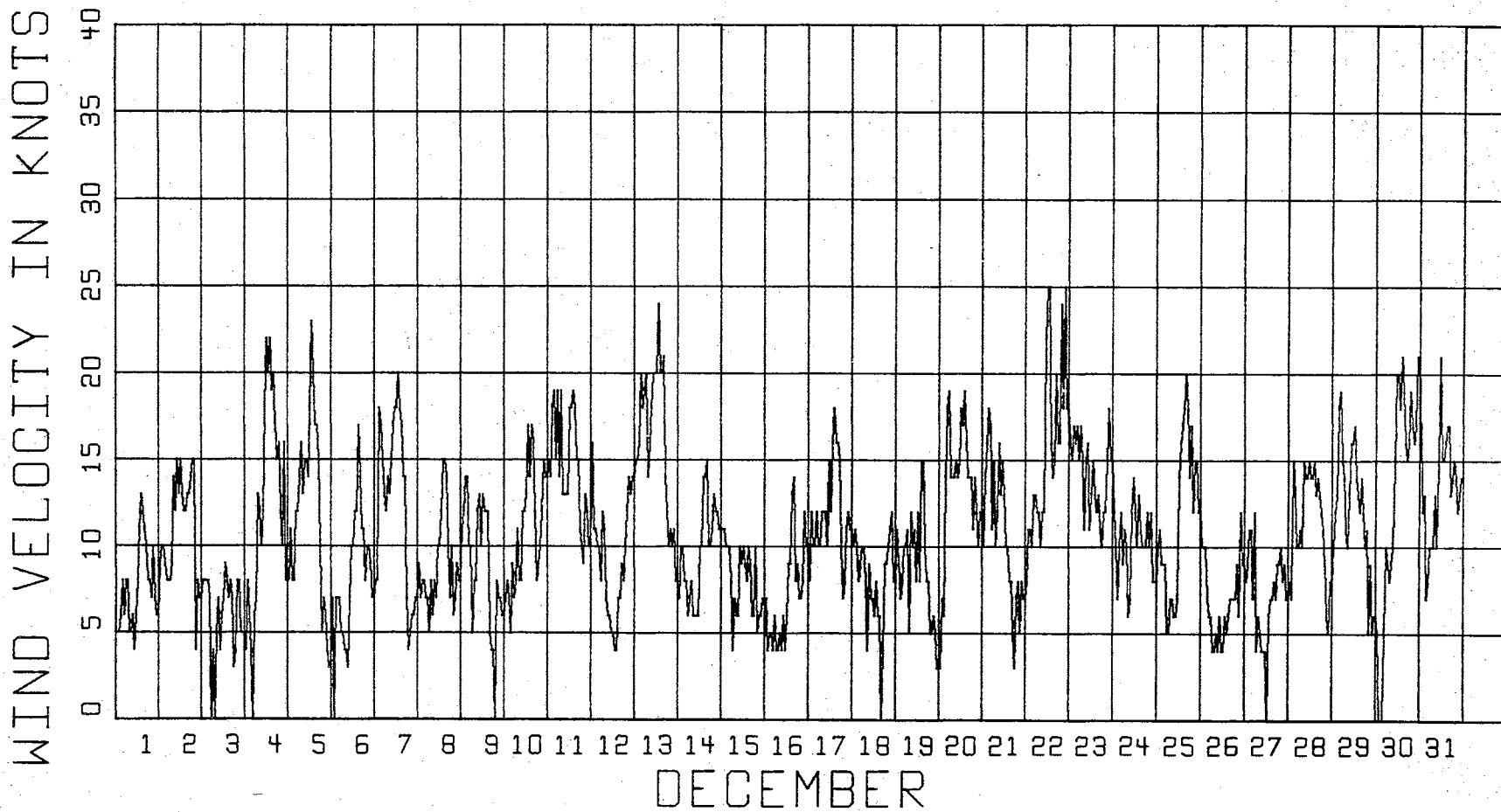
Figure 47. Wind Velocity for December, 1962, Using Standard Meteorological Data

VITA

Le Roy Andrew Gibson

Candidate for the Degree of

Doctor of Philosophy

Thesis: WIND ANALYSIS IN RELATION TO THE DEVELOPMENT OF WIND POWER

Major Field: Electrical Engineering

Biographical:

    Personal Data: Born in Park City, Utah, March 23, 1935, the son of
        Andrew and Priscilla Taylor Gibson.

    Education: Attended high school in Park City, Utah. Attended
        University of Utah from 1953 to 1958 and received a Bachelor
        of Science degree in Electrical Engineering in June, 1958.
        Entered military service in 1958, serving continuously to the
        present. Current rank is Captain in the United States Air
        Force. Attended Oklahoma State University from September,
        1960 to January, 1962, and received Master of Science degree
        in Electrical Engineering in May, 1962. Entered Oklahoma
        State University in January, 1966, and completed requirements
        for the Doctor of Philosophy in May, 1969.

    Professional Experience: Worked as an Electrical Engineer with
        Boeing Airplane Company from June, 1958 to September, 1958.
        Served as Ground Electronics Officer in the Air Defense Command
        from September, 1958 to September, 1960. Worked in various
        test projects which included, testing of Frequency Diversity
        Radards, Man-Pack Radars, Mobile Air Traffic Control Systems,
        and vehicle mounted communications equipment, this being at
        Eglin Air Force Base, Florida. Employed by Florida State
        University as a part time instructor in the Air Force Bootstrap
        education program from January, 1963 to January, 1965.

    Professional Memberships: Institute of Electrical and Electronics
        Engineers.